

V. The Storm

Executive Summary

The following information is presented in this chapter: regional hydrodynamic conditions created by Hurricane Katrina (waves and water levels), local high-resolution hydrodynamic conditions at the levees and floodwalls, as well as, hydrostatic and hydrodynamic forces and loadings that the levees and floodwalls were subjected to during the storm. Of particular interest is the temporal variation of wave and water level conditions, and loadings. Maximum conditions are also of great interest as is the timing and phasing of different types of loadings and forces.

A combination of numerical model results and measured data were used to make the assessment of wave and water level conditions along the entire periphery of the hurricane protection system. The WAM and STWAVE wave models, and the ADCIRC storm surge model, were used to characterize the regional wave and storm surge climate produced by Hurricane Katrina. Models were forced with high-accuracy surface wind and pressure fields, and computations were made on high-performance supercomputers. This report reflects progress to date, and represents a point in time that is 60% through the study process.

Observed peak water levels along the south shore of Lake Pontchartrain were 10.7 to 11.7 ft, which were less than or right at the design peak water levels of 11.8 ft. In the Inner Harbor Navigation Canal (IHNC), north of the intersection of IHNC with the Gulf Intracoastal Waterway (GIWW)/Mississippi River Gulf Outlet (MRGO), there is a large gradient in peak water level, from 15.2 ft just south of the intersection to 11.7 ft at the IHNC entrance to Lake Pontchartrain. In this reach of canal, peak water levels were slightly less than, right at, or above the design levels depending on location. Between this intersection and the IHNC Lock to the south, peak water levels exceeded the design level of 13.2 ft by 1 to 2 ft. Along the east-west oriented GIWW/MRGO channel section, peak water levels exceeded the design value of 13.2 ft by 1 to 5 ft. Along the MRGO adjacent to the St. Bernard Parish hurricane protection levee, peak water levels were over 18 ft, which exceeds the design levels by 5 to 6 ft. Along east-facing hurricane protection levees in south Plaquemines Parish, peak water levels reached 20 ft and they exceeded design levels by as much as 6 ft. All elevations cited are referenced to NAVD 88 2004.65 datum.

Peak significant wave height along the south shore of Lake Pontchartrain reached at least 9.4 ft, exceeding design values by about 1.0 to 1.5 ft. Estimated wave periods were about equal to design values. Along the levees adjacent to Lake Borgne, estimated significant wave heights were less than design values but wave periods exceeded the design wave periods by a factor of 3. Since both wave height and wave period influence the potential for wave run-up and overtopping, the design wave height and period values should be re-examined. In south Plaquemines Parish, design wave height conditions were exceeded by 2 to 4 ft and design wave periods were exceeded by a factor of two to three. Design wave conditions should also be re-examined for these levee systems.

An analysis was performed to examine the influence of the MRGO channel on storm surge propagation into the New Orleans vicinity. The section of waterway where the GIWW and MRGO occupy the same channel allows Lake Pontchartrain and Lake Borgne to be hydraulically connected to each other via the IHNC. Storm surge experienced in the IHNC and the GIWW/MRGO section of waterway is dictated by storm surge conditions in both Lakes due to this hydraulic connection. The long northwest/southeast-oriented section of the MRGO channel to the east of Paris Road Bridge, which seems to be the one that has raised the most concern, only influences the storm surge in the IHNC and GIWW/MRGO canals by a few tenths of a foot for high storm surge events (storms like Hurricanes Betsy and Katrina). It has a more important role for low surges, less than 4 ft in amplitude, but still only creates changes of less than 0.6 ft in some cases and less than 0.3 ft in most cases. The MRGO role in propagation of low amplitude astronomical tide and influx of higher saline water into Lake Pontchartrain has been established; the low-amplitude tide propagates primarily through channels, of which the MRGO is one. However, during high storm surge conditions, when the wetlands become inundated, this reach of the MRGO becomes much less important in storm surge propagation into the IHNC and GIWW/MRGO section. A more detailed analysis is provided in the form of a white paper on the subject.

Detailed analysis of waves, water levels and flow in the 17th street canal was completed. Analysis included surge and detailed wave numerical modeling as well as analytical modeling of flow in and near the breach. Observations from local residents indicate that the breach was initiated before 0630 on August 29. Unconfirmed measured water levels at the pump station appear to confirm this time of breach. Water levels at this time appear to be in the range of 6 – 8 ft and waves were roughly 1 to 2 ft. The predictions indicate that the hydrodynamic loads were primarily hydrostatic during this time period. The results of the surge modeling suggest that the without-breach currents in the canal were negligible. However, the currents were substantial in the neighborhood of the breach. The peak breach discharge occurred at approximately 0900 on August 25, 2005 at slightly greater than 40,000 cfs. The minimum sill elevation also occurred at 0900 and was approximately -12.1 feet. These predictions are preliminary and do not include some effects such as damping of the waves from the bridges and debris at the bridges. Analytical analysis of the barge in the IHNC indicate that the barge impact is a potential contributor to failure of a floodwall and variable draft and details of the collision are primary variables in this determination. Boussinesq simulations of wave and surge on and near the MRGO levees indicate a peak average flow depth over the levee crest of approximately 1.5 ft and an

average velocity of 6.5 ft/s. On the backface of the levee, the gravity driven downrush velocities occur at maximum overtopping, with wave-averaged values near 10 ft/s, and instantaneous velocities reaching 15 ft/s. Simulations suggest that average backface velocities exceeded 10 ft/s continuously for 1 hour (0730-0830), and 5 ft/s for two hours (0700-0900). From 0630-0900, the simulations predict continuous overtopping. Construction of the physical model of the outer portion of the 17th Street Canal is complete and the model is presently being setup for initial runs.

This chapter references a Wave and Storm Surge Analysis Technical Appendix. This appendix will be released with the final report.

Hurricane Katrina Description and History

The approximate storm track for Hurricane Katrina is shown in Figure V-1. The position of the storm center is shown in blue “X’s”, at particular days/times in late August 2005. All times are referenced to UTC.

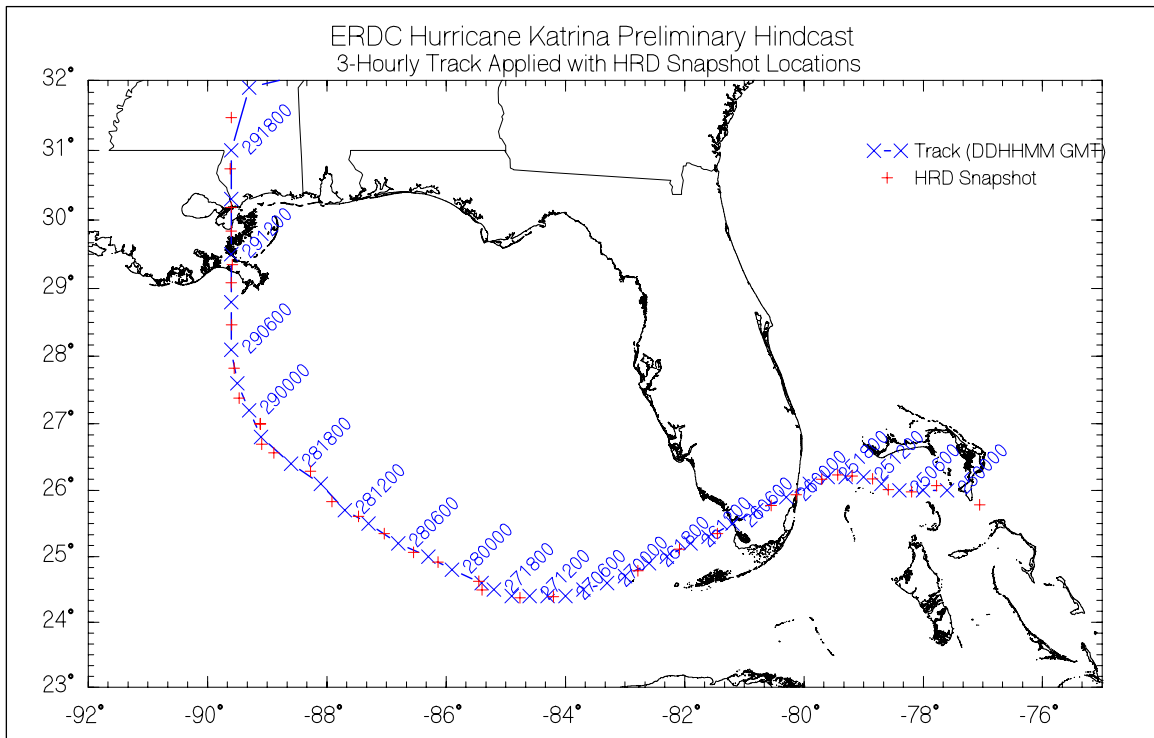


Figure V-1. Hurricane Katrina track

Table V-1 shows the latitude/longitude coordinates for the storm center, the minimum central pressure in the eye of the storm, and the maximum sustained surface wind speed for select times shown in Figure V-1, between 1800 UTC on August 27 and 1800 UTC on August 29. Information in Table V-1 was extracted from the Tropical Cyclone Report for Hurricane Katrina provided by the NOAA

Table V-1 Hurricane Katrina Characteristics				
Date/Time (UTC)	Latitude (deg)	Longitude (deg)	Central Pressure (mb)	Maximum Wind Speed (knots)
Aug 27 1800	24.5	85.3	948	100
Aug 28 0000	24.8	85.9	941	100
Aug 28 0600	25.2	86.7	930	125
Aug 28 1200	25.7	87.7	909	145
Aug 28 1800	26.3	88.6	902	150
Aug 29 0000	27.2	89.2	905	140
Aug 29 0600	28.2	89.6	903	125
Aug 29 1200	29.5	89.6	923	110
Aug 29 1800	31.1	89.6	948	80

National Hurricane Center (Knabb, Rhome, and Brown 2005). The information provides a summary of key hurricane characteristics during the time the storm was at its greatest intensity.

Once Katrina emerged in the Gulf of Mexico after passing over the Florida peninsula, it strengthened quickly and by 0600 UTC on August 26 it had again reached hurricane strength. The storm intensified, and early on August 27 Katrina became a Category 3 storm. The Saffir-Simpson hurricane categories are based on maximum sustained surface wind speed. During that day, August 27, the storm tracked primarily westward. At about 0000 on August 28 the storm turned toward the northwest and experienced rapid intensification; it evolved from a Category 3 intensity storm to a Category 5 storm in about 12 hours. Katrina attained its peak intensity at around 1800 UTC on August 28; the maximum sustained surface wind speed reached 150 knots. At this point, the storm was centered approximately 170 miles south-southeast of the Mississippi River mouth headed to the northwest. At about 0000 on August 29, the storm turned to the north; and as it tracked northward it began to diminish in intensity. By the time it made first landfall near Buras, LA, at 1110 UTC, the maximum sustained wind speed had decreased to 110 knots (upper Category 3 strength). Katrina was a very large storm, in terms of its spatial extent, during its migration through the Gulf, and it remained a very large storm even as it weakened prior to and after first landfall. At approximately 1445 UTC on August 29, the storm crossed the Mississippi Gulf coast near the Mississippi/Louisiana border. The maximum sustained wind speed at final landfall was estimated to be 105 knots. Katrina continued to weaken, and was at Category 1 strength by 1800 August 29. Knabb, Rhome, and Brown (2005) provide a much more detailed description of the storm and its characteristics throughout its history.

Time Line of Performance Events

Hurricane protection system timeline

General. The following is a preliminary hurricane protection system time line summary based on qualitative results of water levels and eyewitness accounts. The primary purpose of these efforts is to aid in the development of a probable timeline for the performance of the hurricane protection system. The timeline will be used as another way to assess the system performance and compare numerical and physical model results with field observations. To date, over 200 high-water marks have been identified and surveyed. With respect to the eyewitness accounts, over 600 people have been contacted and over 175 interviews have been conducted with people who observed flooding induced by Hurricane Katrina. Other means of establishing the timing of events have included documentation of stopped clocks in houses, and the collection of videos and still photos. Attempts have been made to get data from security cameras, but these efforts have produced limited results to date. A USACE news release requesting relocated residents of the greater New Orleans area who stayed during Hurricane Katrina and personally witnessed flooding due to levee overtopping or floodwall breaching before relocating to provide information, photos, and any other related data to IPET was published on 16 February 2006 (Appendix G). This was a nationwide news release with a focus on the gulf south region. In addition to the development of the high-water marks and interviews, considerable effort has been expended in establishing the hydrologic connectivity of this extremely complex system. High-water mark collection is nearly complete, however, additional efforts are required to complete the eyewitness activities and develop a final timeline for the hurricane protection system.

For this preliminary timeline summary, nine sub-areas have been identified. The general locations of these areas are shown in Figures V-2 and V-3. These include: (1) 17th Street; (2) London West; (3) London East; (4) South Gentilly/West Industrial Canal /Upper Ninth Ward; (5) Bartholomew Golf Course; (6) New Orleans East; (7) Lower Ninth Ward and St. Bernard Parish; (8) New Orleans Downtown; and (9) South East Metairie. Although this summary reflects the results of over 175 interviews, it must still be considered preliminary as data are still being collected at this time, and the complete hydrologic picture has yet to be finalized.

1. **17th Street.** Although this area has been covered extensively, the number of people identified as having remained in the area during Hurricane Katrina is fairly small. However, there is some degree of confidence in the results in this area, owing to the credibility and details of the eyewitnesses' accounts. The general consensus is that the initial breach may have occurred early on the morning of Monday, August 29th. While there is the expected wide range of eyewitness times throughout this area, two reliable accounts state that the initial breach was first observed around daybreak (about 0630). One account is from a man in the high-rise building just north of the breach who had a telescope trained on the floodwall area. He reported that just as dawn broke, he saw one section of



Figure V-2. Location of eyewitness sub-areas west of the IHNC



Figure V-3. Location of eyewitness sub-areas east of IHNC

the wall was breached (leaning over). Sometime later when he looked the breach had fully developed. Another eyewitness, viewing from directly across the canal from the west wall observed a single section (panel) leaning over at about day-break. He left and came back about 2 to 3 hours later and observed that there were a number of sections all the way down or gone, suggesting full development of the breach. Other eyewitness accounts in the area generally report seeing the first signs of major flooding in the 0900 to 1000 timeframe, with two accounts near the breach describing rapid flooding between 0900 and 0930. The stopped clock data in the vicinity of the breach also support the 0900 to 0930 timeframe. The eyewitness accounts also generally indicate that there was no significant flooding in the area before 0900, which suggest a possible catastrophic type breaching at that time.

Figure V-4 shows a stage hydrograph developed from Pump Station #6 records on 17th Street. As shown in Figure V-4, the stage on the 29th increases until about 0400 where it flattens out and then the stage drops slightly at about 0630, which would correspond with the eyewitness accounts of the first panel breaching. A dramatic drop in stage occurs around 0930, which corresponds with the eyewitness account of the complete development of the breach. Although the stage changes do correspond with the observed eyewitness accounts, further study is needed to insure that these changes in the stage hydrograph don't reflect the passing of the storm surge, pump operations, gage malfunctions, or other factors. There are also questions about pump Station #6 data that must be addressed before its reliability can be accepted.

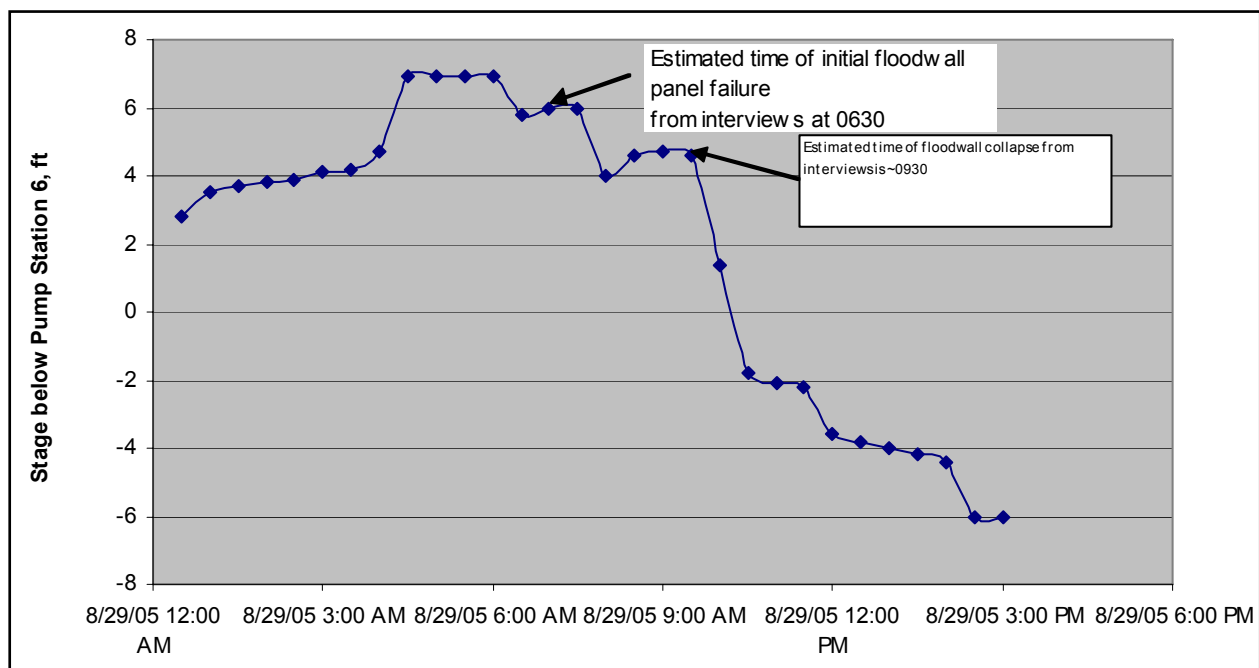


Figure V-4. Stage Hydrograph from Pump Station on 17th Street Canal. This data is being used to supplement eyewitness and clock efforts to determine timing of events, and is not intended to represent absolute elevations

Based on the above data, it appears that the initial failure of the floodwall (single panel) occurred early on the morning of the 29th at least by about 0630, and was probably fully developed (possibly catastrophically) by about 0900 to 0930.

If the initial breach occurred around 0600-0700 in the morning, then according to stage hydrograph data based on digital pictures and eyewitness accounts (Figure V-5), the stage in the canal would only have been at about elevation 6.8 to 7.8 ft NAVD88 (2004.65), which would be well below the top of the wall. According to post-Katrina surveys, the top of the 17th Street floodwall is about 12.4 feet NAVD88 (2004.65) at the breach. The estimated stage at the Lake Pontchartrain end of the 17th Street Canal at 0930 was about 11 ft NAVD88 (2004.65) (Figure V-5).

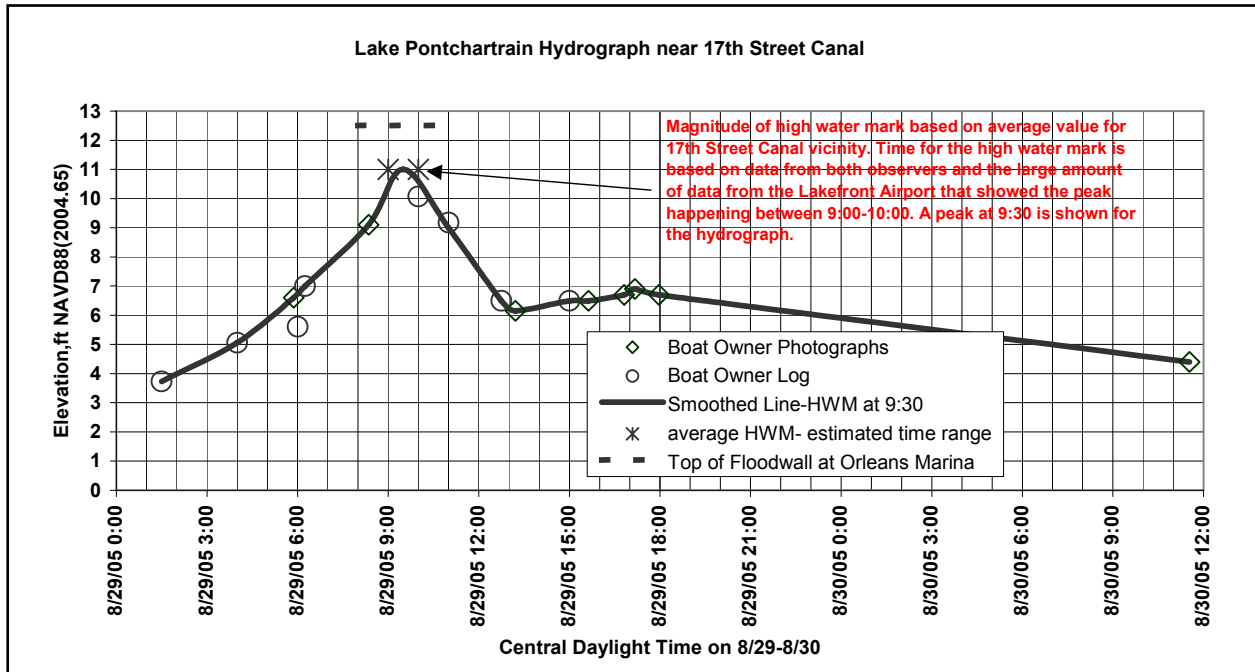


Figure V-5. Stage Hydrograph for 17th Street Canal and Vicinity based on digital photographs and eyewitness account

2. **London West.** Similar to the 17th Street area, there is a scarcity of eyewitness accounts in the London West area. Consequently, there is still some uncertainty with respect to the time of the breach on west side of the London Canal. There are only a few eyewitness accounts in the northern part of the area near the breach. Three of these accounts place the flooding time between 0900 and 1000 on the 29th, and one, which is felt to be a very reliable witness (although he is south of Mirabeau St.) places it between 0700 and 0800. Stopped clock data in the vicinity of the breach is very consistent, with the majority of the times being between 0730 and 0830. Further south (between Mirabeau and I-610), there are more eyewitness accounts. Based on these accounts, it appears that the water began to enter this southern area in the early to mid afternoon period. However, an eyewitness account also reported water flowing south to north over Gentilly Ridge into this area at about 1000.

Based on the accounts at this time, the best current estimate for the time of the breach is sometime before 0900 on the 29th. Additional effort is being expended in the area near the breach to determine if this time estimate can be refined further, and to determine how and when flood waters entered the southern end of the area.

3. **London East.** A large number of eyewitness accounts were conducted in the London East area. Although there is the usual time spread between the data, there seems to be fairly consistent grouping of times between 0700 and 0900, with quite a few reliable accounts between 0700 and 0800 near the east breach. Based on these data, the time of the breach at London East appears to be between 0700 and 0800 on the 29th. It should also be noted that there is video and photography evidence that shows water flowing over Gentilly Ridge into this area from south to north at about 1230 on the 29th.

Assuming the breach occurred between 0700 and 0800, then the corresponding elevation in the canal would have been about 7.8 to 8.8 ft NAVD88 (2004.65), according to the stage hydrograph (Figure V-5). The elevation of the floodwall in this vicinity is about 12.9 ft NAVD88 (2004.65).

4. **South Gentilly Ridge/West Industrial Canal/Upper Ninth Ward.** There are three breach locations on the west side of the Industrial Canal. These include the breach near I-10 through the railroad line, and the breach in the floodwall and earth levee near Pump Station # 19. The elevation of the floodwall along the west side of the canal is about 13 ft while the earth levee is about 10.7 ft.

There are numerous eyewitness accounts in this area that are remarkably consistent. Most recall seeing the first signs of rushing water between 0600 and 0700 on the 29th. Based on these accounts it appears that flood waters may have been coming from the Industrial Canal some time before 0600. Flow over the floodwalls and from the breach or breaches would quickly enter the east-west Florida Canal, thereby providing a possible explanation of the early flooding times as far east as Pump Station #3. The north-south Peoples Canal also provides a direct conduit of water to the northern areas, both north and south of Gentilly Ridge.

The gage records at the Lock and at I-10 (Figure V-6) provide insight into the timing and manner of the breach(s). According to the USGS gage at I-10, there is a dramatic drop in stage of about 5 feet at about 0430 that morning, while the Orleans Levee District Gage flattens out during this same period. Following this period, the stages at both gages continue to rise. While these data should not be viewed as absolute (particularly the 5 foot drop in stage) it does appear that something may have occurred to impact the gage in the 0400 to 0500 timeframe. Thus the preliminary analysis of the gage data may support the eyewitness accounts of early overtopping/breach(s) along the west side of the Industrial Canal. The reliability of this data must be examined closer to ensure that these changes were not due to mechanical problems with the gages. Another complicating factor is that the two large breaches on the east side of the Industrial Canal may have contributed to the stage reduction at the I-10 gages, although

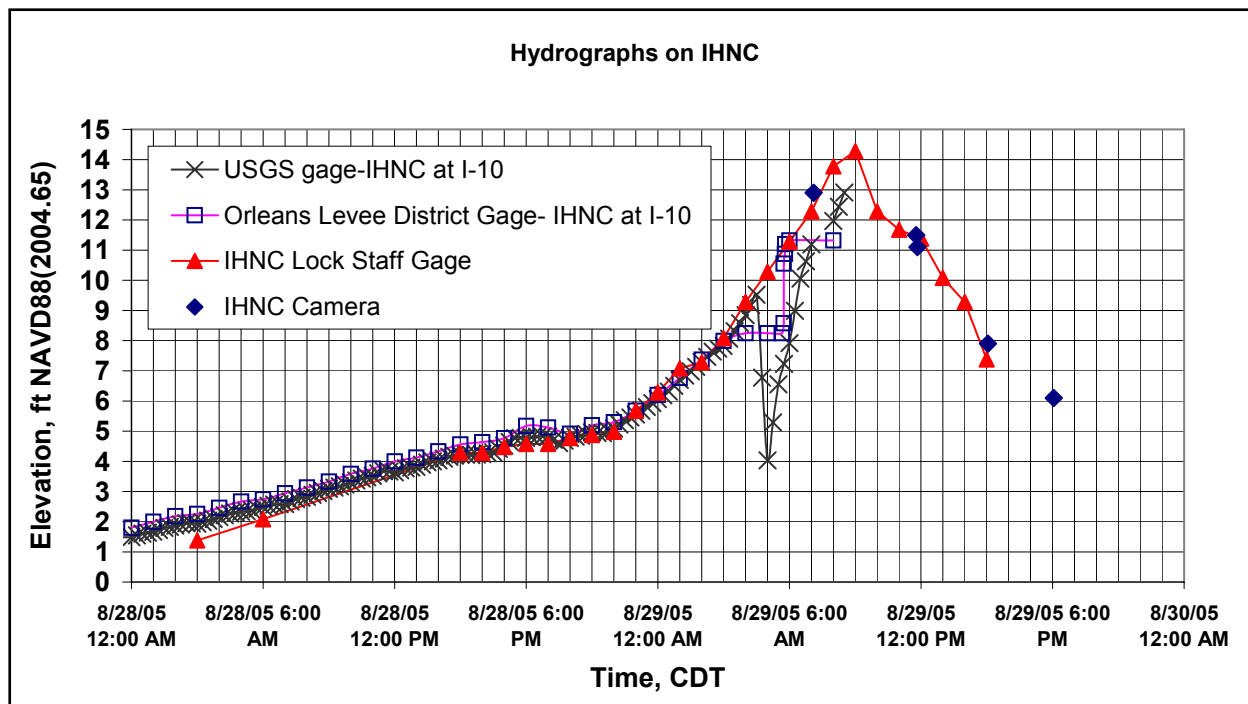


Figure V-6. Stage Hydrographs for IHNC at I-10, and IHNC at Lock

preliminary analyses suggest that they occurred later than the 0400-0500 time-frame. Therefore, while the gage data does provide useful insight, additional hydrologic analysis is needed in order to confirm its reliability.

While the data suggest that this area was inundated very early (between 0600 and 0700, and possibly earlier in some places), the timing of the individual breaches and their timing relative to overtopping is undetermined at this time. Detailed hydrologic analysis of this area is continuing to determine if this can be established with certainty.

5. **Bartholomew Golf Course.** This area is bounded on the north by Lake Pontchartrain, on the east by the Industrial Canal Floodwall, on the south by Gentilly Ridge, and on the west by the railroad grade and Peoples Canal. There are four ways for water to enter this area: (1) overtopping of the hurricane protection levee along Lake Pontchartrain; (2) overtopping of the Industrial Canal floodwall; (3) flow over Gentilly ridge from the south; and (4) from Peoples Canal through the railroad grade. There is considerable uncertainty among the eyewitness accounts in this area, with the majority of the times ranging from mid-morning to late afternoon. There are several reliable accounts that observed the floodwall overtopping early in the morning on the 29th. Both these eyewitnesses noted that this was more wave splashing rather than complete overtopping. They also noted that while this did put water in the street and up to their houses that it ran off quickly, and that the major flooding did not occur till later in the day. Numerous eyewitnesses reported water spewing up through the storms drains consistent with backflow from Peoples Canal. There were also accounts of water coming under the Chef Menteur (Gentilly) overpass into the area from the south. More analyses are needed in this area to narrow this uncertainty.

6. **New Orleans East.** The New Orleans East area is bounded on the south by the Intracoastal Waterway, on the west by the IHNC, and on the north and east by Lake Pontchartrain and marsh lands. Significant levee overtopping and breaches occurred all along the Intracoastal Waterway. There were also a few breaches along the floodwall on the IHNC near I-10, as well as overtopping of the floodwall near the Lakefront Airport. Overtopping also occurred along the levee at Lake Pontchartrain, but to a much lesser degree than on the Intracoastal Waterway. Therefore, the New Orleans East area received flood waters from all directions.

Approximately 25 eyewitness interviews have been conducted in the New Orleans East area. Stopped clock data have also been gathered in this area, as well as video footage of the levee overtopping at the Michoud power plant. Based on these data, it appears that water began overtopping the Intracoastal Waterway levee about 0600 on the 29th, and according to several eyewitnesses, this overtopping continued for about 5 hours. Although there are a number of sources of water for this area, the eyewitness accounts report that the majority of the water came from the south (Intracoastal Waterway). Further hydrological analysis is needed to confirm this. Eyewitness accounts and clock data indicate significant flooding occurred in the area south of Dwyer Road and west of Crowder Road between 0600 and 0800. Video footage shows overtopping of the levee near the Michoud power plant. There is also evidence of from 2 to 5 feet of flow overtopping the railroad grade just south of Chef Menteur from south to north. North of Dwyer Road, the flooding times are a little later, in the 0800 to 1000 timeframe. Several eyewitness accounts just south of the Lake Pontchartrain levee reported flood waters arriving in the 0800 to 0900 timeframe from the south. Farther east of Crowder Road, the times are generally in the late morning to early afternoon. Further analysis is needed to determine if these time differences are due to travel times, topography, or other hydrological factors. Additional efforts are planned for the East New Orleans area to refine these time estimates.

7. **Lower Ninth Ward and St. Bernard Parish.** This area is bounded on the south by the Mississippi River, on the west by the IHNC, and on the north and east by the Intracoastal Waterway and MRGO. The primary sources of flooding for this area are the overtopping and two breaches along the IHNC, and the overtopping and numerous breaches along the Intracoastal Waterway and MRGO. Data in this area includes eyewitness accounts, stopped clocks, and video footage.

To date, there have only been a limited number of interviews in the Lower 9th Ward, primarily due to the fact people have only recently been allowed back in to this area. However, the eyewitness accounts are fairly consistent in this area. Based on these data, the floodwaters appear to have entered the Lower 9th Ward from the IHNC in the 0730 timeframe. Reports at the Jackson Barracks, about 1.5 miles due east of the breaches, indicate a rush of water arriving from the west shortly before 0800.

The stage in the IHNC Lock during the 0730 timeframe was about 13 feet as shown in Figure V-6. Further hydrologic analysis is needed to establish the overtopping and breaching relationships in this area.

To date, no eyewitness accounts of the overtopping or breaching along the Intracoastal Waterway or MRGO have been recorded. Hydrologic analysis is continuing in an effort to establish this timing and the time lag before waters began to enter the Chalmette area. Eyewitness accounts, stopped clock data, and video footage suggest that the floodwaters first entered the areas east of Paris Road (Chalmette) from the northeast (Intracoastal Waterway and MRGO) in the 0800 to 0830 timeframe. Video footage in the Corinne Estates Subdivision in Chalmette provides a good documentation of this flooding. The video also shows large clumps of marsh grass moving in a northeast to southwest direction, clearly indicating flows from the Intracoastal Waterway and MRGO area. These marsh grasses are a common feature on houses and other structures through this entire area, but are rarely, if ever seen west of about Paris Road. Additional analysis is required to refine the time estimates in the Chalmette area, and the area farther east in St. Bernard Parish.

8. **New Orleans Downtown.** At present, only a few interviews have been conducted in this area. Based on these limited interviews, it appears that water started to appear in this area sometime on Monday evening through Tuesday morning. Additional effort will be required to further refine these estimates.

9. **South East Metairie.** A few contacts have been made in this area, but no eyewitness interviews have been conducted yet. Additional efforts are planned for this area.

Regional Hydrodynamics

Summary of Work Accomplished

Development of Wind and Atmospheric Pressure Input

Accurate modeling of waves and storm surge is highly dependent on the accuracy of the wind input to the models. Wind speed is a very important factor influencing the regional wave and storm surge climate, in addition to topographic features which influence wave and surge development and propagation. Surface wind shear stress, the primary forcing to both types of models, dictates the level and frequency of wave energy and storm surge amplitude. Shear stress is non-linearly related to wind speed (a quadratic or cubic dependency) so having accurate winds is crucial. Errors in the input winds are amplified in a non-linear manner. The quality of wave and surge model results is only as good as the meteorological input to the models, particularly wind speed.

Wave and surge models require wind and pressure fields for the entire modeling domain, which for this study included the entire Gulf of Mexico. The work to characterize regional wave and water level conditions was required by several other study tasks, early in the study process. Therefore a spiral development approach was adopted to produce results quickly and then refine the results once other tasks had the information they needed to proceed. The need to produce results quickly dictated the approach that was taken early on.

For the storm surge modeling reflected in this report, wind and atmospheric pressure fields were generated using a Planetary Boundary Layer (PBL) model (Thompson and Cardone 1996). Coupled ADCIRC-PBL models were already in place as a result of prior work done for the U.S. Army Engineer District, New Orleans, so it was utilized while work on the “final” wind and pressure fields was underway. The PBL model employs a moving nested-grid approach (five levels or nests with increasingly higher resolution nearest the storm center) to compute spatially-varying wind and pressure fields as a function of time. For input, the PBL model requires information about the storm position (track), the maximum sustained surface wind speed and central pressure (the type of information shown in Table V-1). Input data for the PBL model were obtained from NOAA. Radius-to-maximum-wind values are computed internally within the five-level model using the method presented in Jelesnianski and Taylor (1973). Radii-to-maximum-winds, which influence spatial variation of the wind field are calculated as a function of central pressure and maximum sustained wind speed. For the final storm surge modeling, wind and pressure fields will be developed using the more rigorous approach outlined below.

For the Gulf-scale and regional-scale wave modeling reflected in this report, preliminary wind fields produced by Oceanweather, Inc. (OWI) were used, which include H*Wind snapshots developed by the NOAA Hurricane Research Division (HRD). An approach which utilized the H*Wind snapshots was taken because the method to link these wind inputs to Gulf-of-Mexico-scale and region-scale wave modeling had been previously developed as part of a National Ocean Partnership Program project, the linkage was readily adaptable for use in this investigation. This methodology for generating surface winds will be adopted to provide input to all final storm surge and wave modeling. The H*Wind snapshots integrated into the preliminary wind fields were primarily based on those created in real-time as part of forecast operations, with some limited re-analysis. The final winds will benefit from a much greater reanalysis effort; which according to HRD staff, is the most intensive analysis of hurricane surface winds that has ever been undertaken by that office.

H*Wind snapshots for the inner core of the hurricane are constructed using a method developed at HRD called the HRD Surface Wind Field Analysis System (Powell et al. 1998, <http://cat5.nhc.noaa.gov/Hwind/>) which utilizes measured meteorological data from a number of different types of sensors and data acquisition processes. All wind measurements are transformed to a standard 10-m elevation, averaging period (1-minute sustained wind speed) and exposure (marine or land). The data are scrutinized for quality. The product of this man-machine mix is a wind streamline and isotach contour plot that is fixed (storm centered) in space and time (see Figure V-7 which is the preliminary snapshot for 1030 UTC on August 29 just prior to landfall). There are 36 unique H*Wind analysis snapshots that comprise the duration of this storm. Snapshots were computed for each of the times denoted with small red crosses (+) in Figure V-1. They represent the best wind estimate for the target domain on which the snapshot is placed. The development of the full domain winds requires two procedures. First, snapshot H*Wind fields are repositioned to the storm track, and then a moving center interpolation algorithm is applied to preserve the characteristics of the tropical storm wind core in space and time.

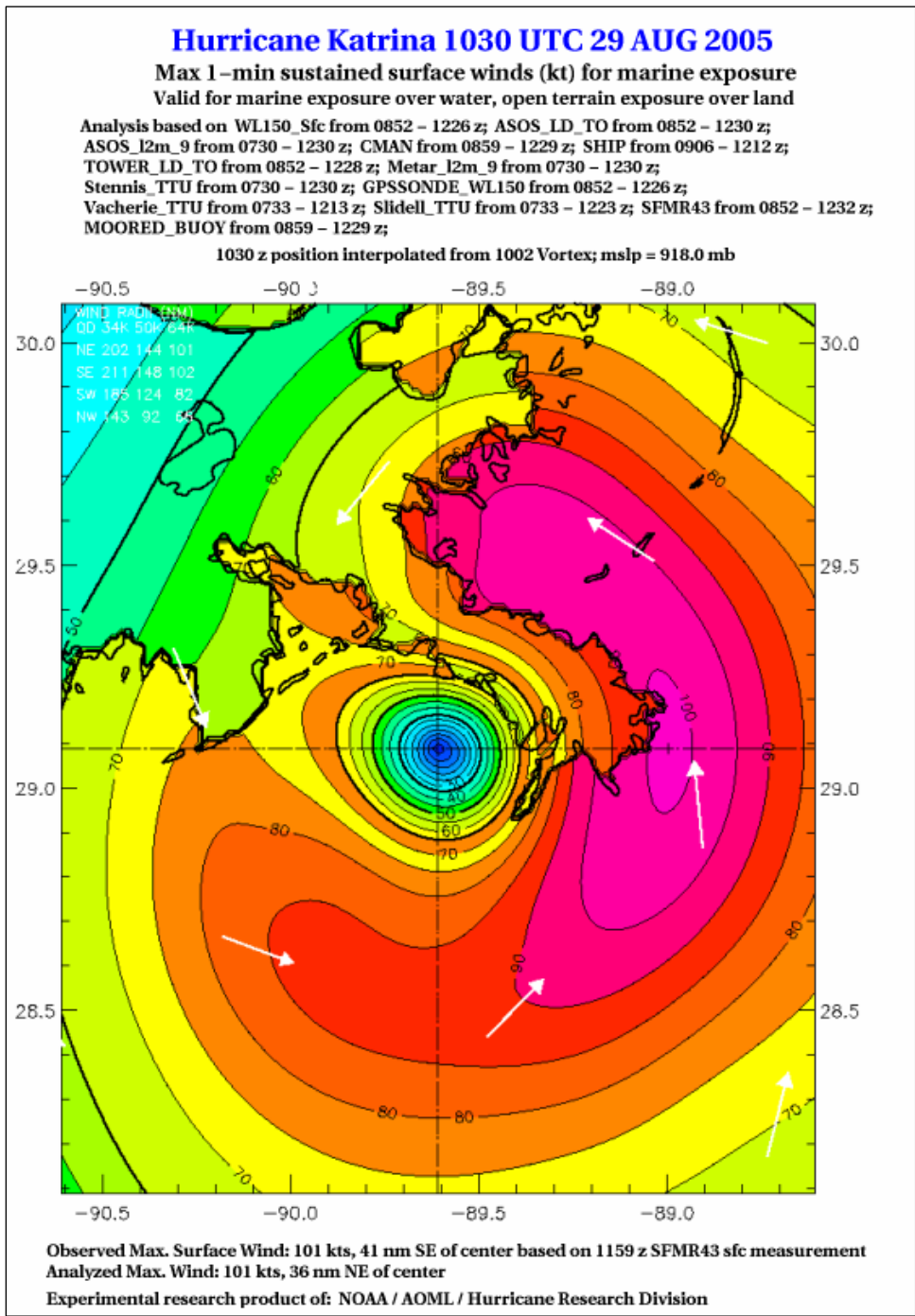


Figure V-7. Preliminary H*Wind snapshot for 1030 UTC on August 29, just prior to landfall (Wind speeds are color contoured in knots, representing 1-minute sustained surface wind speeds. Note this wind field includes both marine and land exposures identified by the abrupt change in color contours over the land)

The wave and surge modeling activities require complete wind field specification for the entire target domain; the H*Wind technique is only used to define wind conditions in the core of the storm. Accomplishing this task requires background estimates which are derived from the NOAA National Centers for Environmental Prediction/National Center for Atmospheric Research (NCEP/NCAR) Reanalysis Project (Kalany et al. 1996). The NCEP/NCAR winds are rigorously analyzed and rely on data assimilation methods using data not originally used in the NCEP operational forecast. A final step is to inject local marine data (adjusted to a consistent 10-m elevation and adjusted for neutral stability). This procedure uses an Interactive Objective Kinematic Analysis (IOKA) System (Cox et al. 1995) developed by Oceanweather, Inc. (OWI). Oceanweather produced the final wind and pressure fields.

Generation of the surface pressure fields follows a slightly different approach using the TC96 model (Thompson and Cardone 1996). This model (TC96) was initially developed over thirty years ago. The model solves, by numerical integration, the vertically averaged equations of motion that govern a boundary layer subject to horizontal and vertical shear stresses. Upgrades and modifications of the TC96 have been made over the development cycle (Cox and Cardone 2000). The pressure fields generated for the Katrina study are built from parameters that are derived from data in meteorological records and the ambient pressure field. The symmetric part of the pressure field is described in terms of an exponential pressure profile from Holland (1980). The pressure field snapshots, aligned to the storm track, are spatially and temporally interpolated in a similar fashion as done for the winds and placed on the identical fixed latitude/longitude grid. No synoptic-scale inputs were considered in this application.

All wind and pressure fields produced by Oceanweather, Inc. (<http://www.oceanweather.com>) were created for two domains, a Gulf-of-Mexico-scale domain (called the basin-scale domain) and a Louisiana/Mississippi regional domain. Specifics of the wind and pressure field domains are provided in Table V-2. Winds and pressures are more highly resolved at the regional scale than at the basin scale. Wind and pressure fields were defined every 15 minutes. Surface winds from OWI represent 30-min average wind speeds. A few results of the wind analysis are presented below. More detail about the process used to generate the wind and pressure fields and the quality of results are contained in the Wave and Storm Surge Analysis Technical Appendix.

Table V-2 Wind and Pressure Field and Offshore Wave Model Domain Characterization							
Domain	Longitude (deg)		Latitude (deg)		Res. (deg)	Duration (yr/mon/day/hr)	Wind Input Interval (sec)
	West	East	South	North			
Basin	98 W	80 W	18 N	30.8 N	0.1	2005082500 – 2005083100	900 (30-min avg winds)
Region	91 W	88 W	28.5 N	30.8 N	0.00833	2005082906 - 2005082918	900 (30-min avg winds)

Wind Conditions During Katrina

Figure V-7 shows the sustained surface wind field just prior to landfall. The white vectors in the figure indicate the general wind direction and they reflect the counterclockwise rotation of the wind fields about the storm center. Peak wind speeds are seen to the right of the storm center, which is typical for hurricanes. Maximum surface wind speeds exceed 100 knots. At landfall, along the entire southeastern Louisiana coast, east of the MS River, surface winds are at hurricane force (64 knots) or greater.

Considerable effort is being expended to maximize use of measured meteorological data in the process to create H*Wind snapshots as well as the IOKA process to develop the basin and regional-scale wind fields, because of the critical nature of winds in the wave and storm surge modeling. In many locations, model results are the only source of information for quantifying the wave and water level conditions along the periphery of the hurricane protection system. So it is very important to understand and quantify the accuracy of model input and model-generated results. Comparison of model results to measurements is a very high priority in all facets of the IPET wave and water level analysis.

Figures V-8 and V-9 show comparisons between measured wind speed and direction with the preliminary wind product produced by OWI for two locations, at Southwest Pass to the Mississippi River (Figure V-8) and at the NOAA National Data Buoy Center Buoy 42007 (Figure V-9). Both of these locations (see the map in Figure V-10) are in positions that were east of the storm's path.

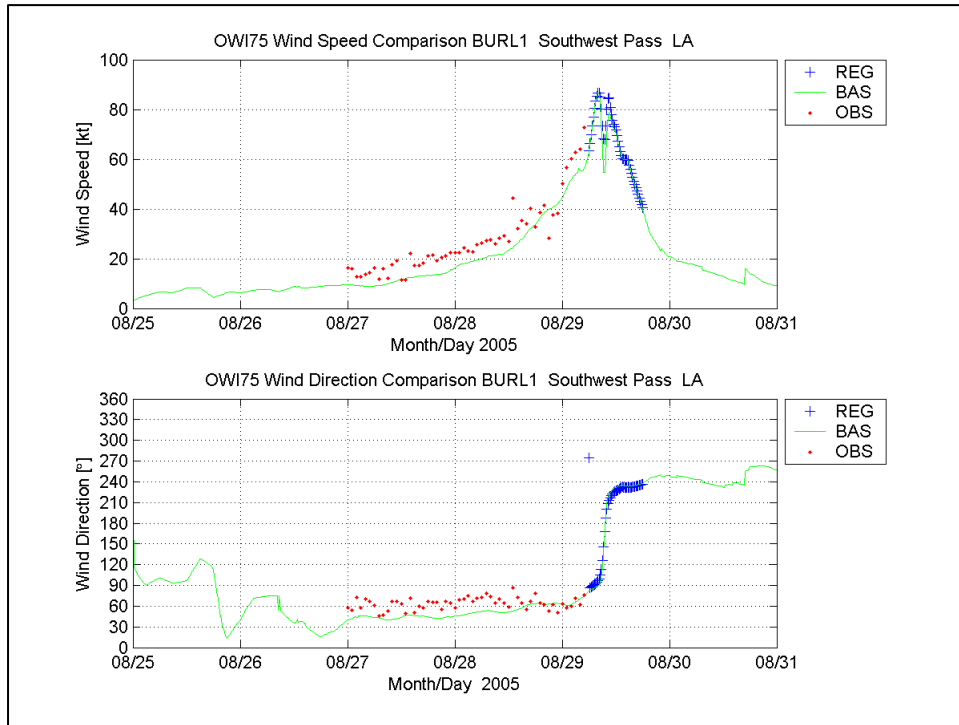


Figure V-8. Comparison of wind speed (upper panel) and direction (bottom panel) at Southwest Pass, LA

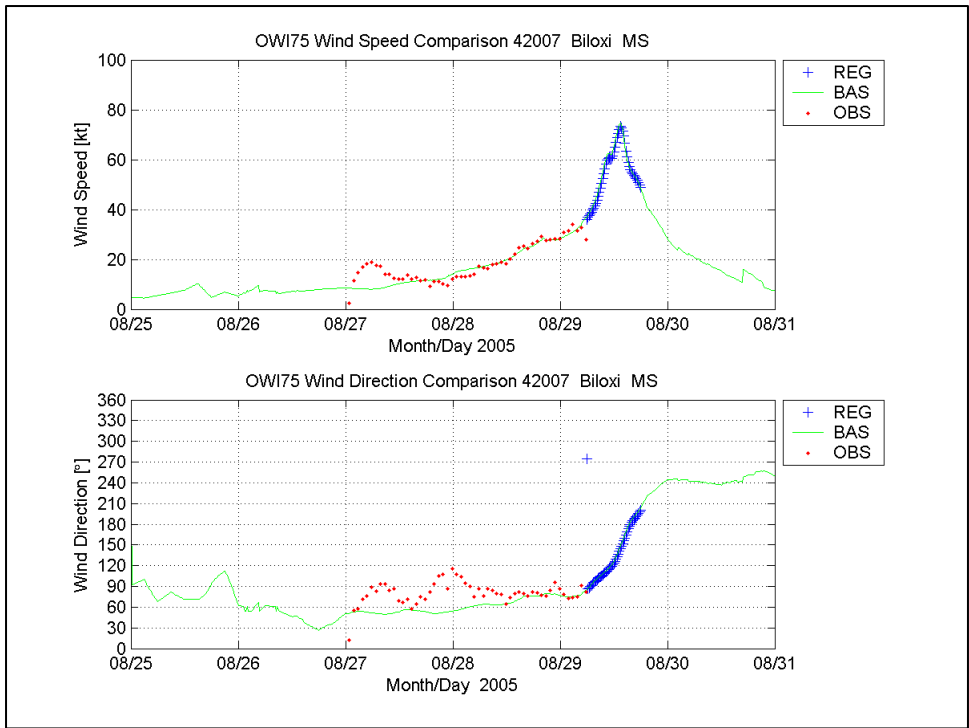


Figure V-9. Comparison of wind speed (upper panel) and direction (bottom panel) at NOAA NDBC Buoy 42007

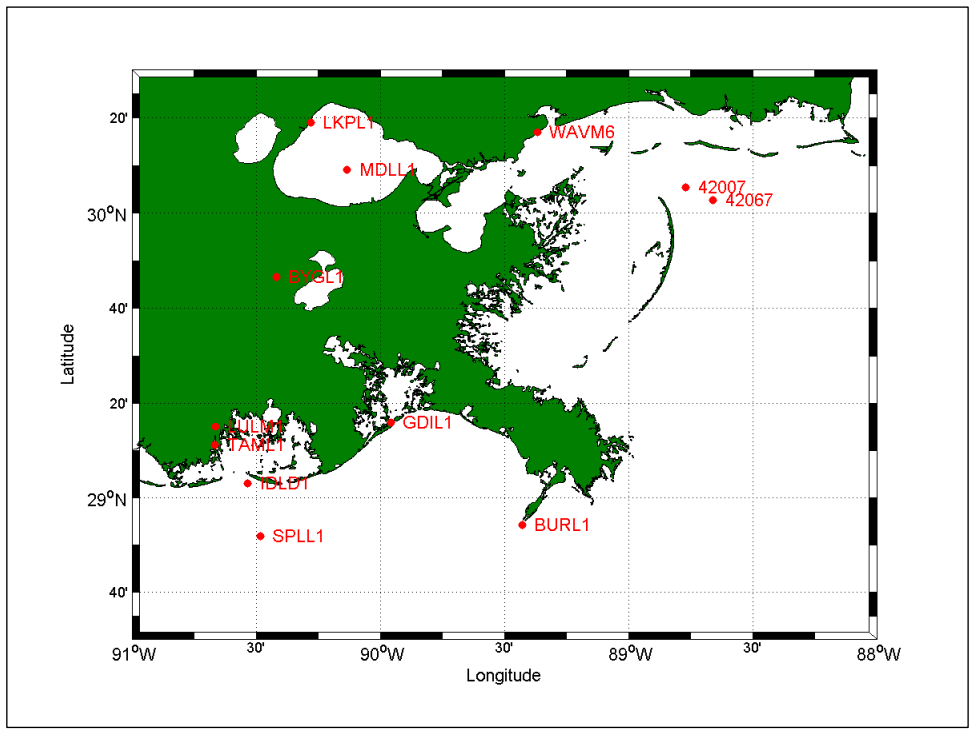


Figure V-10. Wind measurement sites within the regional domain

Figure V-11 shows a comparison for Grand Isle, LA, which was to the west of the storm path. Computed basin-scale winds are indicated by the green line, regional-scale computed winds are shown with blue crosses, and measured winds are indicated with red dots. Note that regional winds were developed for a shorter period of time that encompasses the peak of the storm.

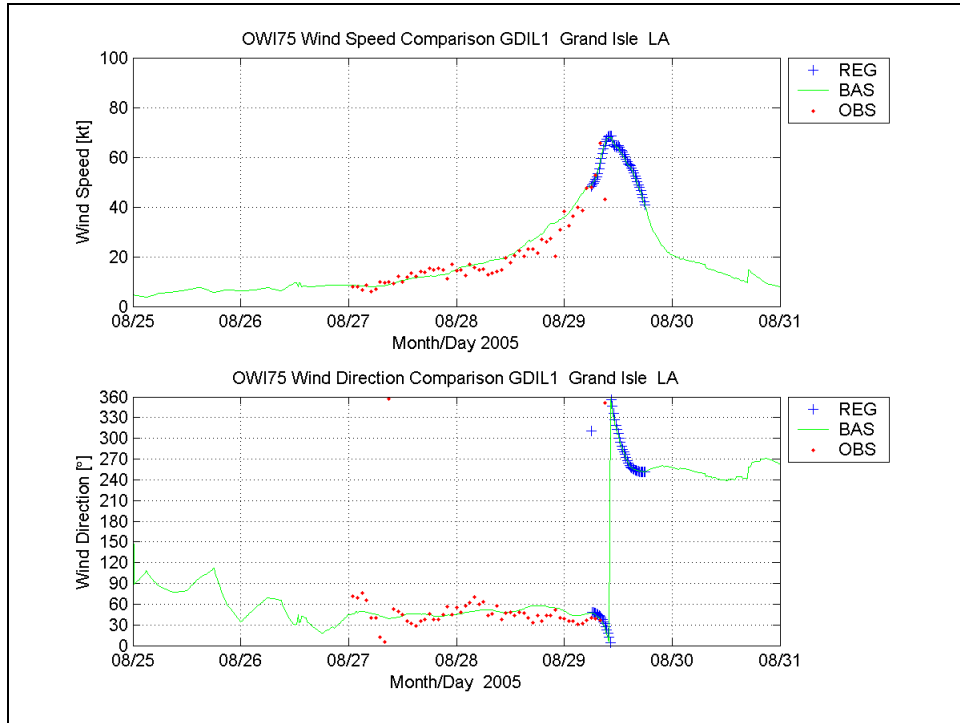


Figure V-11. Comparison of wind speed (upper panel) and direction (bottom panel) at Grand Isle, LA

The H*Wind/IOKA winds show that for at least four to five days prior to landfall, winds were steadily out of the east and northeast and gradually increasing in speed. This trend is confirmed by the measurements. Persistent winds blowing from east to west are notable in that for several days prior to landfall, these winds were acting to push water from east to west along the Mississippi/Alabama continental shelf toward the Mississippi River delta and southeastern Louisiana. This regional-scale movement of water began to build the storm surge in southeastern Louisiana and flood low-lying wetlands well in advance of the storm's arrival. The figures also provide an indication of the accuracy of the windfield products that are being created for use in the wave and storm surge modeling. Overall trends are captured well and magnitudes are reasonably accurate. The greatest errors are in wind direction. Errors are smallest during the day prior to landfall, when wind speeds rapidly increase in magnitude. Additional comparisons are provided in the Wave and Storm Surge Analysis Technical Appendix.

Note that each of the wind measurement sensors near the path of the storm failed prior to the peak of the storm. This was a recurring theme, for wind sensors and water level sensors; failure of instrumentation to function or survive and

capture conditions just prior to, during, and after the storm peak, i.e., the crucial part of the storm. There is great need for instruments that can measure surface wind conditions (and water level) reliably during the peaks of severe hurricanes.

Regional Waves Approach

Wave modeling was done to characterize wave conditions just seaward of the hurricane protection system, throughout the entire study region. With one exception (at essentially a single point in Lake Pontchartrain just north of the 17th Street Canal), no shallow-water wave measurements were available that captured wave conditions during the storm just seaward of the levees and floodwalls. Wave measurements were available at a few offshore sites, some of which survived the peak of the storm; but these sites are too far away and in much deeper water, and they can not be used to characterize conditions adjacent to the hurricane protection system. The paucity of nearshore wave data highlights the need for shallow-water wave measurements that are routinely collected for storms and made in ways that can withstand, survive, and record during severe hurricane conditions, and capture the peak conditions. In light of the limited amount of nearshore wave measurements, wave modeling was employed to provide the required information, at the resolution needed, for the very large study area.

Wave modeling was done using a nested approach, with three levels of nesting: 1) basin-scale modeling for the entire Gulf of Mexico; 2) regional-scale modeling at higher resolution for a much smaller domain that encompassed southeastern Louisiana and part of the Mississippi coast, with more resolved wind field input, and 3) nearshore, shallow-water, local-scale modeling which was done at very high 200-m resolution. At each successive nest level, additional resolution was employed to maximize accuracy (resolution is directly related to accuracy) and to treat the important physical processes such as depth effects as accurately as was computationally feasible. Wave boundary conditions for modeling done in each successively refined domain are derived from modeling done at the next coarser domain. The effects of storm surge on water depth were only addressed in the nearshore, shallow-water wave modeling.

The key output product from the most refined nearshore wave modeling work is information to characterize the temporal variation of significant wave height, peak spectral wave period, mean wave direction computed using the full energy spectrum, along the entire periphery of the hurricane protection system that was considered in this study. Maximum wave conditions are also of great interest, and local maxima were compared to the design wave conditions and to the limited set of wave measurements that was available (comparisons to design wave conditions are presented later). Frequency-direction energy spectra were computed at locations where the high-resolution hydrodynamic analysis was done, which required the energy spectra.

Every effort was made to compare model predictions with measured wave data, to assess model accuracy and provide a level of confidence in model-derived results. These comparisons also help assess uncertainty in model predictions. Comparisons were made using measurements from several sources:

1) two small buoys (nearly co-located) that were deployed in Lake Pontchartrain just prior to the storm by the U.S. Army Corps of Engineers, New Orleans District, functioned during the storm, and were recovered after the storm, 2) a number of large NOAA NDBC buoys that are located in deeper water (see Figure V-12 for buoy locations), and 3) satellite-mounted altimeter.

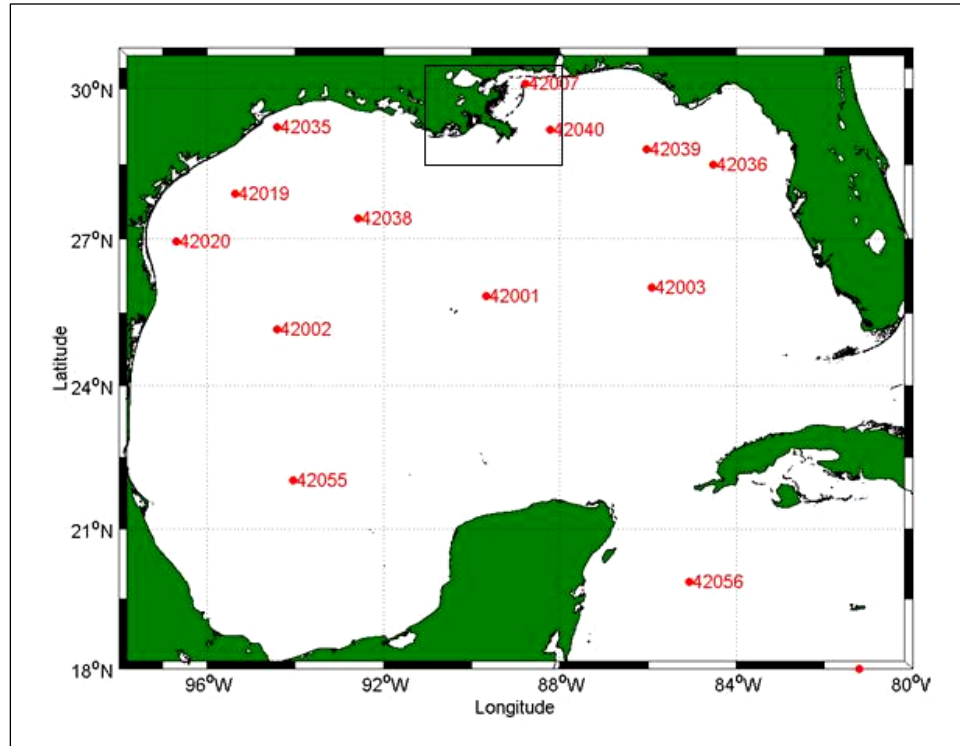


Figure V-12. Offshore wave modeling domains and location of NOAA NDBC buoys

Offshore Waves

Offshore wave-modeling was done using two models, WAM Cycle 4.5 (Komen et al. 1994) and WAVEWATCH III (Tolman 1998, 1999). The WAM model was selected to generate wave conditions for the “production” modeling, since it has been used during the past decade or so by the Corps of Engineers for its detailed wave generation modeling (particularly for hurricanes). The WAM model was applied for basin- and regional-scale domains, the same ones defined in Table V-2. Both domains correspond to those employed in development of wind and pressure fields. Figure V-12 shows the basin-scale domain (entire Gulf) and the regional domain (the black box in the figure that encompasses the Louisiana/Mississippi coastal region). The exact regional domain and the local bathymetry in this area are shown in more detail in Figure V-13.

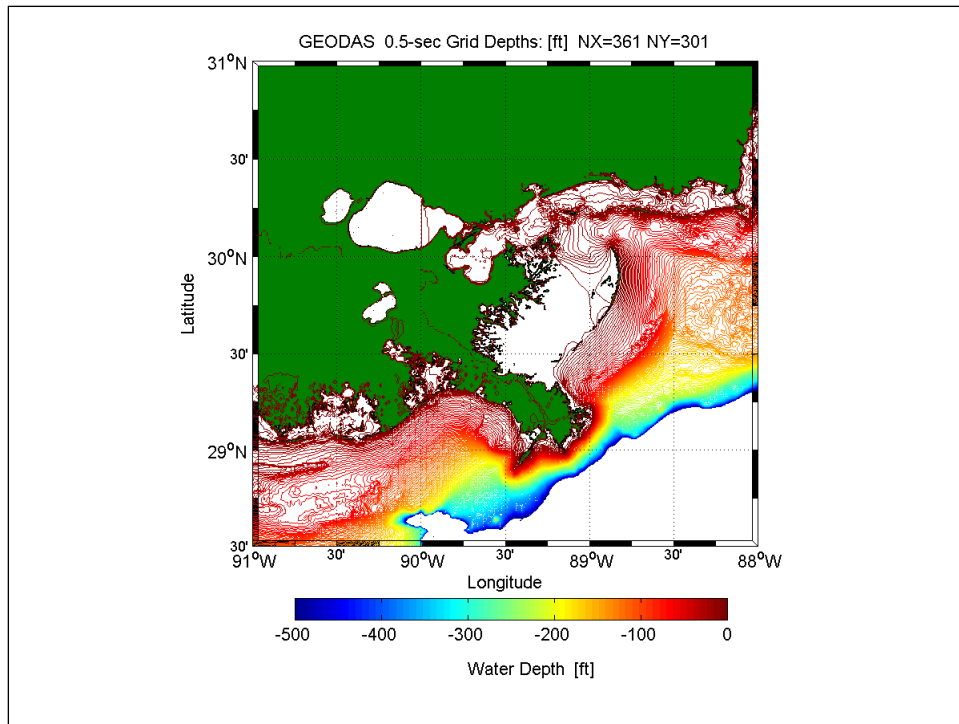


Figure V-13. Regional wave modeling domain and bathymetry

The WAVEWATCH III model was also applied; it is another commonly used model for ocean-scale wave generation and it is the standard model used by NOAA. Wind input for all wave modeling was done using the wind fields described previously based on the H*Wind/IOKA process. The model-to-model comparisons also shed light on uncertainty inherent in the model results.

For the model-to-model comparisons, done for Katrina only, WAM produced slightly better results than WAVEWATCH III at all NDBC buoy locations, particularly in the vicinity of NDBC buoy 42007. Many more details regarding the model-to-model comparisons, using a wide range of statistical error measures, are provided in the Wave and Storm Surge Analysis Technical Appendix.

Figure V-14 illustrates the complexities of the wave field generated by Hurricane Katrina. The figure shows the maximum significant wave height computed at each point in the regional modeling domain, at any time during the simulation. The regional-scale simulation is 12 hr in duration, starting on 29 August 0600 UTC and ending at 29 August 1800 UTC. The overall maximum significant wave height occurs at 89.1417W 28.966N with a value of approximately 53 ft. These wave conditions are extreme. It is important to note that while Katrina was a Category 5 storm prior to landfall, it generated wave conditions that are characteristic of a storm at that intensity. Those large waves propagated outwards from the storm and impacted coastal Louisiana and Mississippi.

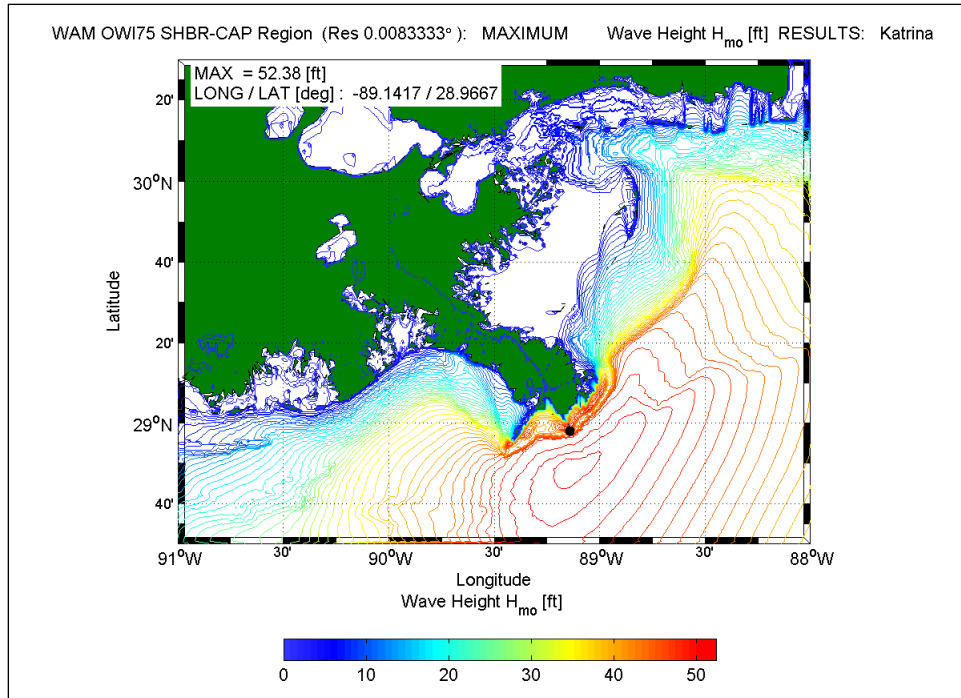


Figure V-14. Color contour of the maximum wave height conditions in the Region domain for the simulation period 2005082906 through 2005082918 UTC

Shallow water effects of shoaling and more importantly refraction focus the offshore energy towards the Mississippi River delta. When waves break due to their arrival in shallow water, wave energy decreases. In areas dominated by depth-induced breaking, significant wave heights are generally on the order of 60% of the local water depth. For example, a sea state in which the significant wave height is about 40 ft would begin to experience considerable depth-limiting breaking in about 65 feet of water. This tendency is evident in the dramatic decrease in wave height along the Mississippi River Delta. It is also apparent along the southeastern Louisiana barrier island chain where considerable energy dissipation takes place well seaward of the barrier islands due to depth-induced breaking. The pattern of wave height maxima follow the bathymetry pattern closely (compare Figures V-13 and V-14), an indication of depth limited breaking effects. Offshore, deeper-water wave conditions along the southeastern Louisiana coast are computed to be 35 ft in the northern areas, increasing to approximately 50 ft adjacent to the Mississippi River delta.

The WAM simulation assumes constant water depths, i.e., no changes due to storm surge. Therefore WAM results landward of the barrier islands indicated in Figure V-14 will be lower compared to expected results when storm surge effects on water depth (increases) are considered. The nearshore wave modeling considers this effect.

The maximum mean wave period results for the regional WAM simulation are shown in Figure V-15. This figure illustrates the diverging wave climate east and west of Hurricane Katrina's path. To the west, the mean wave period is

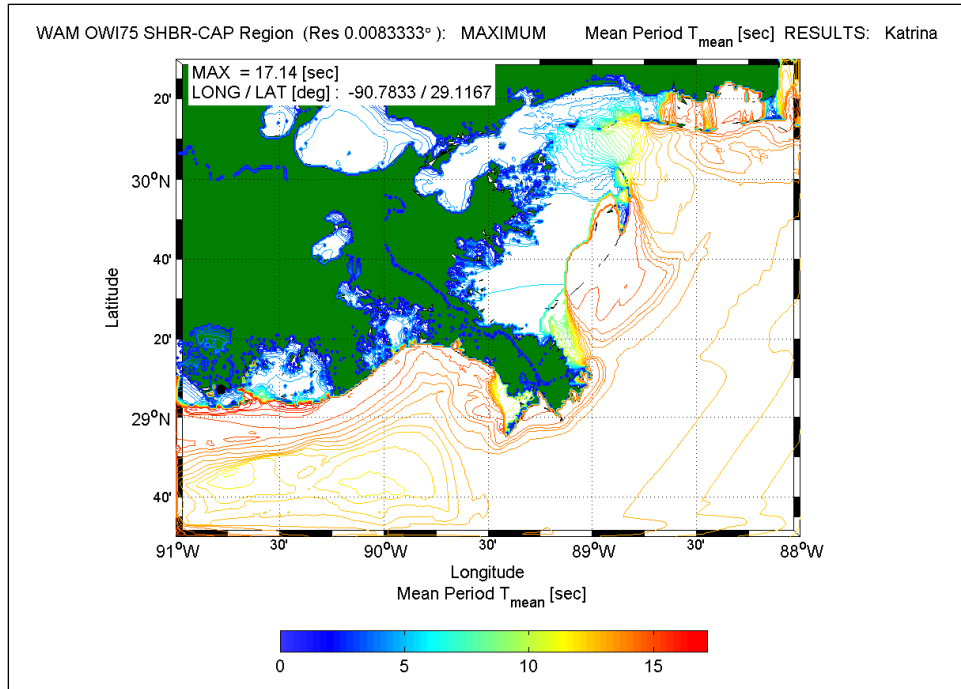


Figure V-15. Color contour of the maximum mean wave period conditions in the region domain for the simulation period 2005082906 through 2005082918 UTC

dominated by swells, having periods ranging from 12 to more than 15 sec; whereas, in the front right hand quadrant of Katrina, local wind seas abound with limited, yet distinct long period swell lobes. Long-period swells are present, but considerable energy is also present at higher frequencies. Shadow zones in wave period appear (lower T_{mean} values) also are evident in the lee of capes or islands. Also evident are zones of large mean period values landward of island gaps (around Horn and Dauphin Islands along the Mississippi coast) in the eastern portion of the Mississippi Sound.

Comparisons of wave model results with measurements are an important facet of the work. A few of those comparisons are presented below. A much more detailed description of the offshore wave modeling work, additional model-to-measurement comparisons, and much more information on the model-to-model comparisons are presented in the Wave and Storm Surge Analysis Technical Appendix.

Comparisons of WAM results to measurements made at NOAA NDBC Buoys 42040 and 42007 are shown here. Of all the buoys for which data are available, these two are in locations that best reflect the wave climate that southeastern Louisiana was subjected to during the storm. Buoy locations are shown in Figure V-12. Comparisons for Buoy 42040 are shown in Figure V-16 and comparisons for Buoy 42007 are shown in Figure V-17. Each figure shows a comparison for energy-based significant wave height, peak and mean spectral wave periods, mean wave direction, wind speed, and wind direction.

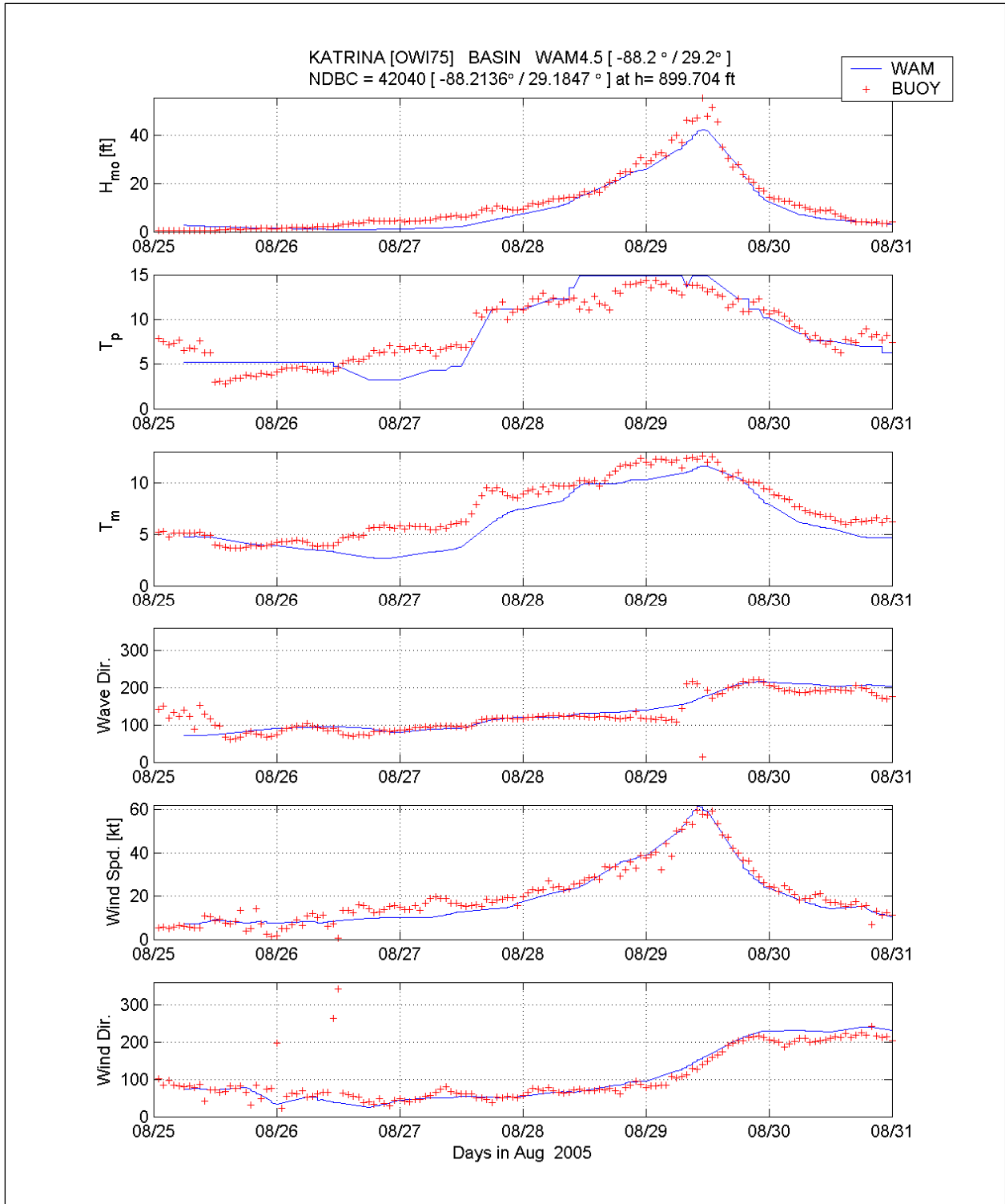


Figure V-16. Comparison of WAM Cycle 4.5 basin-scale (blue line) to the measurements at NDBC 42040

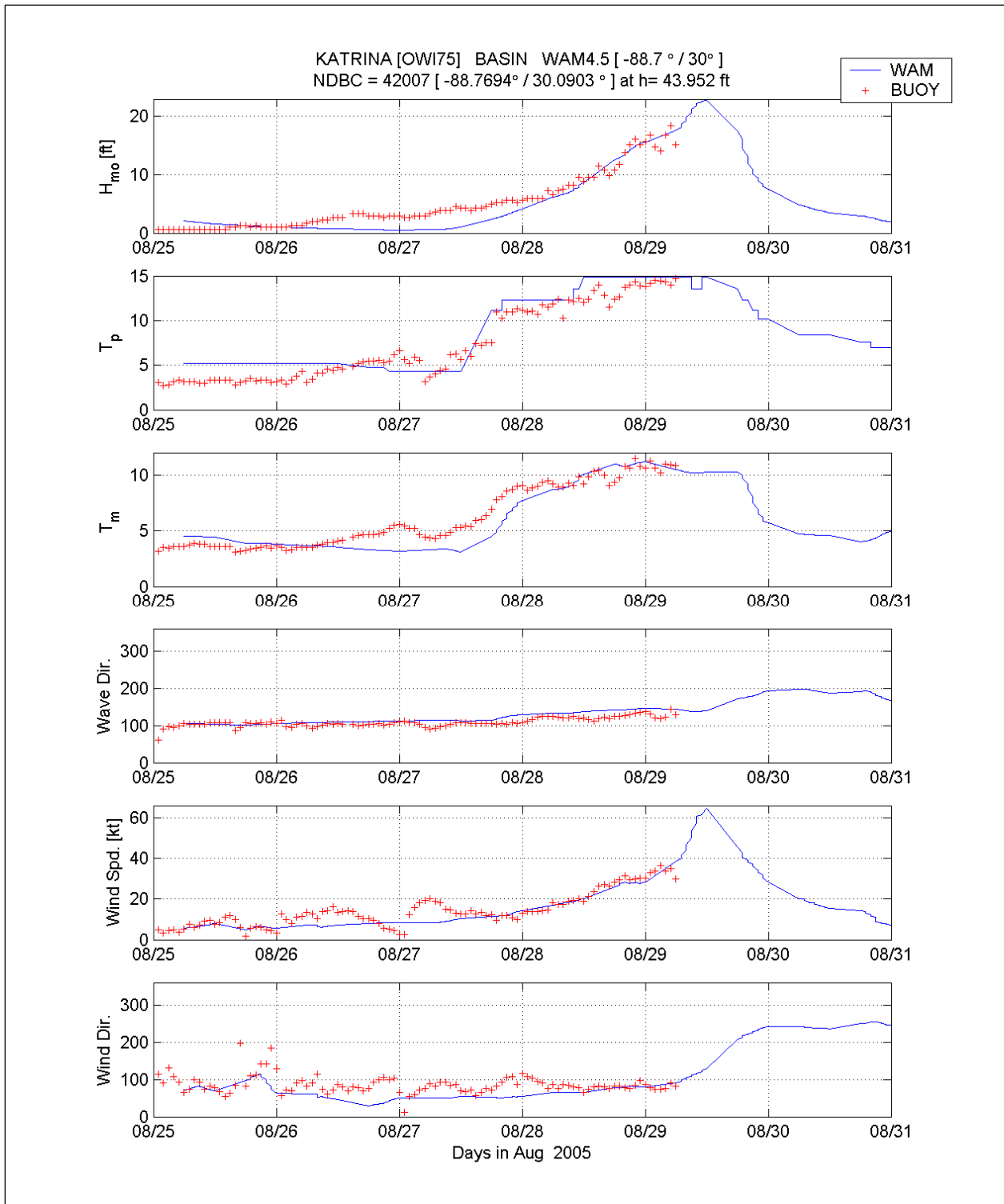


Figure V-17. Comparison of WAM Cycle 4.5 basin-scale (blue line) to the measurements at NDBC 42007

The maximum height measured at 42040 is approximately 55 ft, which is believed to be the largest significant wave height ever recorded by an NDBC buoy. Measured peak wave periods are between 13 and 15 sec near the storm peak. The maximum computed significant wave height is about 42 ft, and the computed peak periods at this time are 15 sec. At this point, it is unclear how the final winds will influence these results, but there are indications that the preliminary wind fields are low during some of the most intense stages of the storm. Computed wave directions agree reasonably well with measured wave directions.

The final comparison is made to the most landward buoy, located in the shallowest water depth in the NDBC Gulf of Mexico array. Buoy 42007 is located just west of the northern tip of the Chandeleur Island chain in a water depth of 44 ft. It is unfortunate though that this buoy did not survive Katrina and as evidenced by the wave record; it failed well before the storm peak. During the growth stage of the storm, measurements indicate a methodical, slowly increasing wave height that is dominated by wind-seas (characterized by short periods on the order of 5 sec) until 27 August 1800 UTC where there is a dramatic shift in T_p , an indication of the early arriving swell energy that reaches southeastern Louisiana well before (2 days) arrival of the intense core of the storm. The downshifting in frequency (or increasing T_p) continues, with the increase in wave energy until failure of the buoy. Approaching the time of failure, there is only a modest change in the vector mean wave direction, changing by at most 30 deg. This should not be surprising because to the south, west, and north there is considerable sheltering due to the influence of land features. Thus there is a very small window available to receive wave energy at this location. Prior to 28 August, wave heights are under-predicted. After 28 August, model results agree reasonably well with measurements. The maximum computed significant wave height at this location is approximately 23 ft, with peak wave periods of 15 sec. Computed wave directions agree well with measured directions. It is clear that the hurricane has spawned energetic long-period swells which propagate into the region.

The primary purpose of the offshore wave modeling task is to provide boundary condition information to the nearshore wave modeling effort (all the nearshore domains). An example of the directional wave spectrum provided as a boundary condition to the nearshore wave modeling is shown in Figure V-18. The spectrum reflects the directional distribution of the incident wave energy as a function of wave frequency (frequency is inversely related to wave period). In Figure V-18, the red vector indicates a mean wave direction, here showing waves approaching from the southeast. The colored area indicates the spectral region encompassing all wave frequencies and directions that are present in the sea state at this location. The red colors indicate the frequency-direction characteristics that contain the highest energy levels (the integrated energy-based significant wave height is almost 13 ft).

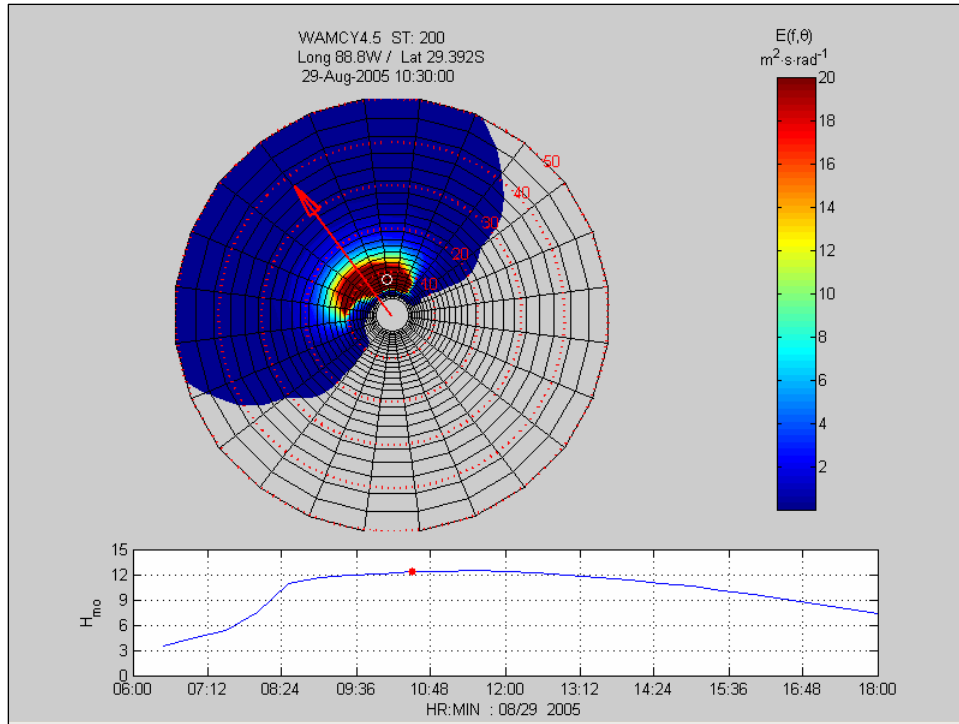


Figure V-18. Example of the directional wave spectra color contoured in the upper panel and the significant wave height trace in the lower panel (note units are in CGS system)

Nearshore Waves

The STWAVE model (Smith, Sherlock, and Resio 2001) was adopted for the nearshore wave transformation modeling; it is the standard model used by the Corps of Engineers to simulate nearshore wave transformation. All “production” runs and results presented in this report were made with STWAVE.

STWAVE was applied on three grids for the southern Louisiana area (Lake Pontchartrain, Louisiana Southeast, and Louisiana South). The input for each grid includes the bathymetry (interpolated from the storm surge model bathymetry), surge fields (interpolated from storm surge model output), and wind (the preliminary OWI/H*Wind wind fields). For the Pontchartrain and Louisiana South grids, the wind applied in STWAVE is constant over the entire domain and is taken from approximately the center of each grid. Spatially variable winds were simulated on the Louisiana Southeast grid, and STWAVE was run at 30-min intervals from 0630 to 1800 UTM on 29 August 2005 for the Southeast and South domains (matching the regional wave simulation that supplied input boundary conditions) and at 30-min intervals from 0000 on 29 August 2005 to 1200 on 30 August 2005 for the Pontchartrain domain.

A few modeling results are presented below for two of the three model domains, Lake Pontchartrain and Louisiana Southeast, where the greatest wave action occurred along the hurricane protection system. The Wave and Storm Surge Analysis Technical Appendix describes the nearshore wave modeling

work in more detail, and it contains more results including those for the Louisiana South domain.

Lake Pontchartrain Grid. The first grid covers Lake Pontchartrain at a resolution of 656 ft (200 m) (north-south) by 656 ft (200 m) (east-west). The domain is approximately 15.5 by 24.9 miles (25 by 40 km). Lake Pontchartrain is run with the full-plane STWAVE to include generation and transformation along the entire lake shoreline. The full-plane version of the model considers wave growth, propagation, and transformation for the complete 360-degree plane. The grid parameters are given in Table V-3. Figure V-19 shows the bathymetry for the Lake Pontchartrain Grid relative to NGVD 29. Brown areas in the bathymetry plots indicate land areas at 0 ft relative to the datum.

Lake Pontchartrain Results. The peak wave conditions on the south shore of Lake Pontchartrain occur at approximately 1400 UTC on 29 August 2005 (9:00 a.m. CDT). The wind at this time is 59.5 knots (30.6 m/sec) approximately from the north. Figure V-20 shows the maximum significant wave height for the entire simulation period for each grid cell within the domain. The wave direction that corresponds to the time of maximum wave height is also shown. The maximum wave height is 9.5 ft with a peak wave period of approximately 7 sec. The maximum wave heights range from 8.5 to 9.5 ft on the New Orleans vicinity lakefront and the associated peak periods are approximately 7 sec.

Table V-3 STWAVE Grid Specifications								
Grid	State Plane	X origin ft	Y origin ft	Δx ft	Δy ft	Orient Deg	X cells	Y cells
Lake Pontchartrain	LA South	3563779.5	690485.6	656	656	270	208	337
Louisiana Southeast	LA Offshore	4294586.6	1639491.5	656	656	141	683	744
Louisiana South	LA Offshore	3997126.0	1264895.0	656	656	108	664	839

At the entrance to the 17th Street Canal, the maximum significant wave height was computed to be 8.7 ft; and the peak period at that time was 6.7 sec. At the time of maximum wave conditions, waves were approaching from directions just to the west of north. At the entrances to Orleans Avenue and London Avenue Canals, peak significant wave heights and corresponding peak periods were 8.8 ft and 6.7 sec peak period, and 9.1 ft and 6.7 sec, respectively. Peak waves approached from just west of north at both sites. The maximum computed wave heights along Orleans East (east of IHNC) were 8.8 ft and corresponding peak periods were 6.7 seconds. The peak waves approached from the northwest.

Three small wave buoys were deployed by the U.S. Army Engineers, New Orleans District, in Lake Pontchartrain on 27 August 2005 to capture wave conditions during the storm. Two of those gauges were recovered and provide valuable comparison data. The deployment locations were 30 deg 2.053' North, 90 deg 7.358' West for Gauge 22 and 30 deg 1.989' North, 90 deg 7.932' West

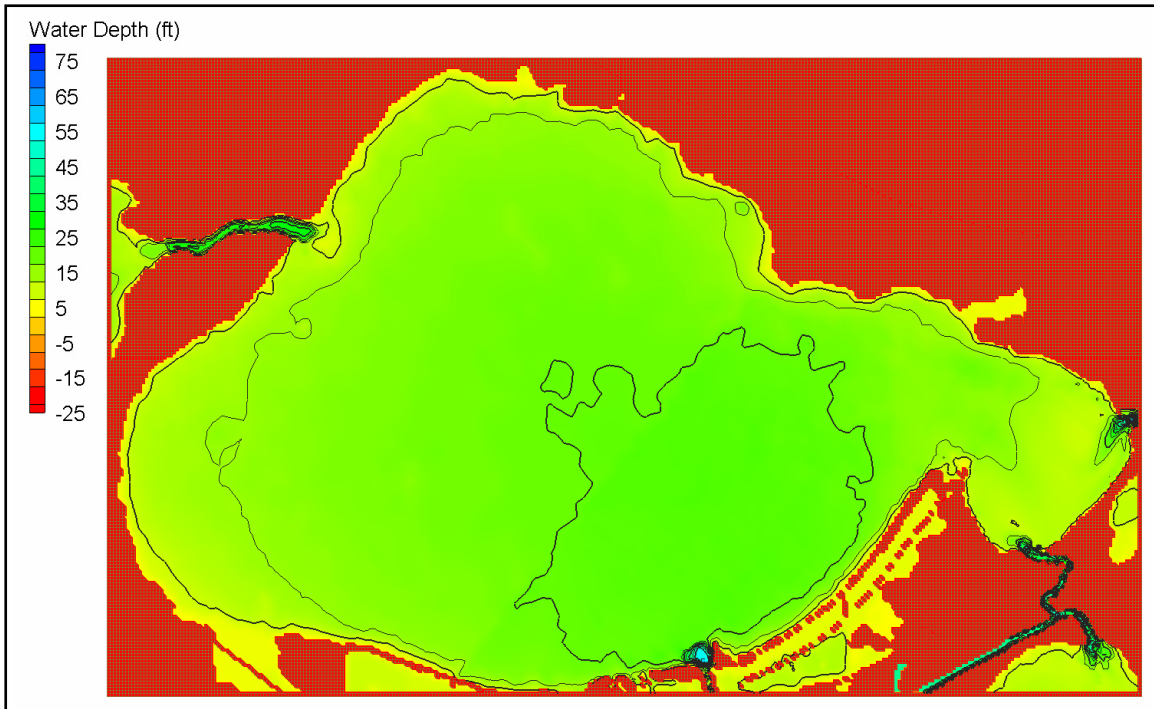


Figure V-19. Lake Pontchartrain bathymetry grid (depths in feet, NGVD 29)

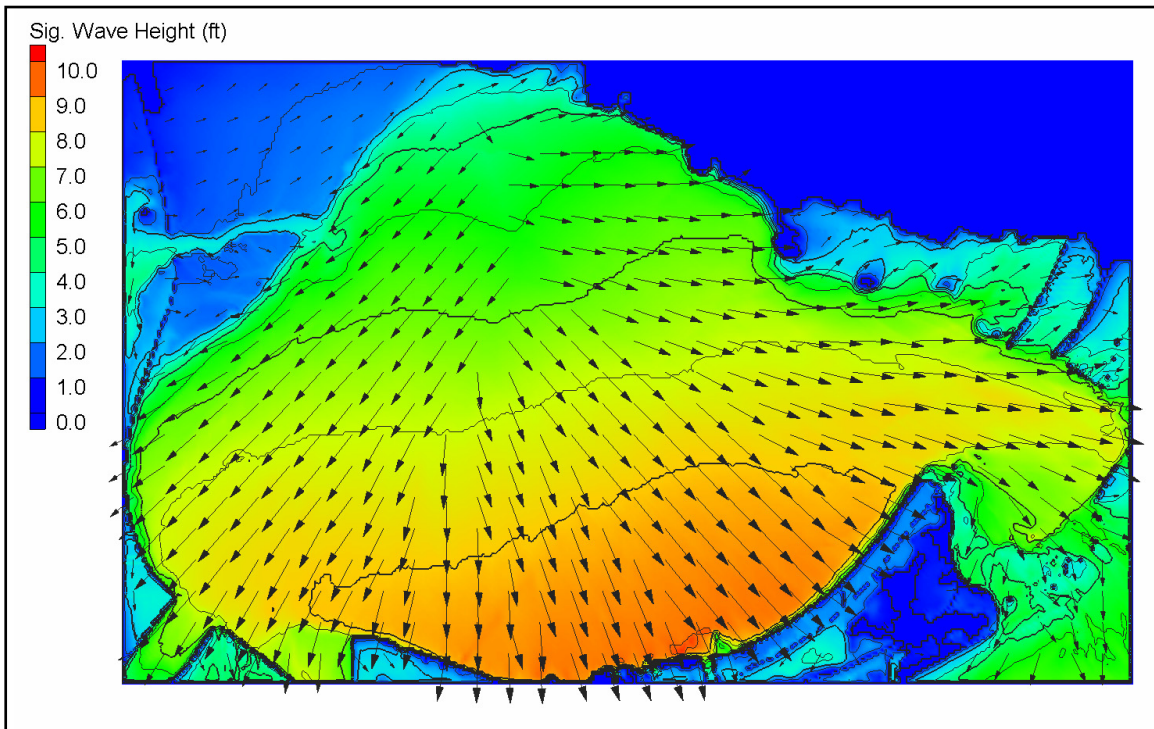


Figure V-20. Lake Pontchartrain maximum modeled significant wave height and corresponding mean direction for 0000 UTC on 29 August to 1200 UTC on 30 August 2005 (wave heights in feet)

for Gauge 23. Gauge 22 was directly north of the 17th Street Canal entrance and Gauge 23 was west of Gauge 22. Both gauges were in approximately 13-ft (4-m) water depth. The sampling records were a relatively short 8.5 min, so there is a lot scatter in the data. Also, at the peak of the storm, the wave heights drop from approximately 8 of 9 ft to 5 ft. The developer of the bouys has examined the data and concurs with our assessment that the data appear to be inaccurate near the peak; the buoy appears to have tilted to an extreme value under the action of the most extreme winds near the peak.

Figures V-21 and V-22 show comparisons of significant wave height and peak spectral wave period for the buoy locations, respectively. The symbols without lines are the 8.5-min measured wave parameters; the blue lines are the measurements with the spectra averaged over 3 records (25.5 min), and the red lines are the modeled parameters (30-min average). The STWAVE results are essentially the same for the two gauge sites. The modeled wave heights are approximately 1 to 2 ft lower than the measurements in the building part of the storm (0630-1200 UTC) and very similar to the measurements in the waning part of the storm (1500-1800 UTC). The measurements at the peak are not reliable. The modeled peak periods are consistent with the measurements, from 0.0 to about 0.5 sec low in the building stage and just prior to the peak,, and 0.5 to 1.5 sec low in the waning stages of the storm.

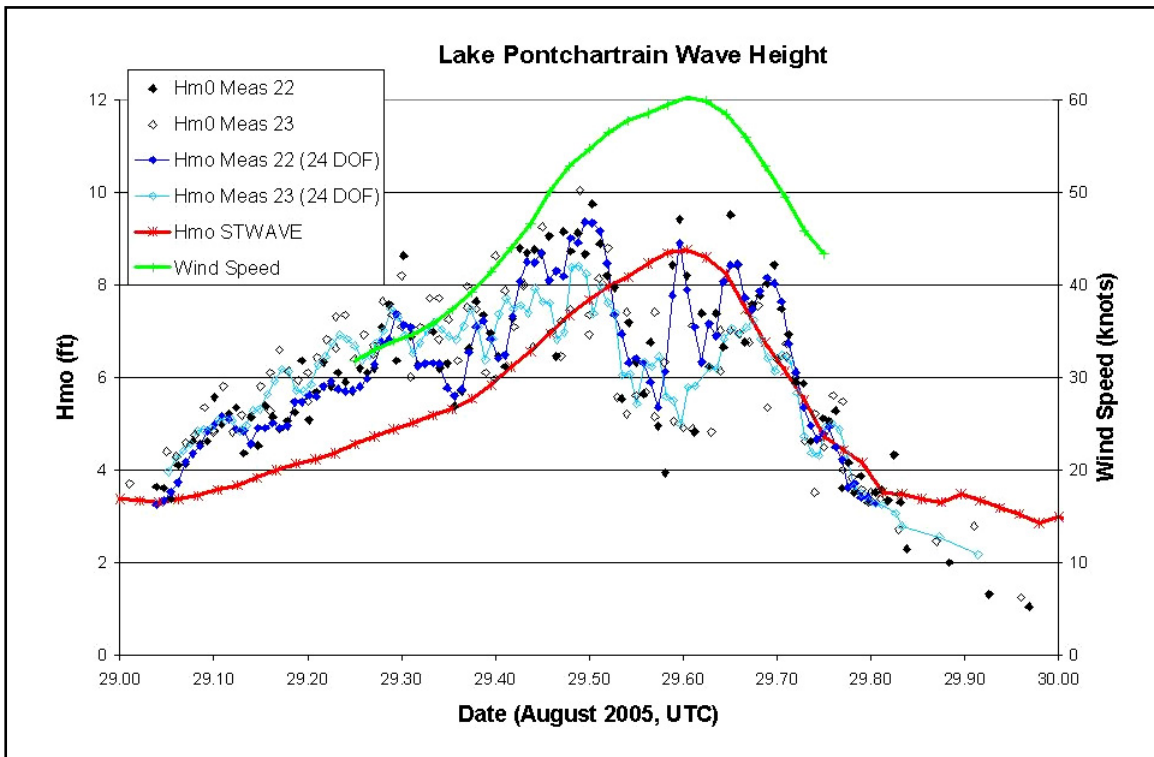


Figure V-21. Lake Pontchartrain measured and modeled significant wave height

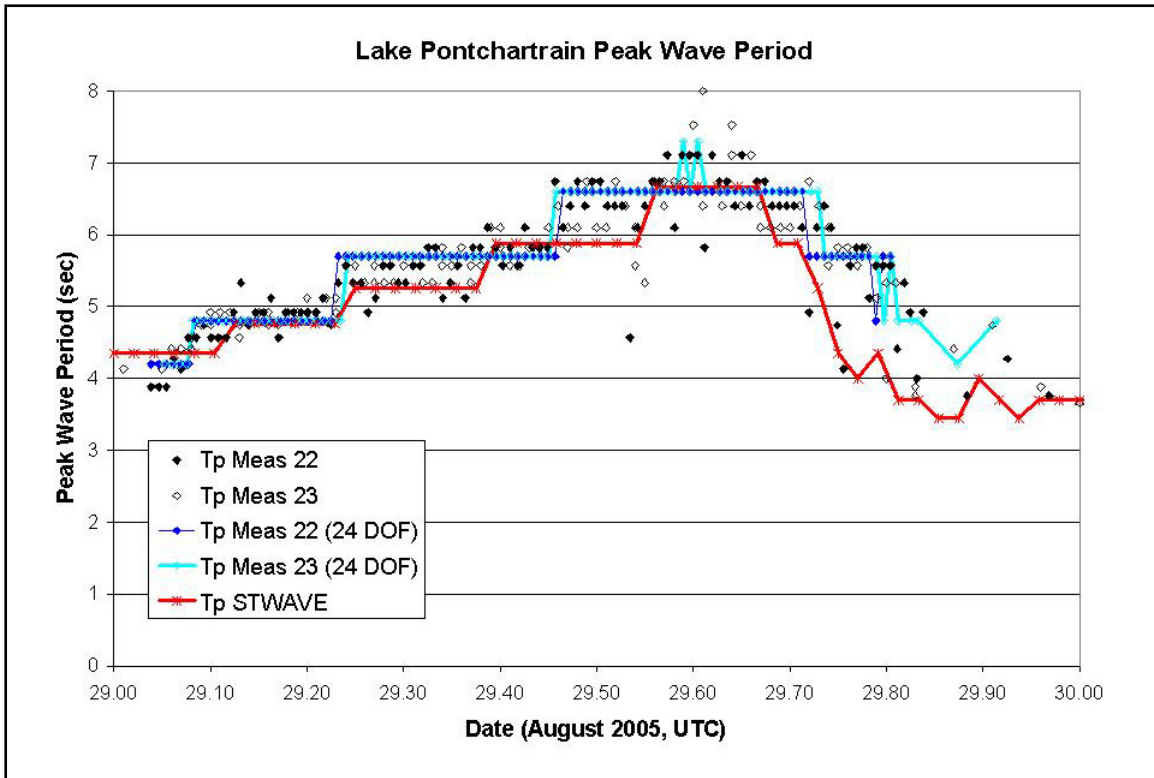


Figure V-22. Lake Pontchartrain measured and modeled peak wave period

STWAVE is a steady-state wave model, which means that the waves reach equilibrium with the local forcing conditions (wind, surge, and boundary waves). Thus, the STWAVE modeling assumes that the winds and surge vary slowly enough for the waves to reach quasi steady state. For Hurricane Katrina, the winds are time varying and the grid domains are relatively large, so the time-dependent SWAN model (Booij, Ris, and Holthuijsen 1999; Booij et al. 2004) was used to evaluate the importance of time variation. Lake Pontchartrain was chosen for this test because the waves are all locally generated and time dependence is expected to have the greatest impact there. Measured data in Lake Pontchartrain (the only available data) enable comparisons between model results obtained using the steady/unsteady approximations and measurements, and assessment of model-to-model differences in light of model-to-measurement differences.

To test the importance of time dependence, SWAN was run in both steady-state and time-dependent modes for 29 August 2005 from 0630 to 1800 UTC. The comparison was made using 1-min time steps for the time-dependent run and forcing the steady-state run to an accuracy of 99 percent with a maximum of 15 iterations (this is a more stringent iteration parameter selection than the default values). All other SWAN model defaults were used. The time-dependent simulation requires about 2.5 hours of simulation time to ramp up (0630-0900), but following this time, the differences in wave height along the southern New Orleans lakeshore are less than 2 percent (average difference is 0.2 percent), with the steady-state simulation giving slightly higher wave heights. The average

directional difference is less than 3 deg and the periods are essentially the same. Based on these results, time dependence is not a concern in the hurricane simulations in the nearshore domains, and steady-state simulations will be used for the 95% solution (final results). Run times are significantly reduced for steady-state compared to time-dependent simulations.

STWAVE wave heights are an average of 2 percent higher than SWAN results. STWAVE wave heights are higher at the peak of the storm and lower height on the building and waning legs of the storm, compared to SWAN results. The computed peak significant wave height using SWAN was 7.7 ft, about 1 ft less than the peak value computed using STWAVE (8.7 ft). The measurements are not reliable at the peak of the storm, when the wave heights are most critical. Just prior to the point in time the measurements appeared to become suspect (decreasing heights despite increasing winds), the maximum wave heights measured at the two buoy locations were 8.4 and 9.4 ft. SWAN results are closer to the measurements on the building portion of the storm and STWAVE results are closer on the waning portion of the storm.

STWAVE peak periods are 9 percent longer than the SWAN peak periods on average. STWAVE shows better agreement with the wave period measurements, but both models are generally within 1 sec of each other. The maximum peak period computed with SWAN was 5.7 sec, about 1 sec less than the maximum computed with STWAVE (6.7 sec). The measurements suggest maximum peak periods of 6.7 to 7.3 sec.

In general, overall, STWAVE produced slightly better results. SWAN predicted a broader wave event, i.e. wave height and period results more slowly varying with time, than did STWAVE. Figures showing results from these comparisons are provided in the Wave and Storm Surge Analysis Technical Appendix.

Louisiana Southeast Grid. The second grid covers the coastal area southeast and south of New Orleans at a resolution of 656 ft (200 m). The domain for the southeast grid is approximately 84.9 by 92.4 miles (136.6 by 148.8 km) and extends from Mississippi Sound in the northeast to the Mississippi River in the southwest. The southeast grid was run with the half-plane version of STWAVE for computational efficiency. The grid parameters are given in Table V-3. Figure V-23 shows bathymetry for the southeast grid.

Louisiana Southeast Results. The peak wave conditions on the southeast grid occur between approximately 1100 and 1200 UTC on 29 August 2005. The highest waves along the Mississippi River levees occur around 1100 UTC (6:00 a.m. CDT) and along the Lake Borgne shoreline around 1200 UTC (7:00 a.m. CDT). Figure V-24 shows the maximum significant wave height and corresponding mean wave direction for the entire simulation period for each grid cell within the domain. Figure V-25 shows the peak wave period field that corresponds to the time of maximum significant wave height.

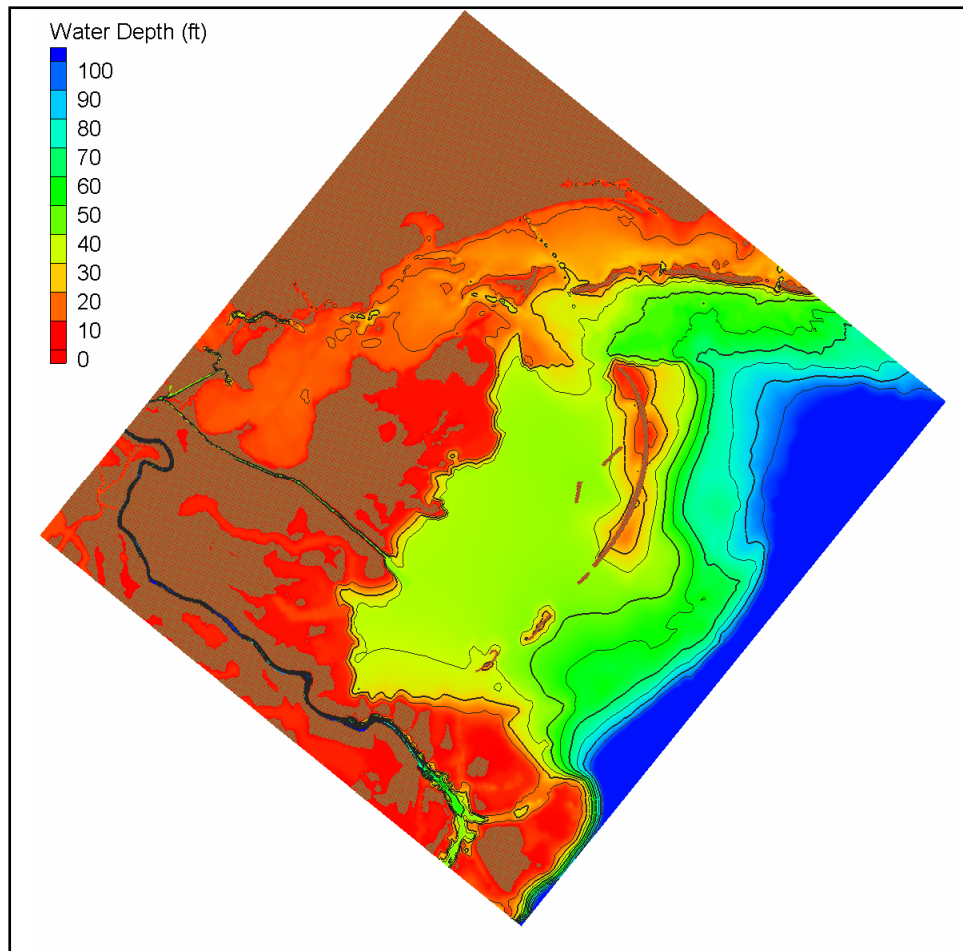


Figure V-23. Louisiana Southeast bathymetry grid (depths in feet, NGVD 29)

The maximum significant wave heights range from 6 to 10 ft along the levee system and the associated peak periods are 7-16 sec. The longer wave periods originate from wave energy traveling between the islands from the Gulf of Mexico. Larger wave heights occur in lower Plaquemines Parish (7-10 ft) and smaller heights in upper Plaquemines and St. Bernard Parishes (5-6 ft). The peak periods are relatively large (up to 16 sec) because of wave penetration through gaps between the barrier islands.

Along the back levee of Orleans Parish, adjacent to the GIWW, maximum computed significant wave heights and peak periods were 5.2 ft and 16.3 sec, respectively. Peak waves approached from the southeast. Along the St. Bernard Parish hurricane protection levee adjacent to the MRGO, with an eastern exposure, peak wave heights and periods were approximately 4.9 to 5.2 ft and 16.3 sec. At the time of peak wave conditions, waves approached from the southeast, rather obliquely, relative to the levee system. Along the portion of the St. Bernard Parish hurricane protection levee with a southern exposure, peak wave heights were less, about 2.3 ft and peak periods were quite long, 18.0 sec. Here, waves approached from the south at their peak conditions.

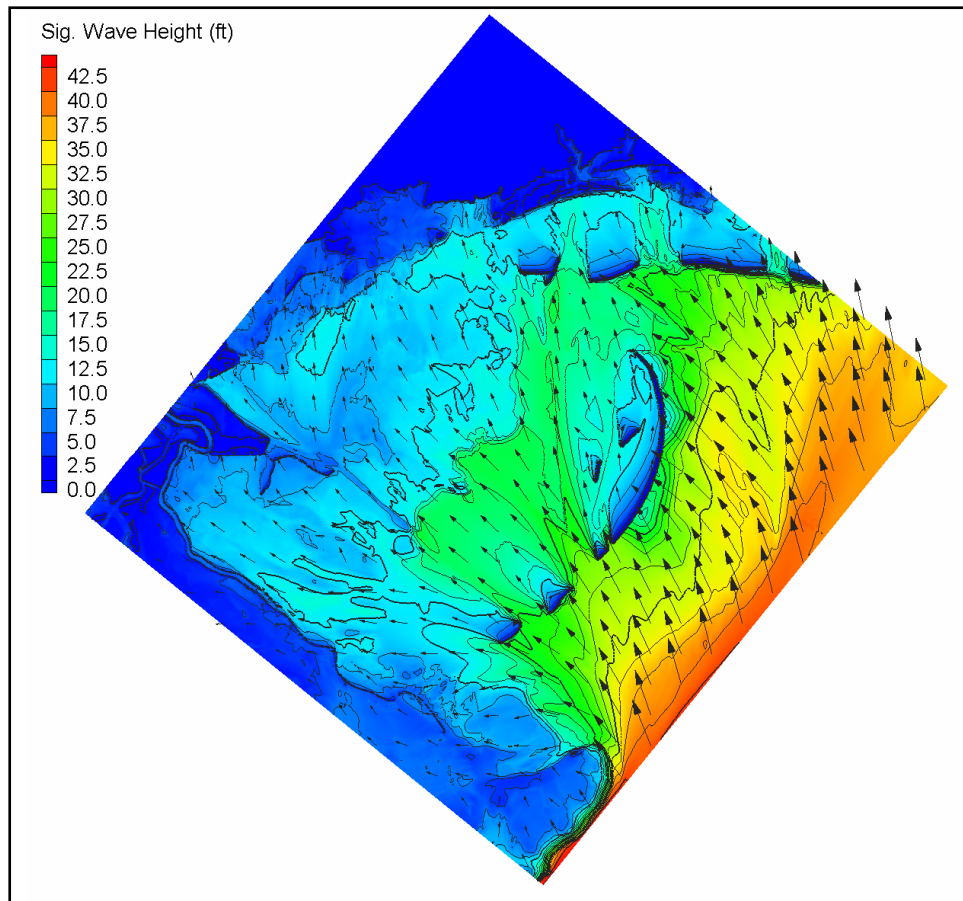


Figure V-24. Maximum significant wave heights, and corresponding mean wave directions, for the Louisiana Southeast domain, for time period 0630 to 1800 UTC on 29 August 2005 (wave heights in feet)

In southern Plaquemines Parish, along east-facing levees of the hurricane protection system on the east side of the Mississippi River, maximum significant wave heights ranged from approximately 7.4 to 9.4 ft, and the associated peak periods were 13.5 sec. The longer wave periods originate from wave energy traveling between the barrier islands from the Gulf of Mexico. In the southernmost portion of Plaquemines Parish, south of Tropical Bend maximum wave heights were 7.2 to 8.0 ft, with periods ranging from 13.5 to 14.9 sec.

Information pertaining to nearshore wave modeling for the Louisiana South domain and information for the levees on the west side of the Mississippi River, is contained in the Wave and Storm Surge Analysis Technical Appendix. Later in this chapter, additional information is presented that compares current best estimates of peak wave conditions with those used in the design of the hurricane protection projects.

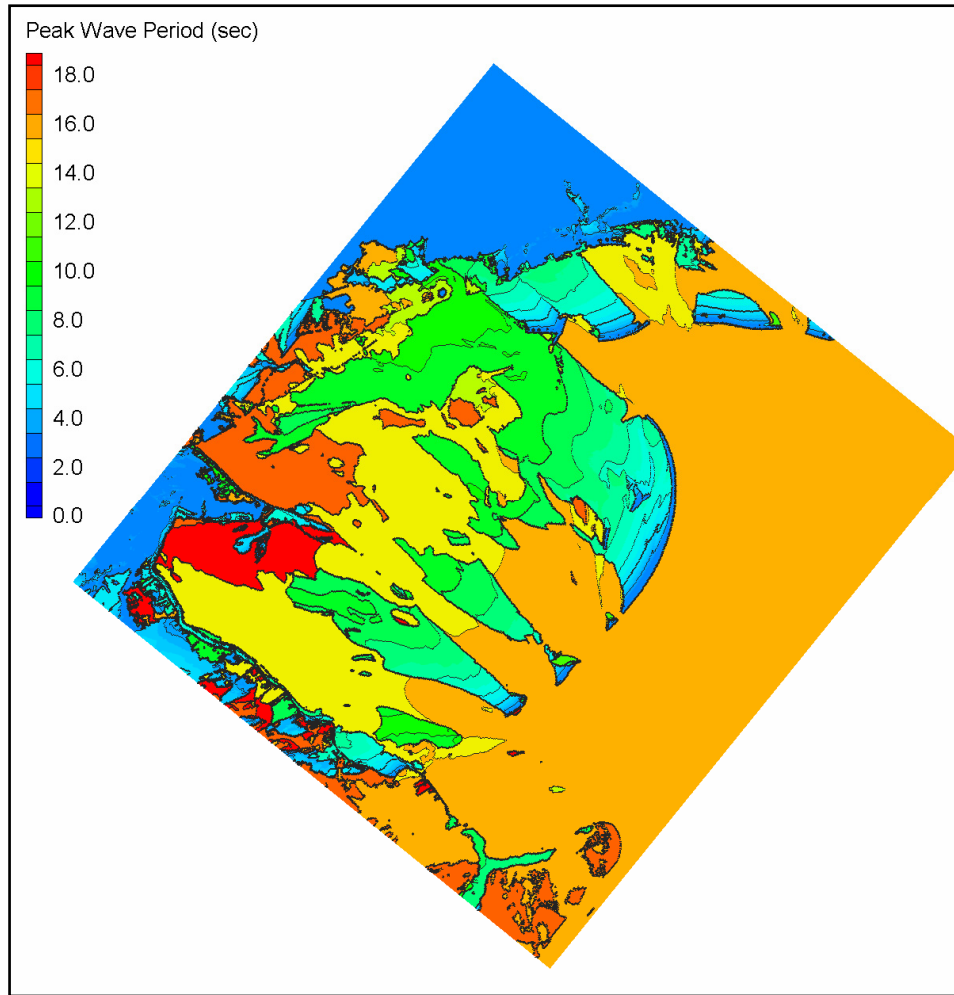


Figure V-25. Southeast Louisiana modeled peak wave period corresponding to the maximum wave height for 0630 to 1800 UTC on 29 August 2005 (periods in sec)

Regional Water Levels Approach

A combination of measurements and numerical modeling using the ADCIRC model was used to develop information with which to characterize the temporal variation of water level and local water level maxima associated with Hurricane Katrina. Development of the ADCIRC model of southeastern coastal Louisiana (Westerink et al. 2005, Feyen et al. 2005) has been underway for several years. The term water level as used in this chapter describes the more slowly varying water surface (variations that occur on the time scales typically associated with the astronomical tide or storm surge, changes of tenths or whole feet per hour). Contributors to water level that are considered in the current modeling are tide, wind and atmospheric-pressure drive storm surge, and water discharge within the Mississippi River. Precipitation and other water inflows are not included.

Variations on these time scales are contrasted with the much more rapidly varying water surface associated with shorter-period wind wave action (oscillatory motions in which the water surface can vary on the order of feet at times scales of up to tens of seconds. Wind waves were discussed in the previous sections.

Measured water level hydrographs are the most reliable source of data for capturing both the temporal variation and the maximum. Water level fluctuations were measured during the build-up stage of the storm at a number of sites throughout the study region; however, few operated throughout the storm. Most failed prior to the peak. Consequently, while there is little measured data that captures both the temporal variation of water level prior to, during, and after the peak conditions and the maximum condition. In a few cases, photographs and other visual images were utilized to provide information about the temporal variation of water level.

An extensive post-storm effort was undertaken to identify and survey high water marks following passage of the storm. While certain high water marks capture the peak water levels well, they contain no information about the temporal variation of water level. High water marks also have their own inherent issues of quality, uncertainty whether they in fact do reflect a peak condition, and whether or not water surface motions due to short wind waves or other factors are reflected in a high water mark.

Water level measurements are able to provide temporal variation and maxima information at only a subset of the locations of interest. Many of the high water marks are of questionable quality. Storm surge modeling was used to complement quality water level measurements where they existed and provide water level information in the many locations where measurements were not available or were of questionable quality. Hydrograph data and the highest quality high water marks also are used to evaluate the accuracy of the storm surge model. As is the case for the wave modeling, model-to-measurement comparisons provide valuable information for quantifying the uncertainty in model predictions.

Hydrograph and High Water Mark Analysis

High Water Marks. The passage of hurricanes results in short-period wind waves on top of the much longer-period storm surge that creates significant entrainment of various types of debris including vegetation, seeds, dirt, man-made trash, and dislodged building material. Depending on local conditions, the entrained debris will deposit on or adhere to some surfaces once the peak stage has been reached and the stages begin to fall. The deposited debris leaves what is referred to as a high water mark (HWM) and the mark is used to quantify the magnitude of peak storm surge. The highest quality marks for estimating storm surge are those that have little or no wave effect (i.e., no influence of wave crests or wave run-up). Some HWMs are collected where significant wave effects are present but that effect is noted.

The HWM data were collected during September through November, 2005. Various organizations participated in the collection of the data including the U.S. Army Corps of Engineers' (USACE) U.S. Army Engineer Research and Development Center (ERDC), the U.S. Army Engineer District, New Orleans (CEMVN), Louisiana State University (LSU), the U.S. Geological Survey (USGS), Levee Districts in the New Orleans area, and the Federal Emergency Management Agency (FEMA).

The HWM and hydrograph data presented are mostly referenced to the latest epoch of NAVD88, 2004.65. Most of the data have been converted to this datum, but a few have not. The datum issue is a significant one. In the vicinity of the Inner Harbor Navigation Channel (IHNC) westward to the vicinity of the 17th Street Canal, the benchmarks complying with 2004.65 result in elevations that are about 0.5 to 0.6 ft lower than elevations derived from benchmarks based on the previous NAVD 88 epoch.

The high water mark data presented herein are rated as excellent, good, and fair/poor, depending on the degree to which the mark is a reliable indicator of the water level, absent wave crest effects or wave run-up effects. Marks rated excellent were those acquired in the interior of buildings, where short wave effects were considered to be absent or minimal. Good marks were typically associated with exterior marks that were consistent with excellent marks measured nearby, or where by the nature of the physical setting for the mark, little to no influence of wind wave action was expected. Excellent water marks were primarily used to characterize local water level maxima, unless no excellent marks were available in an area of interest. In that case marks rated as good were used. Use of fair or poor marks to estimate maximum water level was avoided if at all possible. Both excellent and good marks were used in the comparison with ADCIRC model results.

Along the south Lake Pontchartrain shoreline, at the entrance to the 17th Street Canal, thirteen high water marks rated as "excellent" marks were averaged, and the resultant high water was computed to be 10.8 ft NAVD 88 (2004.65). At the entrance to Orleans Avenue Canal, a single high water mark was available, which was not of high quality. Its value was 10.8 ft NAVD88 (2004.65), the same as the value at the entrance to 17th Street Canal, and similar to the value from London Avenue Canal, so it is considered to be a reliable mark. There were two marks rated as "good" collected at the entrance to London Avenue Canal, and a number of other marks rated to be of lesser quality. The average of the two "good" marks was 10.7 ft NAVD88 (2004.65). Several other marks in the area showed elevations similar to this elevation, so the average of the two marks was considered to be reliable. At the entrance to the Inner Harbor Navigation Canal (IHNC) there were five marks rated "excellent", three to the west side of the entrance and two to the east side at Lakefront Airport. The average of all the five excellent marks was 11.7 ft NAVD88 (2004.65).

Measured high water marks varied considerably within the following series of canals/channels in Orleans and St. Bernard Parishes: the north-south running IHNC that extends from its Lake Pontchartrain entrance to the lock connecting the IHNC to the Mississippi River (the IHNC Lock), and the east-west running

canal which serves as the combined Gulf Intracoastal Waterway (GIWW) and Mississippi River Gulf Outlet (MRGO).

At the Lake Pontchartrain entrance to the IHNC, the peak water level was 11.7 ft NAVD88 (2004.65). To the south of the entrance, in the IHNC, an excellent mark north of the Danzinger Bridge indicated 12.4 ft NAVD88 (2004.65), and an average of two excellent marks immediately adjacent to the Bridge on its north side indicated a peak water level of 12.7 ft NAVD88 (2004.65). Further to the south, just to the south of the confluence of IHNC with GIWW/MRGO, two excellent high water marks indicated 15.2 ft NAVD88 (2004.65). At the end of the IHNC, at the IHNC Lock, the maximum from a gage record was 14.3 ft NAVD88 (2004.65) and there were two excellent high water marks nearby that averaged 13.8 ft NAVD88 (2004.65).

In the 6-mile long GIWW/MRGO channel, an excellent high water mark indicated 16.3 ft NAVD88 at the Paris Road Bridge (not yet referenced to the recent NAVD88 epoch). At the point where the GIWW and MRGO diverge (adjacent to Lake Borgne), at Bayou Beinvenue flood control structure, an excellent mark indicated peak water level of 18.4 ft NAVD88. At the influence of the GIWW/MRGO with the IHNC the peak water level was 15.2 ft NAVD88 (2004.65). The gradient in peak water level (increasing level from Lake Pontchartrain to Lake Borgne) reflects the hydraulic connectivity between Lake Borgne and Lake Pontchartrain via these channels.

The Wave and Storm Surge Analysis Technical Appendix contains much more information concerning the high water marks, including a series of images that show locations where the marks were left. Placement of the marks on images was useful for understanding the setting in which the mark was left and potential for short wave influence. Figure V-26 is an example of a photograph with placed HWMs, for the entrance to the 17th St Canal. The high water mark data are also available in a series of spreadsheets that contain pertinent information regarding each HWM as well as a quality assessment made by the IPET hydrograph and high water mark analysis team. The spreadsheets also indicate the datum for each mark. High water mark data are available for the Louisiana and Mississippi coasts.

Analysis and presentation of high water marks presented in this section focuses on those marks that reflect water level conditions along the outer periphery of the hurricane protection system, for use in analyses of the regional water level conditions. There are many high water marks in the interior areas that were flooded. These data are included in the spreadsheets.

Additional information is also provided later in this chapter that compares estimates of water level maxima to the maximum water level conditions considered in the design of the hurricane protection projects throughout the study region. The results presented there reflect our present best estimates of water level maxima using HWMs where excellent marks exist, maxima from measured hydrographs, or maxima determined from model results in the many locations where no measured data are available.



Figure V-26. High water marks on the west side of the entrance to the 17th Street Canal

Hydrographs. The hydrograph data come from various sources including gage data, staff readings, and surveys of water level position relative to physically identifiable objects that were captured in time tagged digital pictures. Data from the following sources are reflected in this report:

- a. USGS gages.
- b. USACE gages (acquired by the New Orleans District, CEMVN).
- c. NOAA NWS gages
- d. Levee District gages.
- e. Staff gage at the IHNC Lock.
- f. Digital photographs taken by an individual at the Municipal Yacht Club.
- g. Digital photographs taken by various individuals at the Lakefront Airport.

Gage data acquired in the IHNC are shown in Figure V-27 from the USGS gage at Interstate 10 (I-10), the Orleans Levee District gage at I-10, and the staff gage at IHNC Lock which was read by CEMVN lock personnel throughout the storm. The staff gage was set by lock personnel just prior to the storm without being surveyed to an established datum. Subsequent to the storm, the 15.0-ft

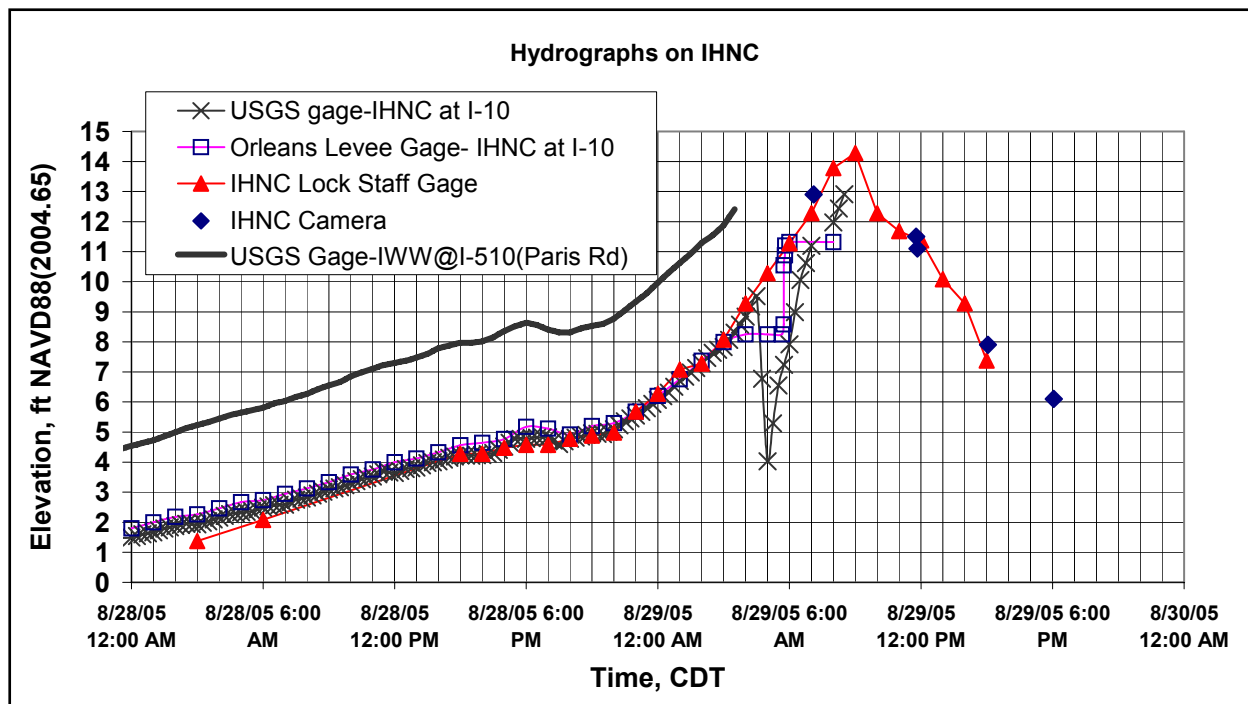


Figure V-27. Hydrographs on the Inner Harbor Navigation Canal (IHNC)

mark on the staff gage was surveyed and found to be at an elevation of 14.28 ft NAVD88 (2004.65). The staff gage readings in the IHNC log were corrected by the 0.72 ft difference and are plotted in the figure. The USGS and the Orleans Levee District gages are located near the railroad floodwall opening just south of I-10. The gate through the floodwall was damaged and sand bags were used to close the opening prior to the storm, based on conversation with a representative of the Orleans Levee District. Based on data from the USGS gage, the sand bags and/or one or both of the breaches on the west side of the IHNC appeared to have failed at approximately 0430 CDT (0930 UTC) on Monday, 29 August. The Orleans Levee District gage, while not showing the large drop, also shows a significant change in water level. The Paris Road gage on the Gulf Intracoastal Waterway/Mississippi River Gulf Outlet (GIWW/MRGO) is about 6 miles east of the intersection of the GIWW/MRGO and the IHNC. The USGS gage at Paris Road requires a datum adjustment to NAVD88 (2004.65), that has not been made yet.

Gages along Lake Pontchartrain were separated into those located west of 90 degrees longitude and those located east of 90 degrees. Figure V-28 shows measured data from gages east of 90 degrees longitude and include USGS Bayou Rigolets near Slidell, USGS Rigolets at Highway 90 near Slidell, and USGS Little Irish Bayou at Highway 11 near Slidell. Only gages providing data throughout a significant portion of the storm are plotted. Since the three curves are similar and Little Irish Bayou survived more of the storm, Little Irish Bayou gage is being surveyed to reference those data to the NAVD88 2004.65 datum.

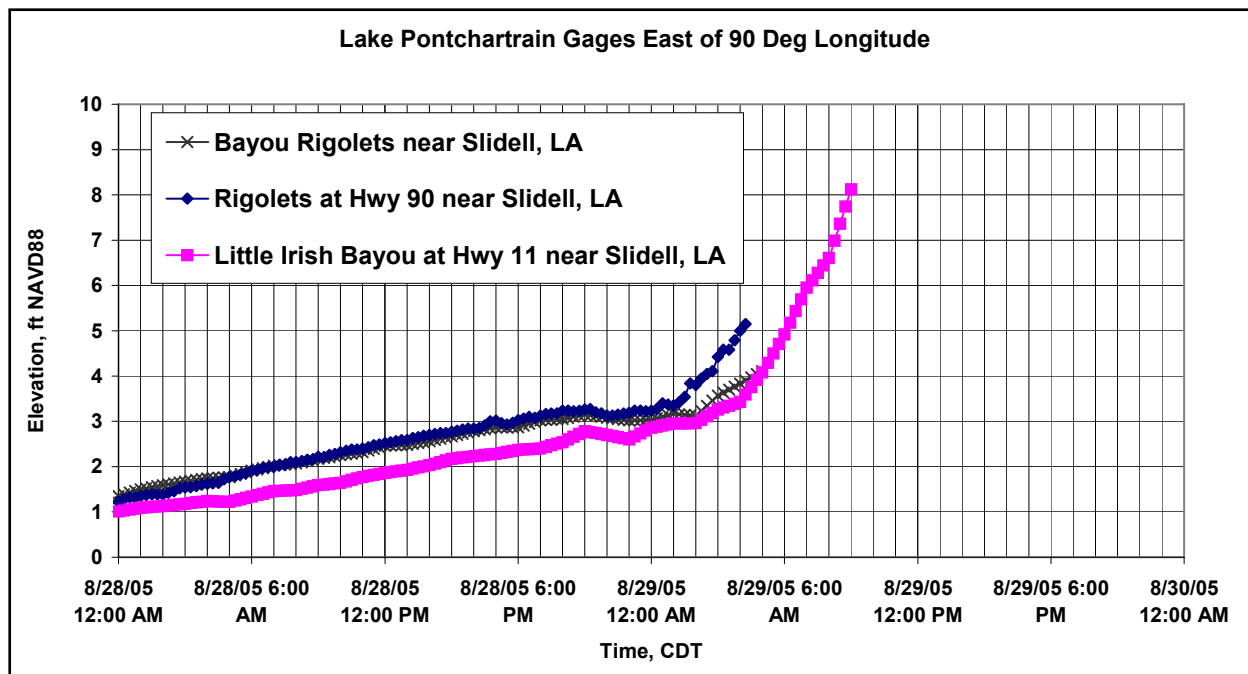


Figure V-28. Hydrographs on Lake Pontchartrain, gages located east of 90 degrees longitude

Figure V-29 shows measured data for gages west of 90 degrees longitude and include the National Weather Service (NWS) gage in Lake Pontchartrain on the Causeway designated Midlake, USGS gage Pass Manchac at Turtle Cove near Pontchatoula, and Orleans Levee District gage at Southshore Marina. After the passage of Katrina, the USGS installed a temporary gage about ¼ mile north of the NWS gage at Midlake on the Causeway. That gage became operational at 4:00 PM on September 2. All four gages are being surveyed to establish the data records relative to NAVD88 2004.65 datum.

Figures V-30 and V-31 are hydrographs acquired by NOAA National Ocean Service (NOS) at stations 8760922 at Southwest Pass, Louisiana and station 8761724 at Grand Isle/East Point, Louisiana. The instruments at these stations are among the few that functioned throughout Katrina's passage and recorded peak water levels. The Grand Isle station recorded a peak water level of 5.70 ft above mean lower-low water (MLLW) at 09:06 UTC on 29 August 2005. The Southwest Pass station recorded a peak water level of 7.61 ft above MLLW at 09:30 UTC on 29 August 2005.

One individual stayed at the Municipal Yacht Harbor (MYH) on his boat, the 53-ft *Manana*, during Katrina. The MYH is located immediately east of the entrance to the 17th Street Canal on Lake Pontchartrain (the largest, northernmost harbor shown in Figure V-26). He moored his 53-ft boat, a trawler-type steel-hull vessel that was built in 1946 and last retrofitted in 1995, with multiple 2-in diameter hawsers. The digital photographs taken on 29 August by that individual were tagged with time that was believed to be one hour behind Central Daylight Time. The LSU personnel examined the camera and confirmed that the camera file times were one hour behind CDT.

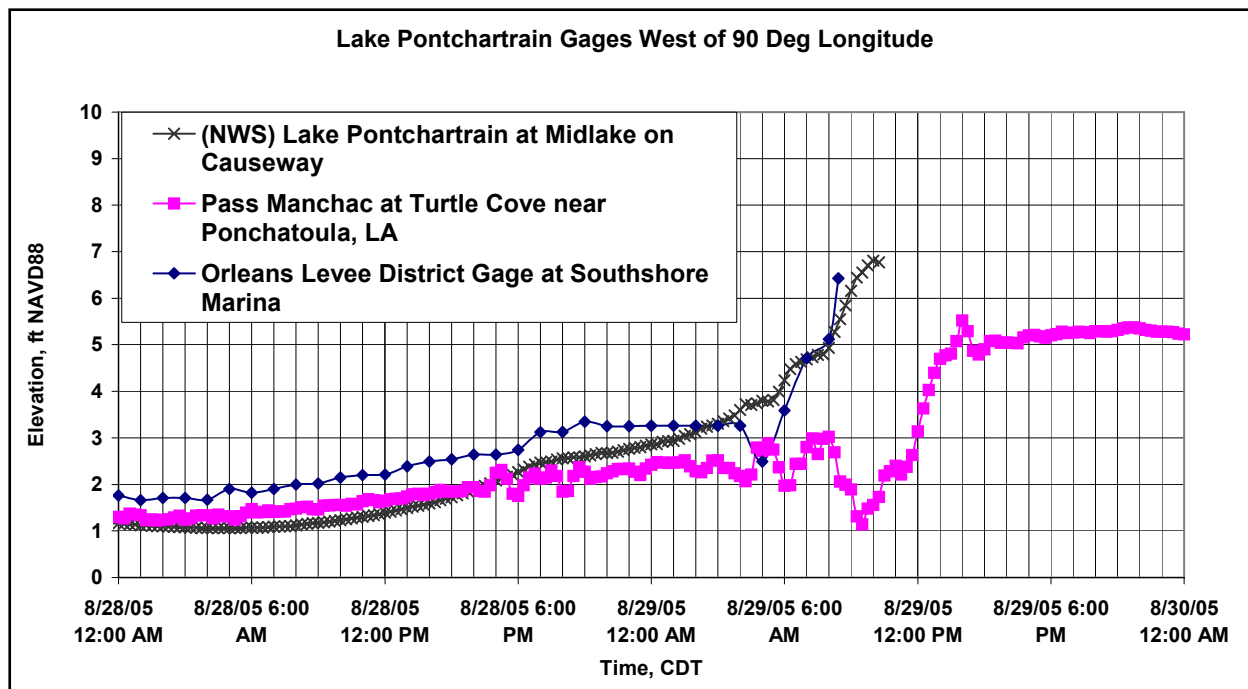


Figure V-29. Hydrographs on Lake Pontchartrain, gages located west of 90 degrees longitude

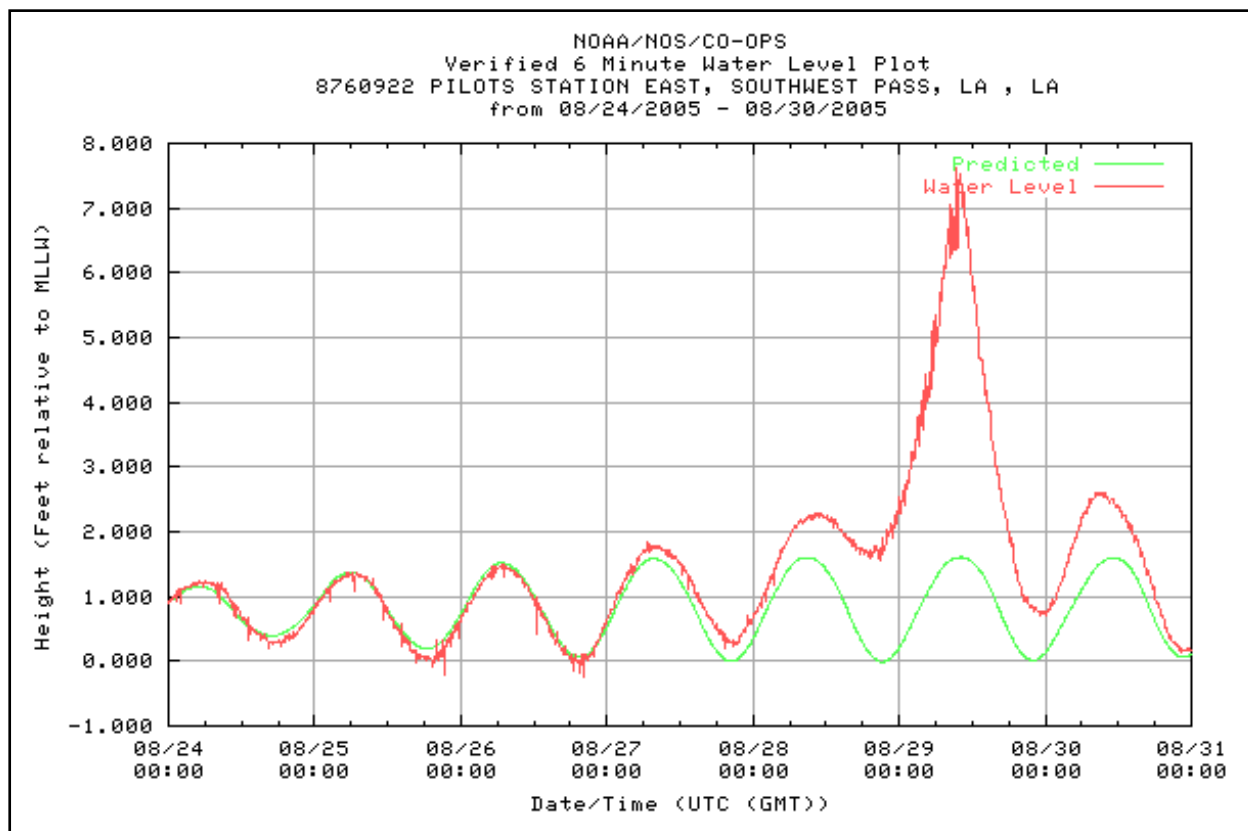


Figure V-30. Hydrograph for NOAA National Ocean Service station at Southwest Pass, Louisiana

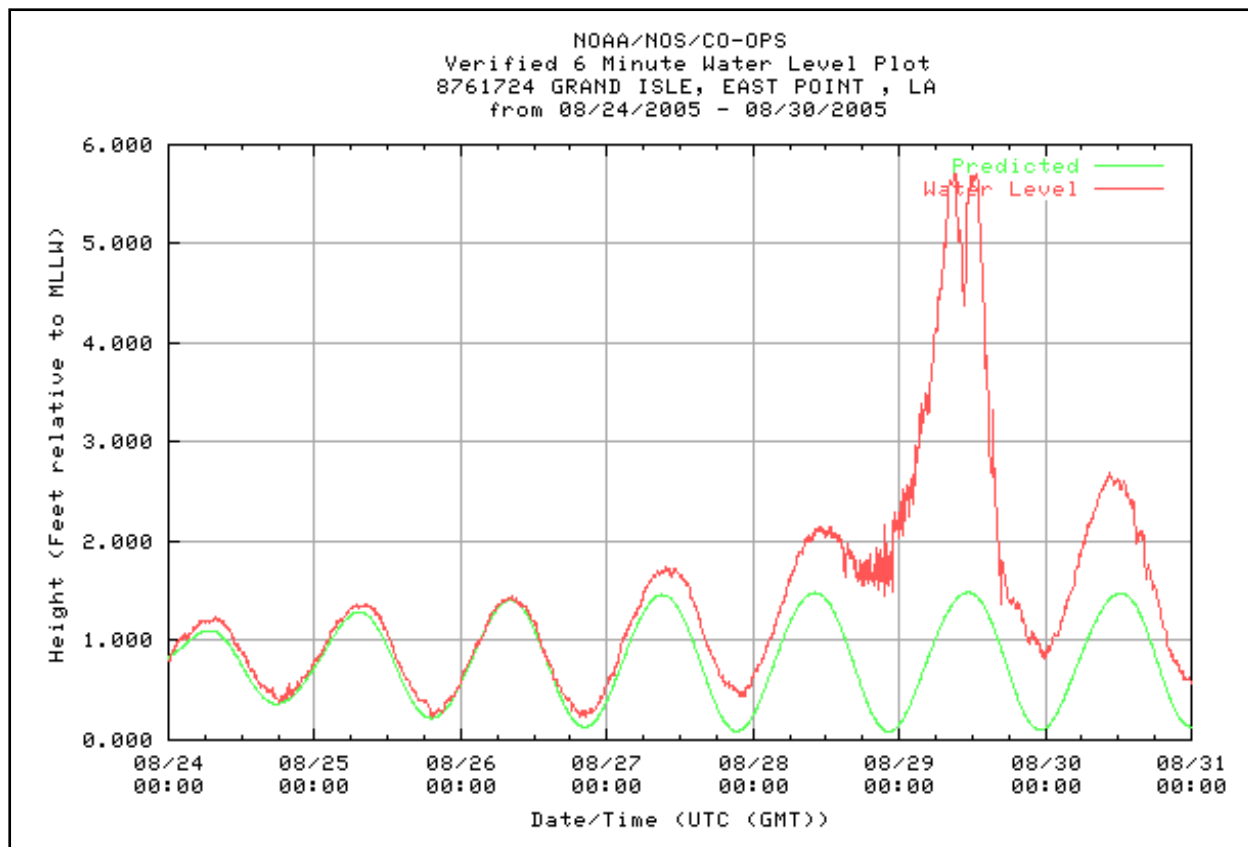


Figure V-31. Hydrograph for NOAA National Ocean Service station at Grand Isle, Louisiana.

A log of visual observations was maintained by another individual on 29 August who remained on his boat at the Orleans Marina near the 17th Street Canal entrance and just south of the Municipal Yacht Harbor. That individual was interviewed and points recorded in his log were surveyed.

The various time-tagged data points in the MYH and the Orleans Marina were surveyed and are plotted in Figure V-32, with their respective times. The survey was conducted using 2004.65 benchmarks. Also shown is the average high water mark elevation computed from high water marks acquired in the vicinity of the entrance to the 17th Street Canal, 10.8 ft NAVD88 2004.65 datum. All marks used are considered to be excellent high water marks, i.e., acquired within the interiors of buildings. The timing of the high water mark is somewhere between 9:00 and 10:00 CDT (1400 and 1500 UTC). A time of 9:30 CDT (1430 UTC) is used on the plot to indicate the time of peak water level until a better estimate is determined.

Digital photographs were taken by members of the Orleans Parish Levee District at the Lakefront Airport on 29 August and the water level location in each of the photographs was surveyed. These data are plotted in Figure V-33. Also shown is an average high water mark elevation, of 11.7 ft NAVD 88 2004.65, computed from five excellent high water marks acquired at the Lake Pontchartrain entrance to the IHNC (both east and west sides).

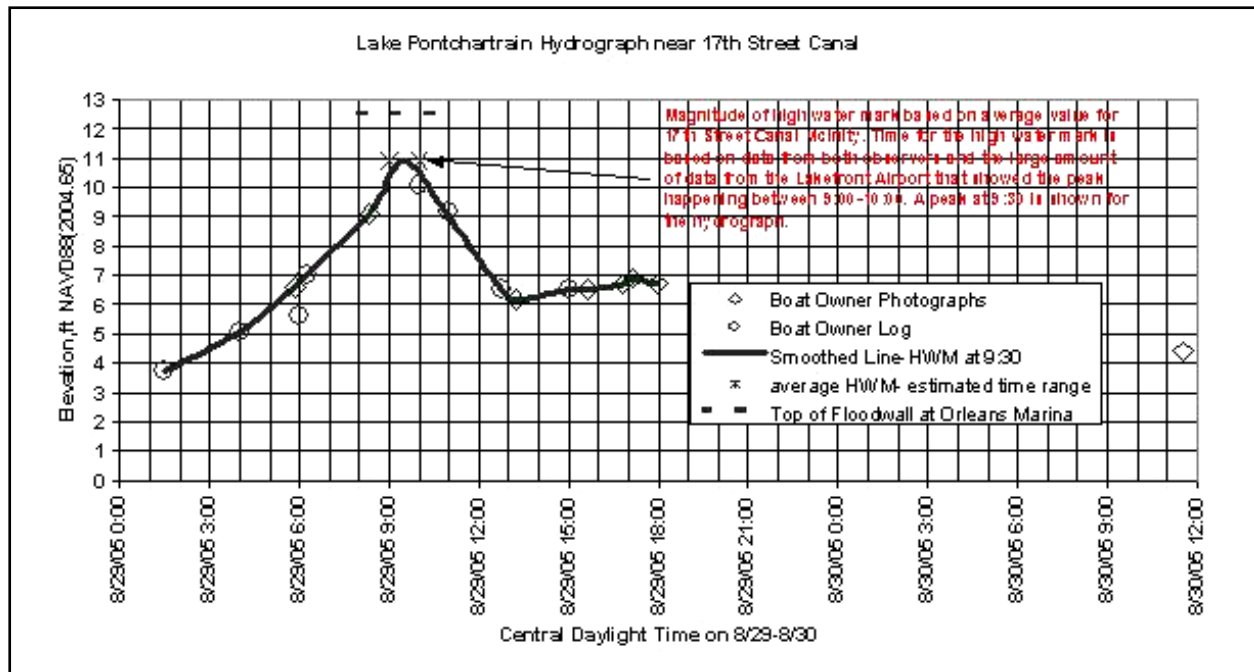


Figure V-32. Reconstructed hydrograph at the entrance to the 17th Street Canal

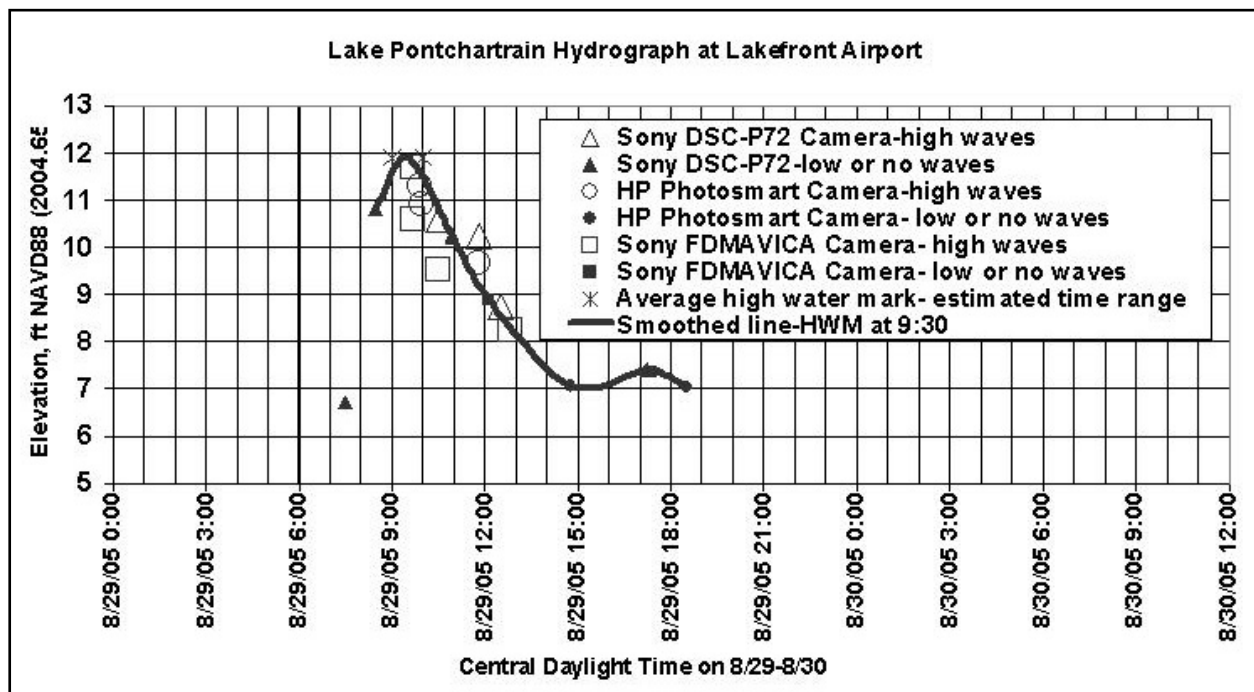


Figure V-33. Reconstructed hydrograph at the Lakefront Airport, entrance to the IHNC

Storm Surge Modeling

In this brief summary, we describe application of the ADCIRC hydrodynamic model to hindcast the storm surge development and propagation during Hurricane Katrina. Over the past decade, extensive storm surge model development, application, and validation efforts have been made in Southern Louisiana. This work has improved storm surge modeling capabilities within a physics-based framework that correctly accounts for and simulates the forcing and response processes (Westerink et al. 2005, Feyen et al. 2005). These efforts have taken advantage of the evolution of unstructured grid computational algorithms as well as massively parallel software and hardware.

TF01 Computational Model. The model domain/grid used in our Katrina simulation is based on an extension of the S08 model (Westerink et al. 2005, Feyen et al. 2005). The S08 model incorporates the western North Atlantic Ocean, the Gulf of Mexico and Caribbean Sea to allow for full dynamic coupling between oceans, continental shelves, and the coastal floodplain without necessitating that these complicated couplings be defined in the boundary conditions (Blain et al. 1994).

The S08 domain/grid has been extensively applied and validated in a number of hindcast studies. These hindcasts included air-sea interaction and forcing as well as tides. Wave-current interaction was not taken into account.

For the Katrina hindcast, the S08 model/domain was extended by adding resolution along the north shore of Lake Pontchartrain as well as the inlets and coastal floodplain (up to the 60-ft contour) along the Mississippi and Alabama coasts. The resulting TF01 model, shown in Figures V-34 and V-35, allows for a better representation of the flooding event as Katrina made its second landfall.

The bathymetric/topographic elevation data were interpolated to the computational mesh by moving progressively from the coarsest to finest areas of the domain. Deep water bathymetric depths were first interpolated from a $5^{\circ} \times 5^{\circ}$ regular grid based on the ETOPO5 values. Subsequently values were obtained from the NOAA NOS depth sounding database and USACE CEMVN and USGS topographic survey values using an element-based gathering/averaging procedure instead of a direct interpolation procedure. The gathering/averaging procedure searches for all available sounding/topographic survey values within the cluster of elements connected to one specific node, averages these values and assigns the average value as the depth/topographic elevation to that node. This gathering/averaging procedure essentially implements grid scale filtering to the bathymetric/topographic data and ensures that bathymetry/topography is consistent with the scale of the grid. Bathymetry/topography was hand-checked; in regions with missing or incorrect data, supplemental data from the CEMVN, USGS or NOS bathymetric/ topographic charts was applied.

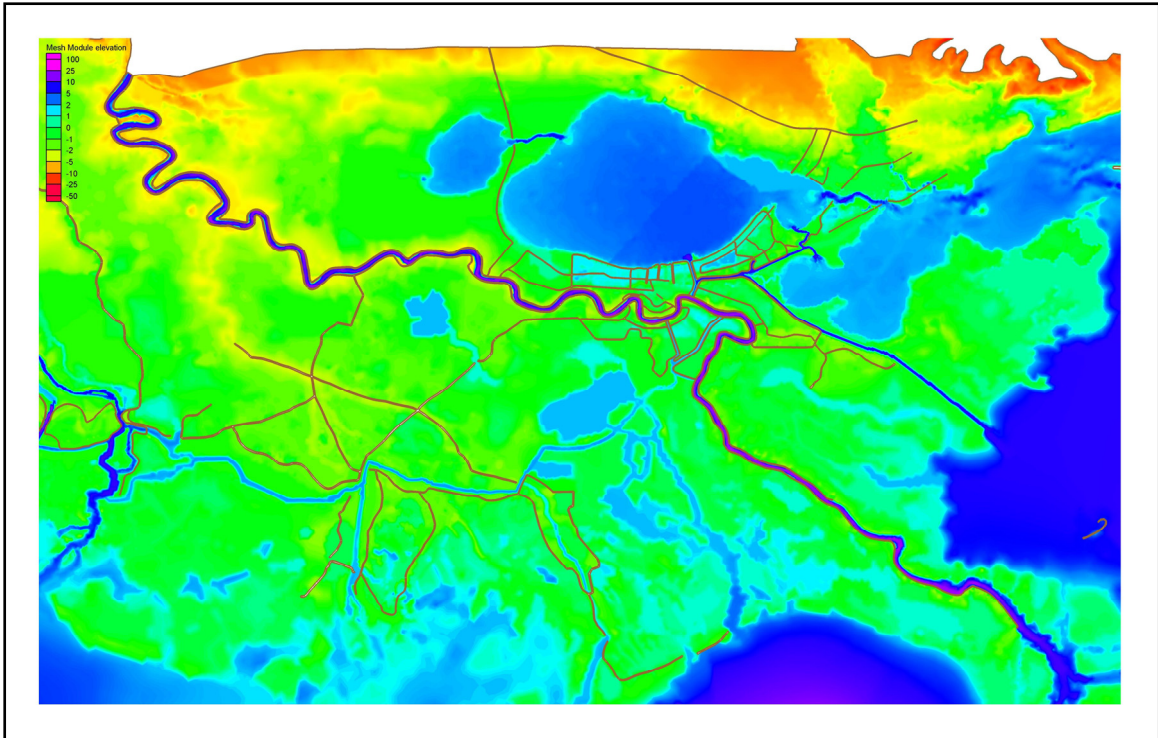


Figure V-34. Bathymetry/topography used in the ADCIRC storm surge model (TF01 grid)

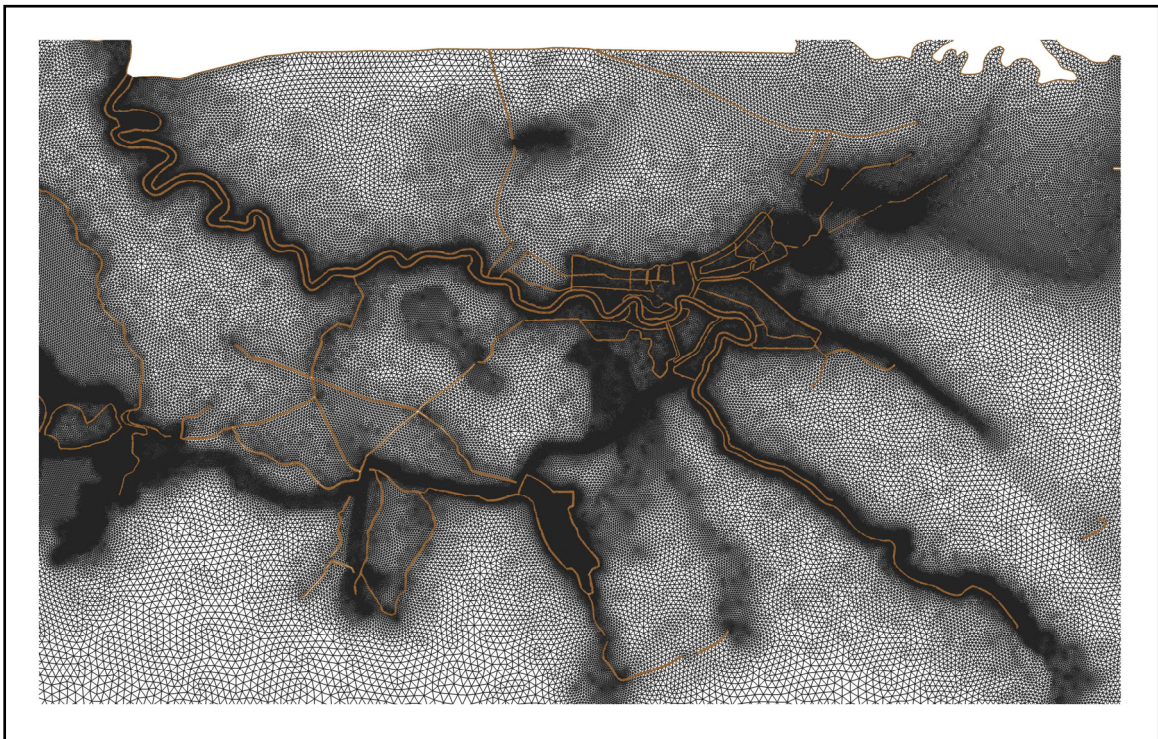


Figure V-35. Grid resolution used in the ADCIRC storm surge model (TF01 grid)

In order to provide a continuous elevation field from offshore on to land and reference these depths to the model's datum, it is necessary to account for the original datums for the bathymetric and topographic data. First, the desired datum for the ADCIRC model is mean sea level offshore. Second, bathymetric data are provided relative to the tidal mean lower low water datum. Examination of NOAA benchmarks in the Southern Louisiana region shows that on average mean sea level is approximately 0.6 ft above mean lower low water datum (MLLW). The topographic data were provided relative to NGVD 29. When the grid was constructed, in light of datum uncertainties, 0.0 ft NGVD 29 was assumed to be approximately 0.0 MLLW, i.e. NGVD 29 was assumed to be about 0.6 ft below mean sea level. The initial water height is raised 0.6 ft so that the modeled mean sea level matches on average the mean sea level relative to bathymetry and topography (the currently used ADCIRC model datum is NGVD29). Note that these adjustments are provided across the domain and will correct the original data to mean sea level on an average regional basis. Recent information acquired during the IPET study suggests that in the New Orleans vicinity NAVD88 2004.65 is about 0.2 to 0.25 ft below local mean sea level (LMSL for the 1983 to 2001 tidal epoch). Therefore, to convert ADCIRC water level results to NAVD88 2004.65, 0.4 ft are subtracted from the model results. Recent information from the IPET datum work suggests that NGVD 29 (1991) is 0.88 ft below local mean sea level for the 1983 to 2001 tidal epoch, along the south shore of Lake Pontchartrain. Bathymetric and topographic data used to construct the ADCIRC model are being re-examined and converted to NAVD88 2004.65.

Storm Forcing and Other Details. Astronomical tides are forced in the simulation reflected in this report; wind waves are not. Work to couple the wave and storm surge models is ongoing. The Mississippi and Atchafalaya rivers are forced with steady flows of 22000 ft³/s and 67000 ft³/s respectively.

Steric effects due to the thermal expansion of surface ocean water during late summer are pronounced in the Gulf of Mexico. This expansion is approximately captured by the long term solar annual and semiannual (*Sa* and *Ssa*) harmonic constituents. Examination of the harmonic constants computed by NOAA for stations across Southern Louisiana shows that the amplitude of the *Sa* and *Ssa* constituents is on average just over 0.61 ft. It is assumed that the hurricanes generally take place during the times when the expansion is at its largest in the late summer. Therefore, the initial water surface was raised an additional amount, a steric adjustment of 0.61 ft.

Marine wind and atmospheric pressure fields were generated using the 5 level version of the Planetary Boundary Layer (PBL) model (Thompson and Cardone 1996). The model was run with 1.5-hourly input minimum atmospheric pressure in the storm eye, maximum wind speed and eye location interpolated from available preliminary NOAA two- to three-hourly values. The input for the PBL simulation is given in the Wave and Storm Surge Analysis Technical Appendix. The PBL model output consists of 30-minute averaged wind and pressure fields available every 15 minutes (necessary to avoid substantial aliasing in ADCIRC's Eulerian wind and pressure field interpolation algorithm). Since the air-sea drag laws have been developed assuming 10-minute averaged winds, a

conversion to 10-minute averaged winds was implemented by multiplying the PBL 30-minute winds by a gust factor of 1.04.

Viscous hydrodynamic parameters are specified globally constant for bottom friction and lateral viscosity using standard physically relevant values as applied in S08 simulations. We emphasize that no tuning or optimization was performed with respect to the selected values and that with the exception of the domain/grid, all model parameters were defined as in previous hindcasts.

Description of Hurricane Katrina Storm Surge. It is noted that the center of the storm tracked largely east of the city of New Orleans (about 28 miles due east at its closest point). However the storm was in the vicinity of critical features in the vicinity of New Orleans, the storm center being as close as 10 miles due east of the St. Bernard Parish/Chalmette hurricane protection levee which runs along the Mississippi River – Gulf Outlet (MRGO) and as close as 20 miles due east of the confluence of the Gulf Intracoastal Waterway (GIWW) and the MRGO. The influence of the MRGO on storm surge that reaches the metropolitan New Orleans area has been the subject of considerable debate. That issue is addressed later in this chapter and in greater detail in the Wave and Storm Surge Analysis Technical Appendix.

Prior to landfall, the counterclockwise rotating winds of Hurricane Katrina began to push water from east to west. This pattern existed several days prior to landfall. This water began to first inundate the wetlands with several feet of water and then pile up water against the east- and northeast-facing levee systems throughout the southeast Louisiana region. As the storm made landfall in southern Louisiana and continued in a north-northeast direction, the buildup in surge along the levee systems increased until the storm center passed, and then the surge began to decrease. The greatest buildup of water occurred about half-way down that portion of the MS River and “back” levee system in Plaquemines Parish, which is located southeast of New Orleans. A slightly smaller buildup in storm surge occurred in Lake Borgne as water piled up against the eastern-facing hurricane protection levees along St. Bernard and Orleans Parishes.

In addition to the local buildup of water against the levees, these local surges propagate away from their region of initial generation. The surge generated against the river and back levees of Plaquemines Parish propagated up the Mississippi River as well as across Breton and Chandeleur Sounds. The latter surge interacts with the wind fields and propagates to the north-northeast paralleling the path of the storm center as it advanced. As the storm pushed this surge to the north-northeast, piling the water up against the Mississippi Gulf coast and combining with more locally generated surge, water levels reached their highest values along the Mississippi coast to the east of the location at second landfall. This local maximum storm surge region to the right of the storm track is typical of land-falling hurricanes.

Figure V-36 shows color-shaded contours of the maximum water level computed for the storm at each grid node, in feet NGVD29, for the entire Louisiana and Mississippi coastal region computed with the ADCIRC model. Figure V-37 shows contours for the metropolitan New Orleans vicinity. Peak water levels in

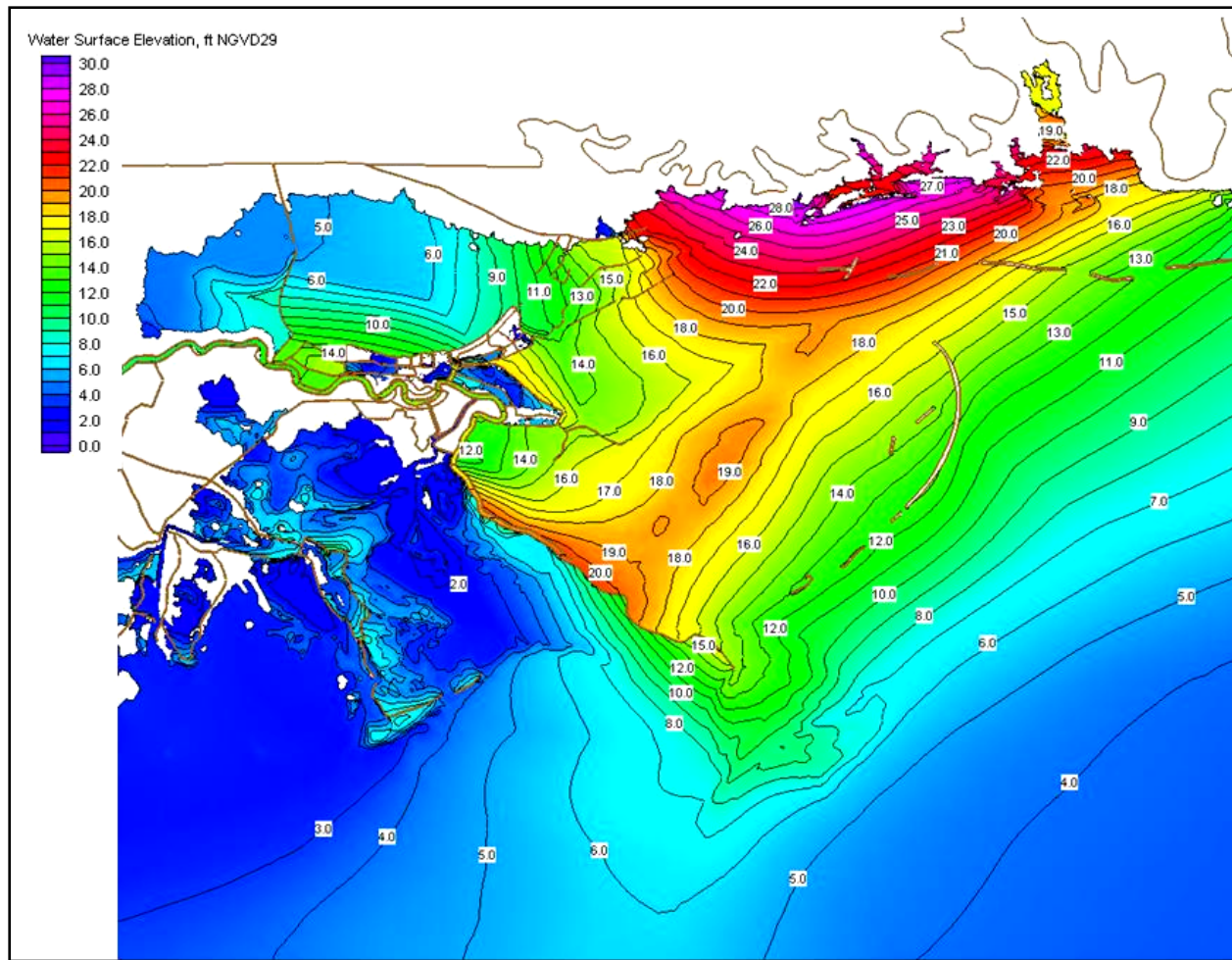


Figure V-36. Maximum computed storm surge using the ADCIRC model, Mississippi to Louisiana region (water levels in feet, NGVD 29)

southeastern Louisiana were computed to be about 20 to 21 ft (dark orange contours), NGVD29, along the east-facing Mississippi River and back levees that protect communities along the river. At the levees facing Lake Borgne along the MRGO, maximum computed water levels were 17 to 18 ft (light orange contours). Along the south shore of Lake Pontchartrain, maximum levels were computed to be between 9 and 13 ft (green contours). Along the coast of Mississippi, maximum water levels were computed to be 27 to 28 ft (pink contours).

Note the pattern of water level gradient within the GIWW/MRGO and the IHNC. The pattern is similar to that reflected in the high water marks.

Figures V-38 through V-40 show computed time series of water surface elevation, in feet NGVD29, at twelve locations throughout the metropolitan New Orleans area. Figure V-38 shows locations along the south shore of Lake Pontchartrain. The computed time of arrival of the peak surge is about 13:59 UTC on August 29, 2005 (or about 9:00 a.m. local time, CDT). The simulated time of arrival for the peak surge is slightly ahead of the observed time of

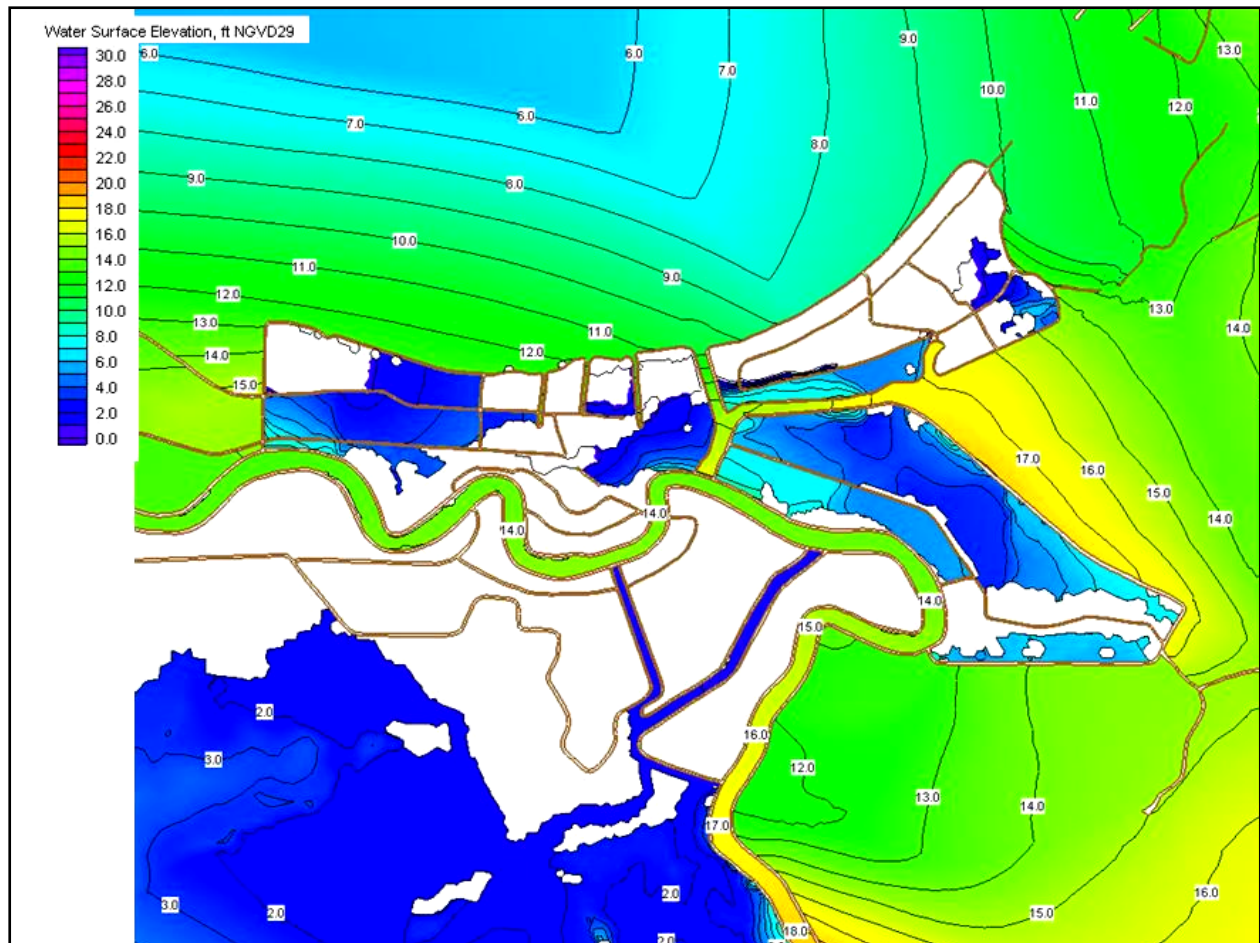


Figure V-37. Maximum computed storm surge using the ADCIRC model, metropolitan New Orleans vicinity (water levels in feet, NGVD 29)

arrival, which is estimated to have occurred sometime between 9:00 a.m. and 10:00 a.m. CDT. Figure V-39 shows the same information for locations along the MRGO and GIWW/MRGO. Model results indicate that the peak of the storm surge wave took approximately 50 min to propagate from the southeastern corner of the levee along the MRGO in St. Bernard Parish to the junction of the IHNC and MRGO, as the storm tracked to the north-northeast. The computed time of arrival of the peak surge at the IHNC Lock is about 13:35 UTC (8:35 a.m. CDT). The observed hydrograph at the Lock shows arrival of the peak surge at about 9:00 a.m. CDT, or slightly later. However, the timing of the peak at the IHNC Lock may be influenced by the breach on the IHNC into the Lower 9th Ward.

Hydrograph data at the IHNC Lock and the reconstructed hydrographs at the entrance to 17th Street Canal and at Lakefront Airport suggest that the time of peak surge arrival predicted by the storm surge model is about 30 min early. This may change once the final winds are incorporated into the modeling.

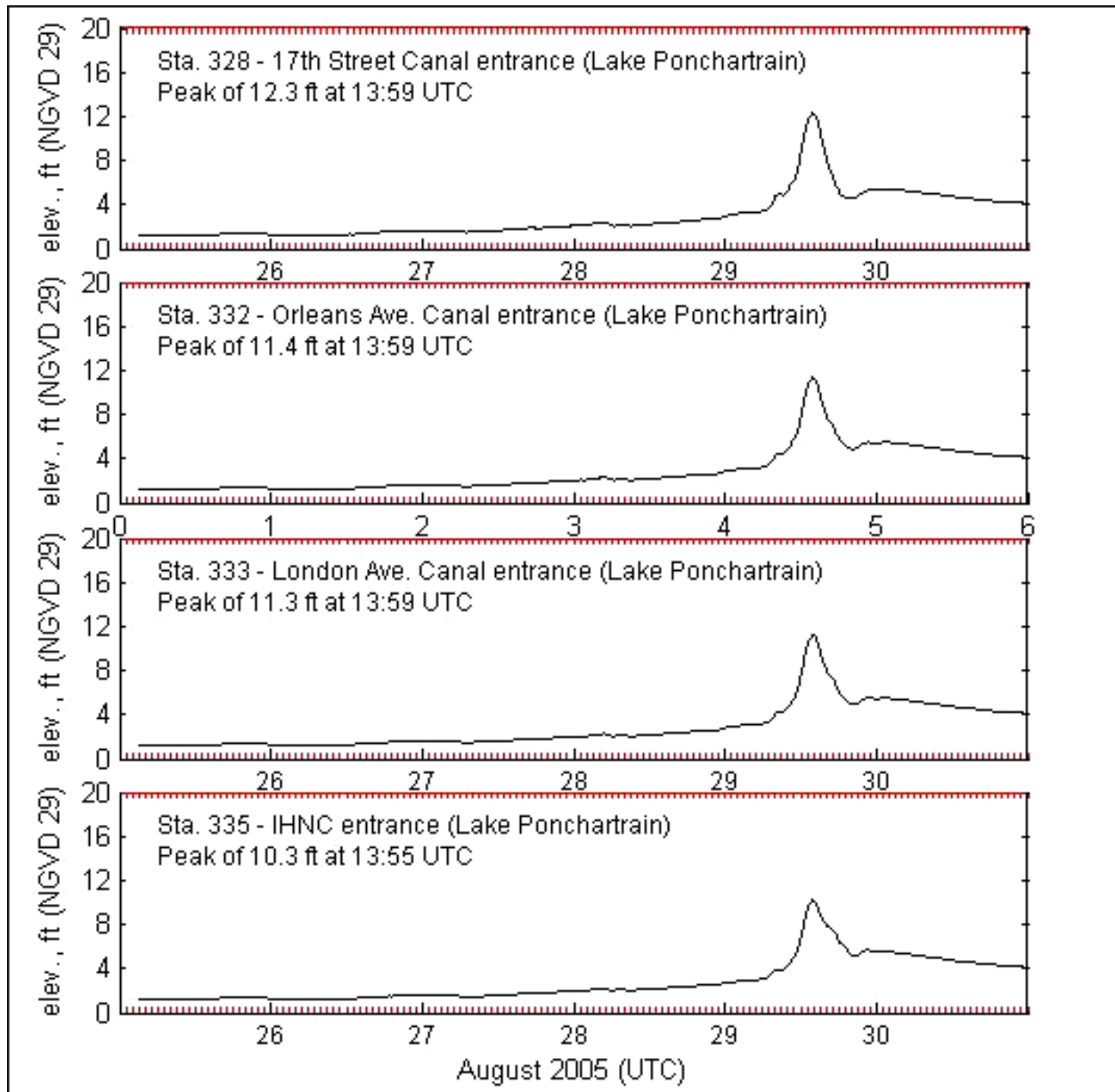


Figure V-38. Change in water surface elevation, with time, for locations along the south shore of Lake Pontchartrain

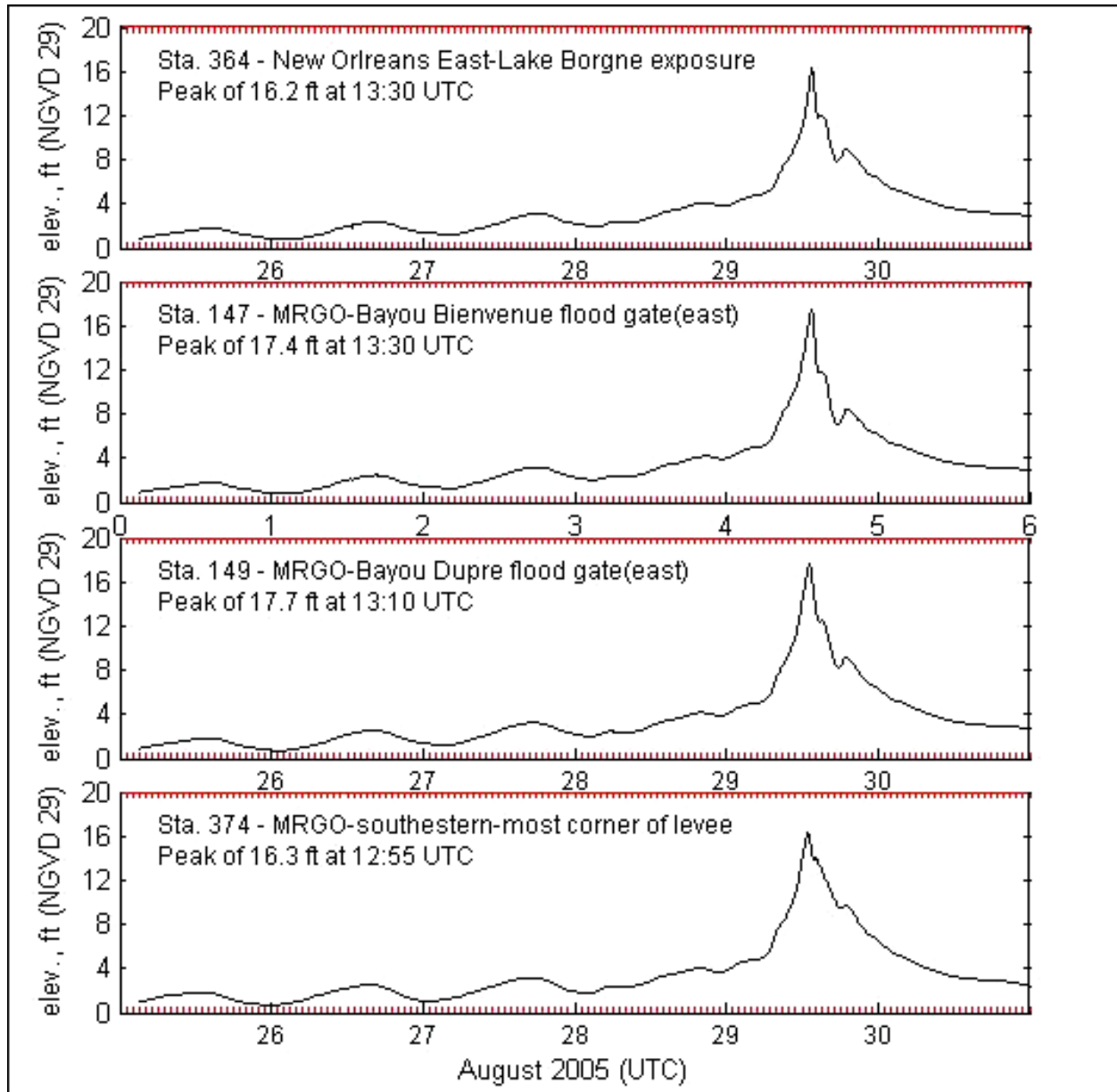


Figure V-39. Change in water surface elevation, with time, for locations in the GIWW and MRGO with exposure to Lake Borgne

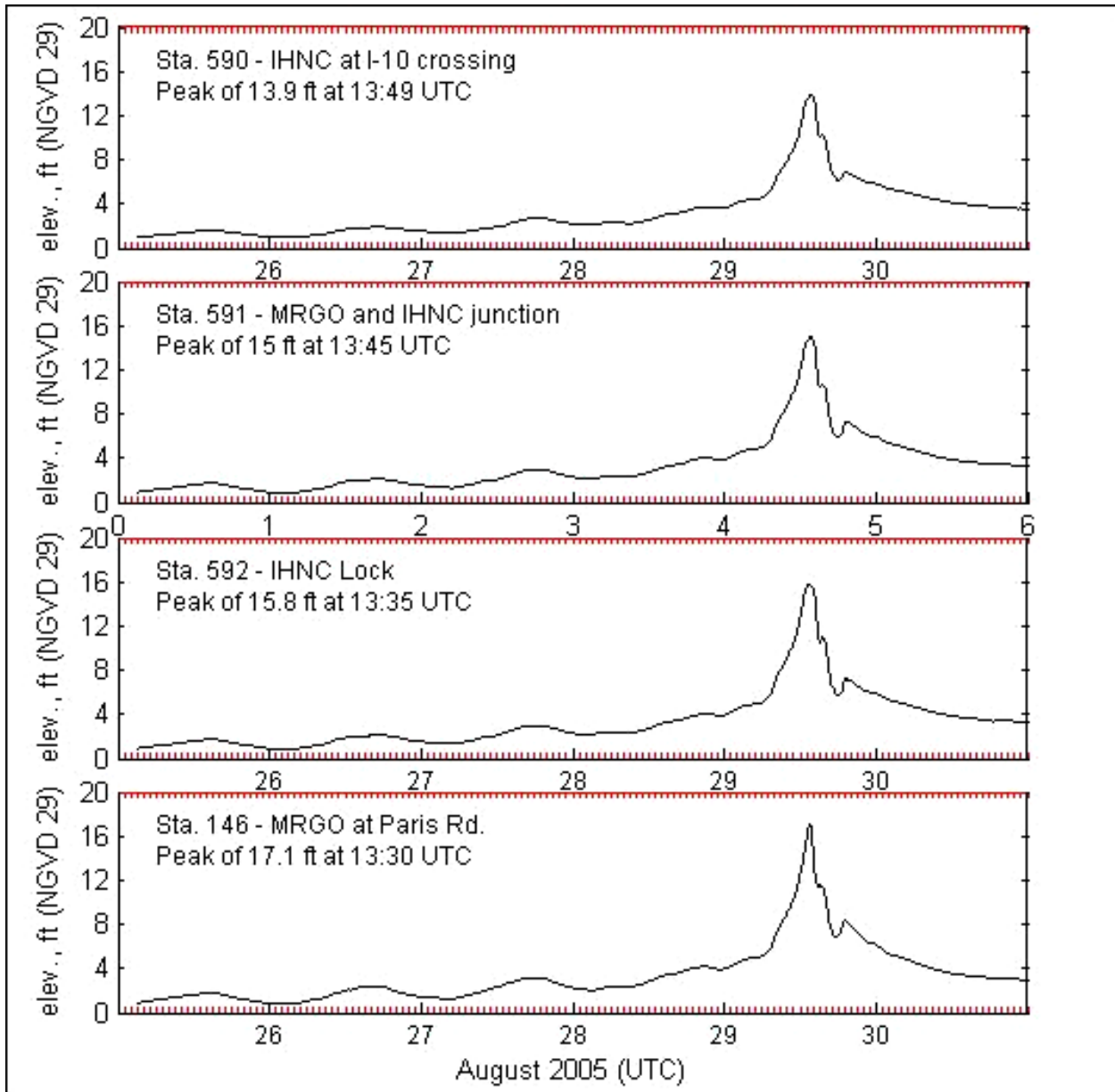


Figure V-40. Change in water surface elevation, with time, for locations along the GIWW/MRGO and IHNC

Model-generated maximum water levels are compared to measured high water marks and to design water levels in the following section. More documentation describing the storm surge modeling, a more detailed description of the storm surge propagation through the region, and additional model-to-measurement comparisons are provided in the Wave and Storm Surge Analysis Technical Appendix.

Comparison of Katrina Wave and Water Level Maxima with Design Values

Peak wave and water level conditions experienced during Hurricane Katrina are compared to values used in the design of the hurricane protection system. In the series of figures that follow, design values are shown in yellow boxes with the label “D”; computed, model-derived values are shown in blue with the label “C”; and where measurements are available, measured values are shown in green boxes with the label “M”. Design values were taken from the original Design Memoranda, which generally cited significant wave height and period. The Design Memoranda do not specify whether a peak or a mean period was used. At the time the projects were designed, this distinction between different measures of wave period was probably not made. Computed wave maxima were estimated using STWAVE model results (significant wave height and peak wave period) and computed water level maxima were estimated using ADCIRC results (maximum water surface elevation).

Peak measured wave conditions were only available at the entrance to the 17th Street Canal; however, the measurements are of questionable accuracy at the peak of the storm. The maximum measured wave height and period values that are used are those measured just prior to the point at which the data appear to become suspect, from both wave buoys. For water level conditions, at sites where hydrographs captured the peak water level, that value is presented. Where high water marks rated “excellent” are available, those values are shown. If no excellent marks are available in an area of interest, then marks rated “good” or the best available quality of mark, were used.

All water levels are converted to a common datum NAVD88 (2004.65) for the purposes of this comparison using datum conversions based on current IPET datum analysis results. To convert from the ADCIRC model datum to NAVD88 2004.65, 0.4 ft are subtracted from model results. The Design Memoranda cite design water levels relative to a number of difference reference frames, mean sea level, MSL, National Geodetic Vertical Datum (without reference to any specific epoch), and to still water level, SWL. The earliest design documents cited SWL and MSL; later design documents cited NGVD. It appears that the intent of the designers has always been to relate design water levels to mean sea level, and this intent has been confirmed with CEMVN staff so that assumption is used. To convert design water levels to NAVD88 (2004.65) datum, 0.25 ft are added to the design water level values along the south shore of Lake Pontchartrain (correction derived from the New Canal datum analysis), and 0.2 ft are added to values in the vicinity of IHNC/GIWW/MRGO canals (an average of corrections derived from the New Canal, 0.25 ft, and Chef Menteur, 0.15 ft, datum analyses). For southern Plaquemines Parish, the same 0.2 ft correction was applied until more definitive information becomes available.

Wave Maxima. Figure V-41 shows wave maxima for the south shore of Lake Pontchartrain in Jefferson and Orleans Parishes. Significant wave heights measured and computed for Katrina exceeded design wave heights by 0.9 to 1.6 ft. Peak wave periods during Katrina were about equal to the design values.

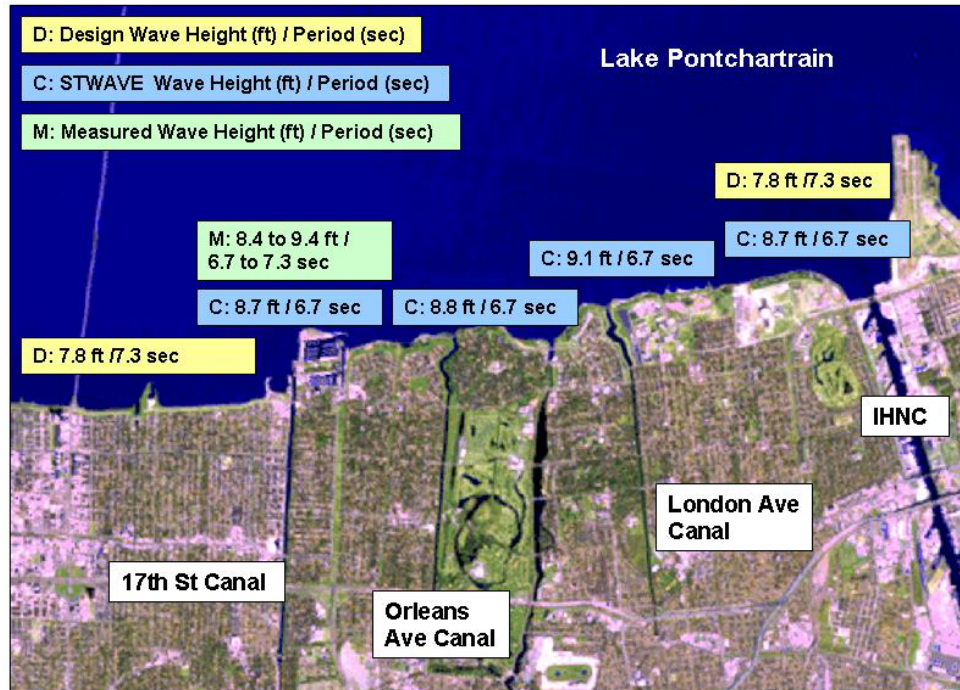


Figure V-41. Wave maxima along the south shore of Lake Pontchartrain hurricane protection system

Figure V-42 shows wave maxima for the eastern portion of Orleans Parish. On Lake Pontchartrain, significant wave heights computed for Katrina exceeded design wave heights by 1 ft; peak wave periods were 0.6 sec less than the design values. On the east-facing side of the Parish, significant wave heights computed for Katrina exceeded the design value by 0.8 ft; and wave period exceeded the design value by 1.3 sec. On the back levee of Orleans Parish, along the GIWW, with exposure to Lake Borgne, maximum significant wave height computed for Katrina only exceeded the design value by 0.3 ft, but the peak wave period exceeds the design value by about a factor of 3. The design wave periods are more typical of those for wind seas. Wave model simulations show that during Katrina, the eastern-facing levee systems were subjected to longer-period energy propagating from the Gulf past the barrier islands. Re-examination of the design wave conditions along the eastern-facing levees at this location is recommended, in light of the large differences between design periods and the wave periods generated by Hurricane Katrina. Both wave heights and wave periods define the potential for wave run-up and overtopping.

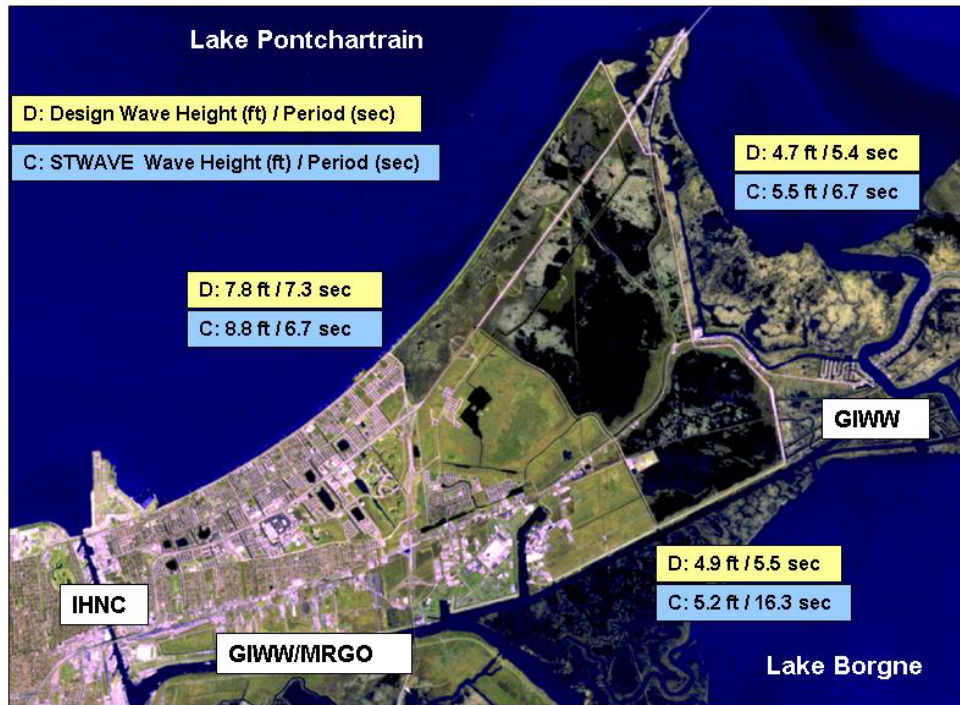


Figure V-42. Wave maxima along eastern Orleans Parish hurricane protection system

Figure V-43 shows wave maxima for the easternmost portion of St. Bernard Parish. Along the MRGO, significant wave heights computed for Katrina were less than the design wave heights by 1.7 to 1.8 ft. However, peak wave periods computed for Katrina were nearly two to three times greater than the design values. On the south-facing portion of the hurricane protection levee, significant wave heights computed for Katrina were less than design values by about 2.2 to 2.3 ft; wave periods exceed design values by a factor of about three. Design wave conditions at these locations should be re-examined as well. Lower wave heights will reduce run-up; higher wave periods will increase wave run-up.

Figure V-44 shows wave maxima for areas of Plaquemines Parish. Along the levees east of the Mississippi River with exposure to waves approaching from the east, significant wave heights computed for Katrina exceeded design wave heights by amounts ranging from 2 to 4 ft. Peak wave periods computed for Katrina were much greater than the design periods, two to three times greater. On the west-facing levees on the west side of the Mississippi River, in some locations, significant wave heights computed for Katrina exceeded the design values and in some locations computed wave heights were less than design values. In all cases the computed wave periods exceeded the design wave periods. Design wave conditions should be re-examined along the west-facing levees.

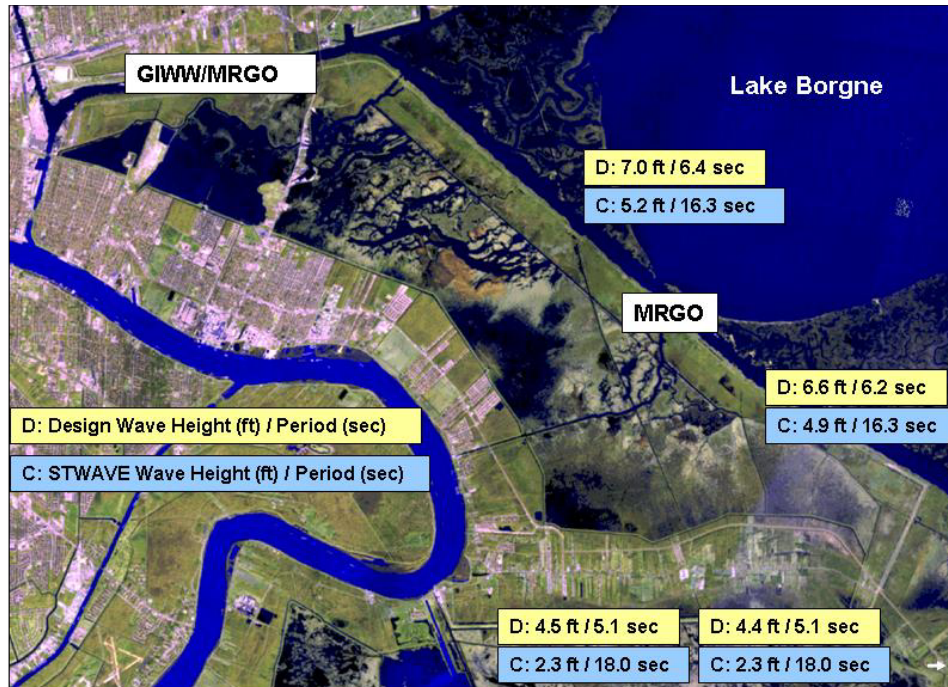


Figure V-43. Wave maxima along hurricane protection system of St. Bernard Parish



Figure V-44. Wave maxima along hurricane protection levees in Plaquemines Parish

Water Level Maxima. Figure V-45 shows water level maxima for the south shore of Lake Pontchartrain in Jefferson and Orleans Parishes. Peak water levels during Katrina at the entrances to 17th Street (10.8 ft NAVD 88, 2004.65), Orleans Avenue (10.8 ft NAVD 88, 2004.65) and London Avenue Canals (10.7 ft NAVD88 2004.65), were about 1 ft less than design values. The peak values were all based on high water marks. The design water level is 11.8 ft NAVD88 (2004.65) throughout the region.

Figure V-46 shows water level maxima for eastern Orleans Parish. On the Lake Pontchartrain side, the design water level is 11.8 ft NAVD88 2004.65 and the measured peak water level at the entrance to the IHNC was 11.7 ft, NAVD88 2004.65. At this location the peak water levels were right at the design levels. On the back levee, adjacent to the GIWW, with exposure to Lake Borgne, and along the GIWW/MRGO, design water levels range from 13.0 to 13.2 ft NAVD88 2004.65. High water mark data suggest that the design water levels were exceeded along these canals, by amounts ranging from 1 to approximately 5 feet. Within the IHNC, north of its junction with the GIWW/MRGO, design water levels range from 11.8 to 13.1 ft NAVD88 2004.65. High water marks suggest that design water levels in this section of channel were right at design levels or slightly below.

Figure V-47 shows water level maxima for eastern St. Bernard Parish. As stated above, the design water levels along the GIWW/MRGO were exceeded by amounts ranging from 1 to 5 feet. In the IHNC, south of its junction with the GIWW/MRGO, design water levels are 13.2 ft NAVD88 2004.65 and an excellent high water mark indicated a peak water level of 15.2 ft. The hydrograph from the IHNC Lock indicates the peak reached 14.3 ft NAVD 88 2004.65. Within the IHNC, south of its junction with the GIWW/MRGO, peak water levels during Katrina exceeded design values by 1 to 2 feet. Along the MRGO, the design water level varies from 13.2 ft to 12.7 ft NAVD88 2004.65. High water marks indicate that design water levels were exceeded along the MRGO hurricane protection levee by amounts ranging from 3 to 5.5 ft.

Figure V-48 shows water level maxima for southern Plaquemines Parish. For the east-facing levees and flood walls, design water levels ranged from 12.8 to 14.2 ft NAVD88 2004.65. Not all high water mark data have been processed for this region; but based on model results, peak water levels during Katrina exceeded the design values south of Phoenix by as much as 6 ft. At the southernmost end, near Venice, computed Katrina peak water levels were right at design levels. On the levees facing west on the west side of the Mississippi River, again based solely on model results, peak water levels during Katrina exceeded the design values in some areas, by amounts up to approximately 1 ft; but in other areas, the peak values were less than the design values by about the same amount.

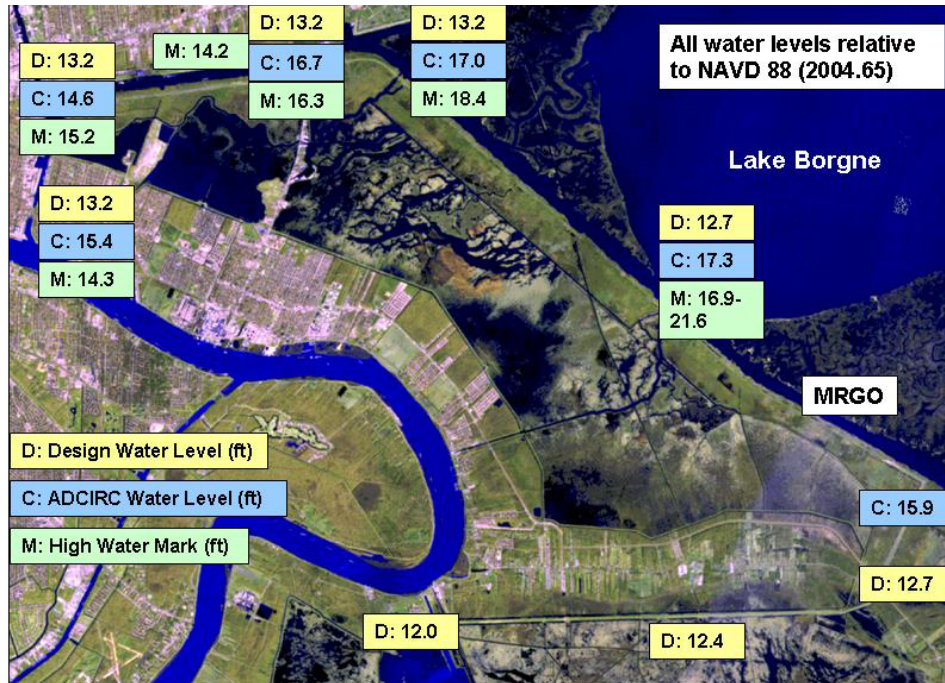


Figure V-47. Water level maxima for eastern St. Bernard Parish hurricane protection system

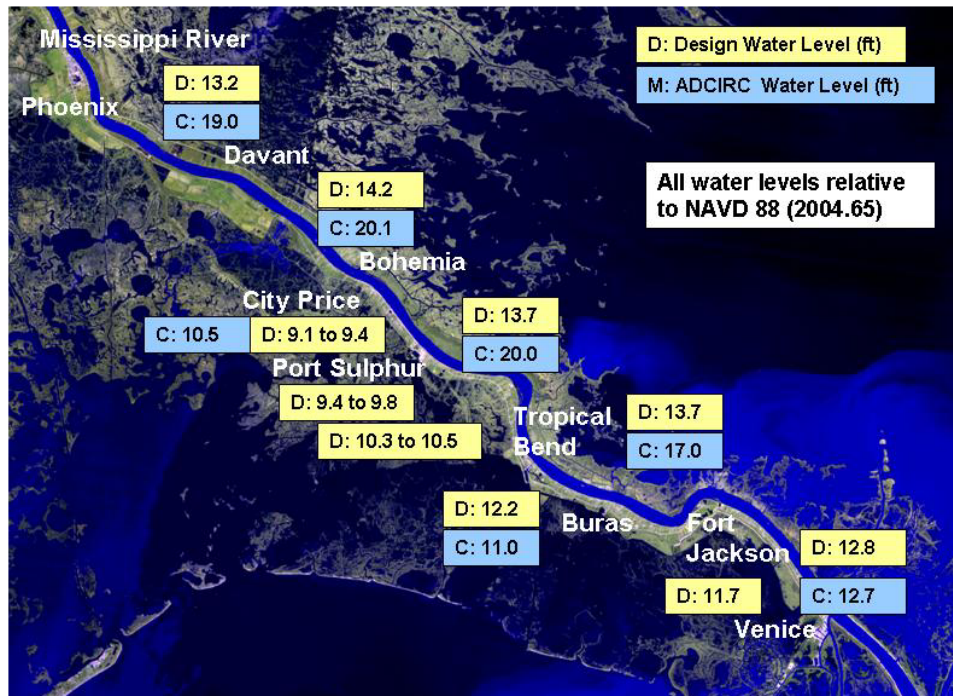


Figure V-48. Water level maxima for Plaquemines Parish hurricane protection system

Influence of the MRGO on Storm Surge in the New Orleans Vicinity

The Mississippi River Gulf Outlet (MRGO) role in propagation of low amplitude astronomical tide and influx of higher saline water into Lake Pontchartrain has been established. Concerns have been raised regarding the role of the MRGO on storm surge propagation into the metropolitan New Orleans vicinity.

From the perspective of long wave propagation, of which the tide and storm surge are examples, the critical section of the MRGO is Reach 1, the section of waterway where the GIWW and MRGO occupy the same channel (see Figure V-49). It is through this channel that Lake Pontchartrain and Lake Borgne are hydraulically connected to one another via the IHNC. The two Lakes are also connected to each other via the Rigolets and Chef Menteur Pass; the IHNC is the smallest of the three connections. Reach 1 existed as the GIWW prior to the construction of the MRGO, although the maintained depth was lower. As a result of this hydraulic connection, the storm surge experienced within the IHNC and Reach 1 (GIWW/MRGO) is a function of storm surge in both Lakes; a water level gradient is established within the IHNC and Reach 1 that is dictated by the surge levels in both Lakes. This is true for both low and high storm surge conditions.



Figure V-49. Location of the MRGO (Reaches 1 and 2)

To prevent storm surge in Lake Borgne from influencing water levels experienced in the IHNC or GIWW/MRGO sections of waterway, flow through the Reach 1 channel must be dramatically reduced or eliminated, either by a permanent closure or some type of structure that temporarily serves to eliminate

this hydraulic connectivity. The presence of an open channel is the key factor. If the hydraulic connectivity between Lake Pontchartrain and Lake Borgne is eliminated at a point within Reach 1, tide or surge to the west of this point will become primarily influenced by conditions at the IHNC entrance to Lake Pontchartrain; and tide or storm surge to the east of this point will become primarily influenced by conditions in Lake Borgne.

Most concern seems to be focused on MRGO/Reach 2 that runs from the GIWW/MRGO confluence, just east of the Paris Road Bridge, to the southeast (see Figure V-49). Three previous studies have been performed to examine the influence of MRGO/Reach 2 on storm surge in New Orleans and vicinity (two initiated by the U.S. Army Corps of Engineers and one commissioned by the Louisiana Department of Natural Resources), in addition to work performed to examine this issue as part of the IPET study. The IPET work to examine the influence of the MRGO/Reach 2 was done with the current version of the ADCIRC model, as reflected in this report. All studies have reached the same conclusion. The change in storm surge induced by MRGO/Reach 2 (computed as a percentage of the peak surge magnitude) is greatest when the amplitude of the storm surge is low, on the order of four feet or less. In these situations, changes induced by the MRGO in the metropolitan New Orleans area are rather small in terms of absolute water surface elevation changes, 0.6 ft or less in all cases and less than 0.3 ft in most cases, but this amount can be as much as 25% of the peak surge amplitude when the amplitude is low. When the long wave amplitude is very low, the surge is more limited to propagation via the channels, and the MRGO has its greatest influence. Once the surge amplitude increases to the point where the wetlands become inundated, this section of the MRGO plays a diminishing role in influencing the amplitude of storm surge that reaches the IHNC. For storm surges of a magnitude produced by Hurricanes Betsy and Katrina which overwhelmed the wetland system, both more than 7 ft peak surge and Katrina near 18 ft in Lake Borgne, the influence of MRGO/Reach 2 on storm surge propagation is quite small, just a few tenths of a foot at most in the IHNC and GIWW/MRGO in terms of absolute water surface elevation changes. These small changes represent only a few percent of the surge amplitude. When the expansive wetland is inundated, the storm surge propagates primarily through the water column over this much larger flooded area, and the channels become a much smaller contributor to water conveyance.

The hurricane protection levees along the south side of Orleans Parish and the eastern side of St. Bernard Parish along the MRGO, which together are referred to as a “funnel”, can locally collect and focus storm surge in this vicinity depending on wind speed and direction. This localized focusing effect can lead to a small local increase in surge amplitude. Strong winds from the east tend to maximize the local funneling effect.

Additional detail concerning the work to examine the influence of the MRGO on storm surge, and a more detailed explanation of why the effect is so small at high storm surge levels, is included in Appendix E titled “Note on the Influence of the Mississippi River Gulf Outlet on Hurricane Induced Storm Surge in New Orleans and Vicinity.”

Status of Remaining Efforts

Remaining work includes incorporating the final wind and pressure fields produced by NOAA Hurricane Research Division and Oceanweather, Inc. into all wave and storm surge modeling. The ADCIRC model set-up will be modified to incorporate recent topographic survey data and recent datum information as well as grid mesh refinements. Coupling between storm surge and wave models will be completed and applied for the storm (WAM, STWAVE and ADCIRC coupling). An STWAVE domain for the Mississippi coast will be set up and applied. Spatially variable wind fields will be integrated into the STWAVE modeling for Lake Pontchartrain and Louisiana South domains (this has been done for Louisiana Southeast). Datum adjustments will be made to high water mark and hydrograph data that have not been corrected yet. Exhaustive model-to-measurement comparisons and model skill assessment will continue. Sensitivity tests will be done for both wave and surge models to examine the role of pre- and post-storm wetland roughness on computed waves and water levels. Sensitivity tests will be done to examine influence of a degraded eastern barrier island chain on wave and storm surge conditions. Other sensitivity runs will be done to examine the role of model parameters and uncertainty in model input on wave and storm surge results. The final report will be prepared and data sets will be prepared for public release.

References

- Booij, N., Haagsma, IJ. G., Holthuijsen, L.H., Kieftenburg, A.T.M.M., Ris, R. C., van der Westhuysen, A. J., and Zijlema, M. 2004. "SWAN Cycle III Version 40.41 Users Manual," Delft University of Technology, Delft, The Netherlands, 118 p, <http://fluidmechanics.tudelft.nl/swan/index.htm>.
- Booij, N., Ris, R. C., and Holthuijsen, L.H. 1999. "A Third-Generation Wave Model for Coastal Regions, Part I: Model Description and Validation," *J. Geophys. Res.*, 104(C4), 7649-7666.
- Blain, C. A., J. J. Westerink, and R. A. Luettich, 1994. The influence of domain size on the response characteristics of a hurricane storm surge model. *J. Geophys. Res. - Oceans*, **99**, C9, 18467-18479.
- Blain, C. A., J. J. Westerink, and R. A. Luettich, 1998. Grid convergence studies for the prediction of hurricane storm surge. *Int. J. Num. Meth. Fluids*, **26**, 369-401.
- Cox, A. T., and V. J. Cardone, 2000. Operational system for the prediction of tropical cyclone generated winds and waves. *6th International Workshop on Wave Hindcasting and Forecasting*, November 6-10, 2000, Monterey, CA
- Cox, A. T., J. A. Greenwood, V. J. Cardone, and V. R. Swail, 1995. An interactive objective kinematic analysis system. Preprints, *Fourth International Workshop on Wave Hindcasting and Forecasting*, Banff, Alberta, Canada, Atmospheric Environment Service, 109-118.

- Feyen, J. C., J. J. Westerink, J. H. Atkinson, R. A. Luetlich, C. Dawson, M. D. Powell, J. P. Dunion, H. J. Roberts, E. J. Kubatko, H. Pourtaheri, 2005. A Basin to Channel Scale Unstructured Grid Hurricane Storm Surge Model for Southern Louisiana, *Monthly Weather Review*, In Preparation.
- Holland, G. L., 1980. An analytical model of the wind and pressure profiles in hurricanes. *Mon. Wea. Rev.*, Vol 108, 1212-1218.
- Jelesnianski, C. P., and A. D. Taylor, 1973. A Preliminary View of Storm Surges Before and After Storm Modifications, *NOAA Technical Memorandum ERL WMPO-3*
- Kalany, E., M. Kanamitsu, R. Kistler, W. Collins, D. Deaven, L. Gandin, M. Iredell, S. Saha, G. White, J. Woollen, Y. Zhu, M. Chelliah, W. Ebisuzaki, W. Higgins, J. Janowiak, K.C. Mo, C. Ropelewski, J. Wang, A. Leetmaa, R. Reynolds, R. Jenne, and D. Joseph, 1996. The NCEP/NCAR 40-year reanalysis project. *Bull. American Met. Society*, Vol. 77, No. 3, 437-471.
- Knabb, R. D., J. R. Rhome, and D. P. Brown, 2005. Tropical Storm Report Hurricane Katrina 23-30 August 2005, National Hurricane Center, Dec 2005.
- Komen, G. J., L. Cavaleri, M. Donelan, K. Hasselmann, S. Hasselmann and P.A.E.M. Janssen, 1994. Dynamics and modelling of ocean waves. Cambridge University Press, Cambridge, UK, 560 pages.
- Powell, M. D., S. H. Houston, L. R. Amat, and N. Morisseau-Leroy, 1998. The HRD real-time hurricane wind analysis system. *J. Wind Engineer. Ind. Aerody.*, 77&78, 53-64.
- Smith, J. M., A. R. Sherlock, and D. T. Resio, 2001. "STWAVE: Steady-State spectral Wave Model User's manual for STWAVE, Version 3.0," ERDC/CHL SR-01-1, U.S. Army Corps of Engineers Engineer Research and Development Center, Vicksburg, MS.
- Thompson, E. F., and V. J. Cardone, 1996. Practical modeling of hurricane surface wind fields. *ASCE J. of Waterway, Port, Coastal and Ocean Engineering*, Vol 122, No. 4, 195-205.
- Tolman, H. L. 1998. A New Global Wave Forecast System at NCEP. In: *Ocean Wave Measurements and Analysis*, Vol. 2, (Ed: B. L. Edge and J. M. Helmsley), ASCE, 777-786.
- Tolman, H. L. 1999: User Manual and System Documentation of WAVEWATCH-III version 1.18. Technical Note, 110pp.
- Westerink, J. J., J. C. Feyen, J. H. Atkinson, R. A. Luetlich, C. N. Dawson, M. D. Powell, J. P. Dunion, H. J. Roberts, E. J. Kubatko, H. Pourtaheri, 2005. A New Generation Hurricane Storm Surge Model for Southern Louisiana, *Bulletin of the American Meteorological Society*, In Review, 2005.

High Resolution Hydrodynamics

Summary of Accomplishments

The present report is an extension of Report 1 and does not include discussion of the goals and objectives of this task.

As discussed in Report 1, the task Estimation of Forces on Levees is focused on providing high resolution time histories of water levels, waves and related forces on levees and floodwalls in the New Orleans area, along with an analysis. Report 1 contained descriptions of the types of models and methods that will be used in these analyses and the reasons for their application to this problem. As required, additional supplemental technical information will be presented in Appendices in the present report to build upon the technical content contained in Report 1.

Initial timelines indicated that we would provide information for all of New Orleans canals and the large flood-protection levees in St. Bernard and Plaquemines Parish in this report; however, sufficient bathymetric and topographic information to allow accurate high resolution computations of the type undertaken here was available only for the 17th Street Canal in time for model runs required for this report. In order to avoid undo speculative results, this report will only examine conditions in these latter areas.

It should be noted that delays in the availability of bathymetric and topographic information required for construction of the 17th Street physical model have also delayed that model somewhat; however, it is hoped that an aggressive testing schedule will allow us to still meet our goal of completing initial testing for waves passing through the entrance to the canal and under the flood-proof bridge near the site of the levee/floodwall failure by mid-March.

Analyses of Water Levels

In areas exposed to the open Gulf, massive quantities of water were driven against miles of coastal levees. Since the appropriate levee heights were modeled in the large-scale ADCIRC and STWAVE runs performed within the Surge and Wave Model Group, the effects of levee overtopping are implicitly included in the boundary conditions provided for the high resolution calculations undertaken here. Levee breaching was not represented in the Surge and Wave Model Group's calculations; however, these effects should be quite small in the St. Bernard and Plaquemines areas.

In contrast to the situation along the open Gulf, water levels within canals can depend strongly on the time of breaching and size of the breaches relative to the canal cross section. As a baseline study, a series of ADCIRC model tests were performed to examine the variation of water surface elevation (WSE) and current speeds within the 17th Street Canal for the case of no breaching. In idealized tests with no wind forcing on water within the canal, the WSE time series throughout varied little (less than 3 cm) from the input forcing hydrograph at the Lake Pontchartrain boundary for simulated conditions during Katrina. This

shows that water levels within these canals will tend to be approximately equal to the level at the boundary, plus the effect of wind set-up along the canal. During these tests, steady currents were quite small (less than 0.1 m/sec) with some seiching, possibly due to numerical effects, producing velocities in the range of 0.35 m/sec.

Detailed Time History of Water Levels, Waves, and Related Forces

St. Bernard and Plaquemines Parish. Boussinesq simulations at four specific levee transects along the Mississippi River Gulf Outlet (MRGO) provide time histories of combined wave and surge water levels, overtopping rates, and flow velocities along the back and front sides of the levees. The northernmost transect is a few miles south of the intersection of MRGO and the Intercoastal Waterway, while the southernmost transect is near the Bayou Dupre Control Structure. Simulations cover the time from 0100 to 1100 CDT on August 29th. The largest waves and surge occur at roughly the same time (0700-0800). Maximum surge values were near 18 feet along MRGO, while maximum wave heights were 2-3 ft. The levees at the four transects experience similar conditions. Wave spectra were taken from STWAVE simulations (Surge and Wave Model Group) at locations inside the MRGO, and thus predicted wave heights were relatively low due to dissipative propagation over the marshes of Lake Bourne. At peak wave height, the predicted wave-induced increase in the mean water level (setup) at the levee toe was 1-1.5 ft.

Maximum overtopping rates occur at 0800, with wave-averaged values near 10 ft³/s per ft of levee length. This corresponds to an average flow depth over the levee crest of approximately 1.5 ft and an average velocity of 6.5 ft/s. On the backface of the levee, the gravity driven downrush velocities occur at maximum overtopping, with wave-averaged values near 10 ft/s, and instantaneous velocities reaching 15 ft/s. Simulations suggest that average backface velocities exceeded 10 ft/s continuously for 1 hour (0730-0830), and 5 ft/s for two hours (0700-0900). From 0630-0900, the simulations predict continuous overtopping. For approximately one hour before and one after this time period, predicted overtopping was intermittent and due to only wave overwash. During these times, the predicted uprush and downrush velocities along the front face of the levees are maximum. These velocities are related to the swash oscillations, with maximum runup velocities near 10 ft/s, and downrush velocities of 5 ft/s. These values are peak values, with time and depth-averaged values of horizontal velocity on the front face very small during periods of non-continuous overtopping. The vertical profile of the time-averaged velocities (undertow) will be investigated further if needed.

17th Street Canal. As noted above information on the timing of breaching and the size of the breach are extremely important to the estimation of water levels within a canal. The following provides an analysis of the nature of this interrelation. As shown, for sufficient breach size, it is possible for water levels at the breach to remain constant or even become lower while water levels at the entrance continue to rise. In this context, observed water levels and eye-witness accounts become a vital part of the methodology for estimating water levels during the storm.

Figure V-50 shows valuable information collected by Data Collection and Management Group, along with the time series of ADCIRC water levels at a point near the entrance of the canal. The data cover the period during and immediately after passage of Hurricane Katrina. In Figure V-50, the solid line denotes the “best fit” to observed and photographed water levels throughout Katrina. Open circles, open triangles, and x’s denote the sources of data used in this compilation. The dashed line and black dots show the ADCIRC results; and the red dots show reports of water levels observed by the pump operator at the south end of this canal. Also shown in this figure is an estimate of the water level shortly after 1100 CDT on the same day, obtained from a frame of an amateur video taken from a nearby high-rise building near the shore of Lake Pontchartrain. Figure V-51 shows the video frame. The top of the levee on the west side of the canal, inside the canal, is estimated to be at elevation +3 ft NAVD88 2004.65. The top of the wall is at approximately +12.5 feet NAVD88 2004.65. The estimated water level from this photo is approximately +2 ft, ± 2 feet, NAVD88 2004.65. The estimated water level from this photo is approximately +1 ft, ± 2 feet, NAVD88 2004.65.

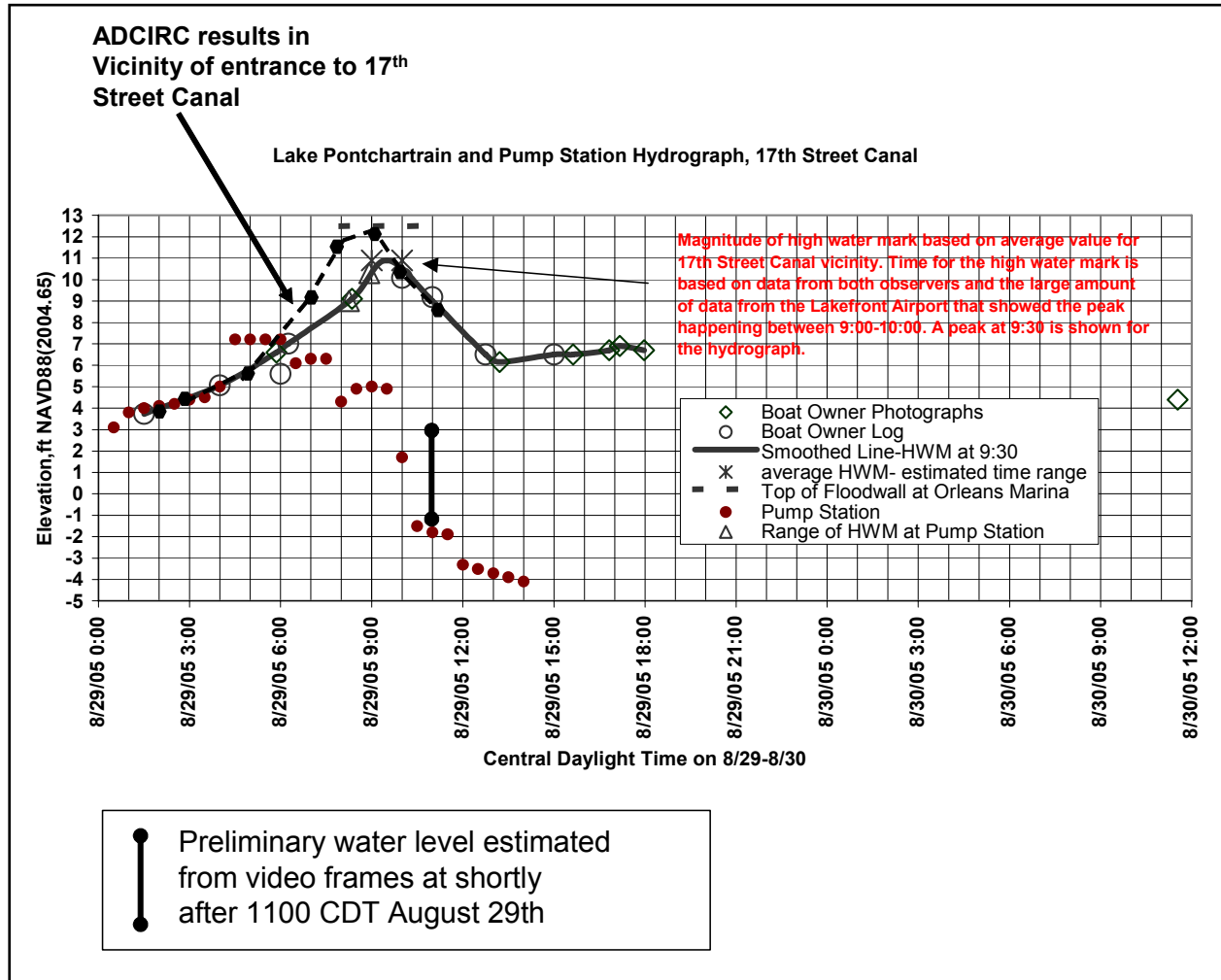


Figure V-50. Observed and estimated water levels inside and in the entrance to the 17th Street Canal during Hurricane Katrina



Figure V-51. Frame from a video of the breach in the 17th Street Canal shortly after 11:00 on August 29th

At this point, we can say with some certainty, as confirmed by at least two independent observers, that the floodwall had already failed by daybreak on the morning of Katrina. Examination of the water levels in Figure V-50 suggests that the water level at the time of failure was in the range of +6 to +7 feet (NAVD88 2004.65). Subsequent analyses and discussions with the pump operator who made the observations at the south end of the canal are in progress and once these are complete, we will be able to provide appropriate results, including estimates of uncertainties, for the critical period near the peak of Katrina.

As can be seen from the above discussion, there is some uncertainty in the water levels that should be used in analyses of wave conditions within this canal. It is also important to recognize that results from the physical model should provide valuable information for subsequent model runs within this canal. However, in spite of these potential complications, we believe that it is possible to provide reasonable first estimates of wave conditions during the storm. Figure V-52 shows estimated wave heights at the site of the breach based on two different sets of assumptions. The line labeled “wave height 1” includes an estimated decay due to the bridge and debris on the north side of the bridge; whereas, the line

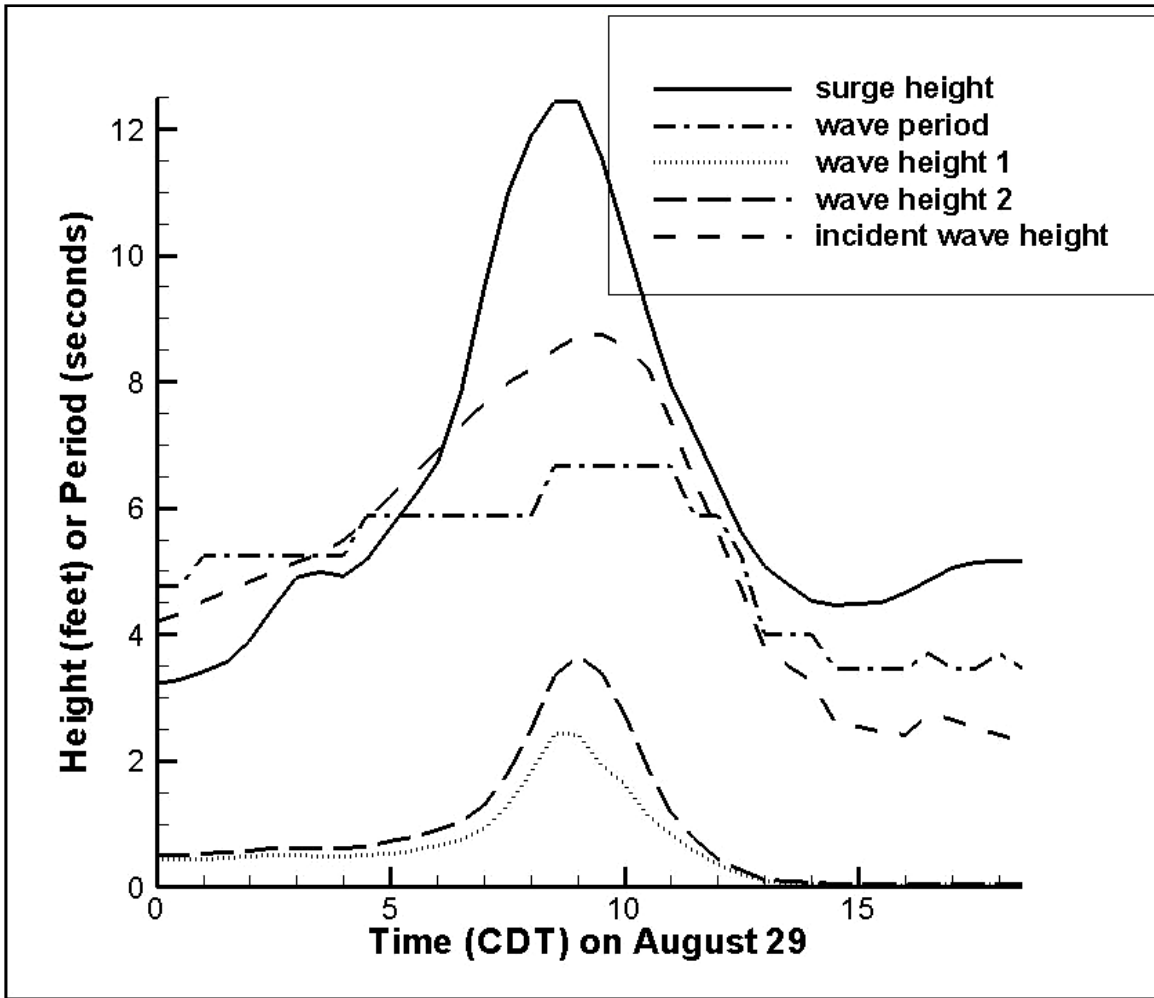


Figure V-52. Time series of estimated water level and wave conditions at the site of the 17th Street canal breach, under the assumption that water levels at the breach are equal to those at the entrance

labeled “wave height 2” neglects this decay. Water levels throughout the storm are set to the water levels shown in Figure V-52. Wave periods are essentially the same for the entrance of the canal as reported by the Surge and Wave Model Group.

Boussinesq simulations indicate that wave heights in the canal at the time of breach (~0600 CDT) were less than 1 ft. These simulations do not yet include any dissipation or reflection due to debris or the bridge, and also do not include wave growth due to wind forcing. These simulations do capture the complex, 3D bathymetry-driven wave transformation at the canal entrance. The small predicted wave height in the early morning leads to pressure predictions that are dominantly hydrostatic, with wave-related bottom pressure oscillations of 21 – 25 psf in amplitude with period of 5 - 8 seconds, or a wavelength of 110 - 210 ft in 26 ft of water. Hydrostatic bottom pressures at this time were approximately 1600 psf. Simulations at later times, when the wind and wave direction was better aligned with the canal orientation (roughly 1200 CDT), predict larger wave

heights in the canal, approaching 3 ft. Preliminary runs also indicate the possible existence of a complex 3D wave field inside the canal, with certain sections of the canal experiencing cross-channel oscillations. Physical modeling is necessary to investigate the existence of such modes.

The dynamic forces and moments acting on the flood walls due to waves could be significant to wall stability. For purposes of illustration here, we consider the reasonably representative case of a mean water level of 5 ft against the floodwall and a wave height of 2 ft propagating along the wall. The static hydraulic force and moment about the base per unit wall length for this scenario are 800 lb/ft and 1333 ft-lb/ft, respectively. Applying linear wave theory for this example, the percentage fluctuating force and moment contributions relative to static values at the wave crest and trough are shown in Table V-4 below.

Table V-4 Percentage Change From Hydrostatic Forces and Moments on a Floodwall With a Mean Water Depth of 5 feet and a 2 foot Wave Height		
Percentage Change in	Under Crest	Under Trough
Force	+ 44 %	- 36 %
Moment	+73 %	- 49 %

The results of the simple calculation in Table V-4 illustrate that waves can play a potentially significant role in the integrity of a flood wall. Additionally, the effect of fluctuating forces and moments may be relevant to foundation stability. Finally, the fluctuating forces and moments would propagate along the flood wall, thereby causing shear forces between the adjacent wall panels. In summary, the role of fluctuating loads on the flood walls may be significant and should be considered in this evaluation. Although the simple example here has considered only a single linear wave, the final results will evaluate the forces and moments associated with irregular and nonlinear waves.

Barge Motions and Forces in the Inner Harbor Navigation Canal

A limited description of the work conducted on this issue was presented in Report 1. The complete treatment and summary is presented in the following paragraphs.

This analysis relates to the motions of and potential collision forces due to a free floating barge under the action of wind forces. The issue addressed is whether the barge that floated through the east floodwall of the IHNC Canal could have contributed to its failure through impact.

The equations governing the effective wind speed acting on a barge present in the wind boundary layer are examined and an effective wind speed defined for drag force calculations. Static wind forces and moments acting on a lightly loaded barge and then transferred to the east IHNC floodwall due to a wind speed of 100 miles per hour have been examined and found to represent a reasonably

small fraction of the hydrostatic forces and moments exerted directly on the floodwall. These forces and moments have been expressed as averages per unit length on the floodwall although the barge related forces were likely transferred as a concentrated loading rather than uniformly.

The equation of motion of a freely floating barge has been developed and cast in non-dimensional form for easy application. The equations include development of the terminal velocity of the barge. The equation is solved for the non-dimensional velocity and displacement.

It is found that the terminal velocity of the barge is achieved rather quickly for the wind speed examined (100 miles per hour) and that for barge conditions in the INHC the momentum and energy impact on the east flood wall depend primarily on the draft of the barge during the event. Simplified equations have been presented for terminal momentum and energy for use by others in evaluating whether the barge was a contributor to the failure of the INHC flood wall in the Lower Ninth Ward area. The forces depend on the details of the collision including the time over which the momentum is transferred from the barge to the floodwall and the orientation of the barge relative to the wall during impact.

Hydraulics of 17th Street Canal Including Breach Characteristics

The availability of data relating to the hydraulics and breach characteristics in the 17th Street Canal provide a unique opportunity to evaluate the contribution of this breach to the flooding during Hurricane Katrina.

The water level time history in Lake Pontchartrain was established through interviews and collection of other perishable information by the Data Collection and Management Group. Additionally, the pump operator at the south end of the 17th Street Canal recorded visual observations of the water level on a staff at this location. These results combined with limited eyewitness accounts of the timing of breach width characteristics provide the basis for the preliminary hydraulic analysis. The main results of that analysis are reviewed in the following paragraphs.

The initial breach appeared to have occurred at approximately 0600 (CDT) on August 29, 2005 and was later observed to be wider at 0900 on the same day. Standard steady state hydraulic calculations were carried out to estimate the time history of discharges into the canal from Lake Pontchartrain and through the breach. With these estimates available, the consideration was made that the flow through the breach was critical which allowed the breach sill elevation to be estimated.

The peak breach discharge occurred at approximately 0900 on August 25, 2005 at slightly greater than 40,000 cfs. The minimum sill elevation also occurred at 0900 and was approximately -12.1 feet. The next phase of this analysis will reduce uncertainties in the observational data to the degree possible and will evaluate the reasonableness of the calculations. It is noted that the

ADCIRC numerical model is also being applied to evaluate the hydraulics in this canal.

Physical Model

The 14,000 sq ft, 1:50 scale, physical model of the 17th St Outfall Canal has been constructed as of this report date and is being readied for testing. Construction was performed in 6 weeks for a model area that would typically require 4 months to construct. A physical model at this scale is a useful tool in providing objective results for wave conditions in the canal during the storm. The physical model includes reproduction of over one mile along the lakefront, the Hammond Highway Bridge, and a portion of the canal 1200 ft beyond the breach zone. Figure V-53 shows the model during the final stages of construction. Data collection will now be initiated with wave and water level conditions determined from numerical models conducted by the Surge and Wave Model Group. Wave data from the physical model will aid in the calibration of numerical wave models for wave transmission and these models will provide detailed response of the entire canal to short and long wave energy. Tests will proceed from the present to April 15. Appendix E discusses the physical model work in greater detail.



Figure V-53. Physical model during construction; left photo showing overall view, and right view looking south, down the 17th St Canal

Interim Results

ADCIRC Model Tests

A series of ADCIRC (Luetlich and Westerink, 2004) model tests were performed to examine the variation of water surface elevation (WSE) within the 17th Street and London Avenue Canals. In addition, a series of sensitivity tests were performed to investigate the effect of boundary condition specification and bottom friction on predicted WSE's and current speeds. The grid domains used for these tests are shown in Figure V-54.

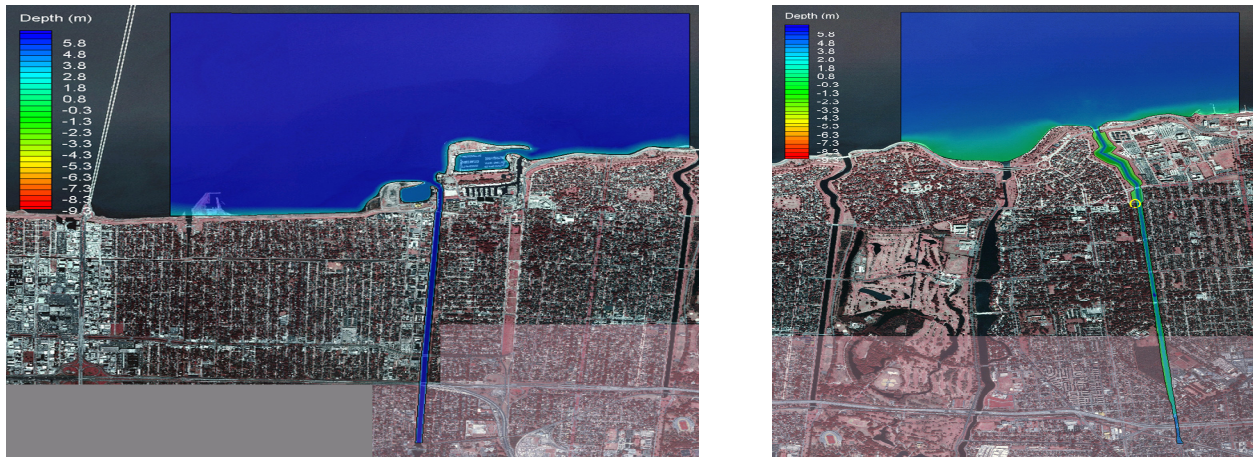


Figure V-54. 17th Street (left) and London Avenue (right) Canals grid domains

Simulations to date have been performed using Lake Pontchartrain WSE boundary forcing only (provided by regional surge and wave modeling efforts). Therefore, all results presented herein do not include additional water level and velocity contributions from locally-generated wave and wind effects. Furthermore, all simulations to date were performed without allowing the canals to breach.

In both the 17th Street and London Avenue Canals, maximum velocity magnitudes during the storm, in the absence of a breach, were small, on the order of 0.35 m/s. A long-period (on the order of one hour) oscillation in the velocity field was simulated in both canals during rising surge.

The WSE time series throughout both canals varied little from the input forcing hydrograph at the Lake boundary (Figure V-55). At the storm peak, water level inside the canal was less than 3 cm different from that in the Lake. No long-period oscillation in water level was observed in the simulated results.

Lateral Boundary Condition. The effect of the specification of lateral boundary conditions is shown in Figure V-56. The lakeward boundary condition is a time series of WSE from the Katrina ADCIRC output provided by Surge and Wave Model Group. The lateral boundaries are specified as combinations of radiation and slip wall (zero-gradient). “West Rad” corresponds to a radiation boundary condition on the west boundary and a slip wall on the east. The “Both Rad” and “Both Wall” are what they state. It is seen in Figure V-56 that WSE variations at the breach are essentially the same regardless of the boundary condition specified, with the exception that the case without radiation boundaries (“Both Wall”), which traps a reflected wave.

The time variation of the WSE as a function of position within the 17th St. Canal is shown in Figure V-57, in which the WSE at the Breach location, Mid-Canal and at the pump station are nearly identical.

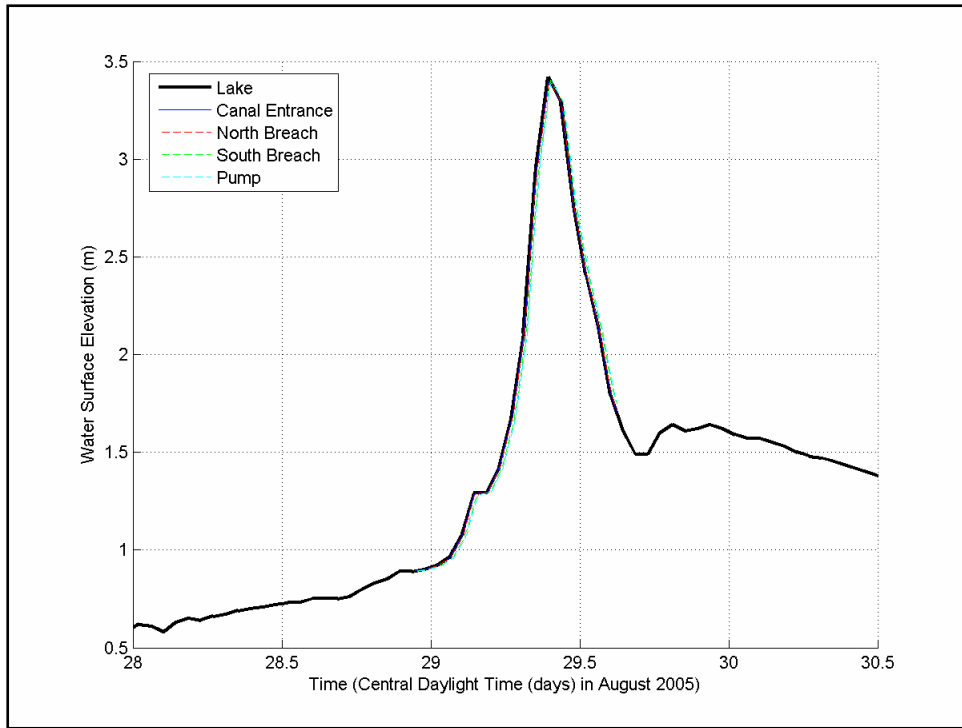


Figure V-55. London Avenue Canal water surface elevation timeseries compared with input Lake forcing timeseries

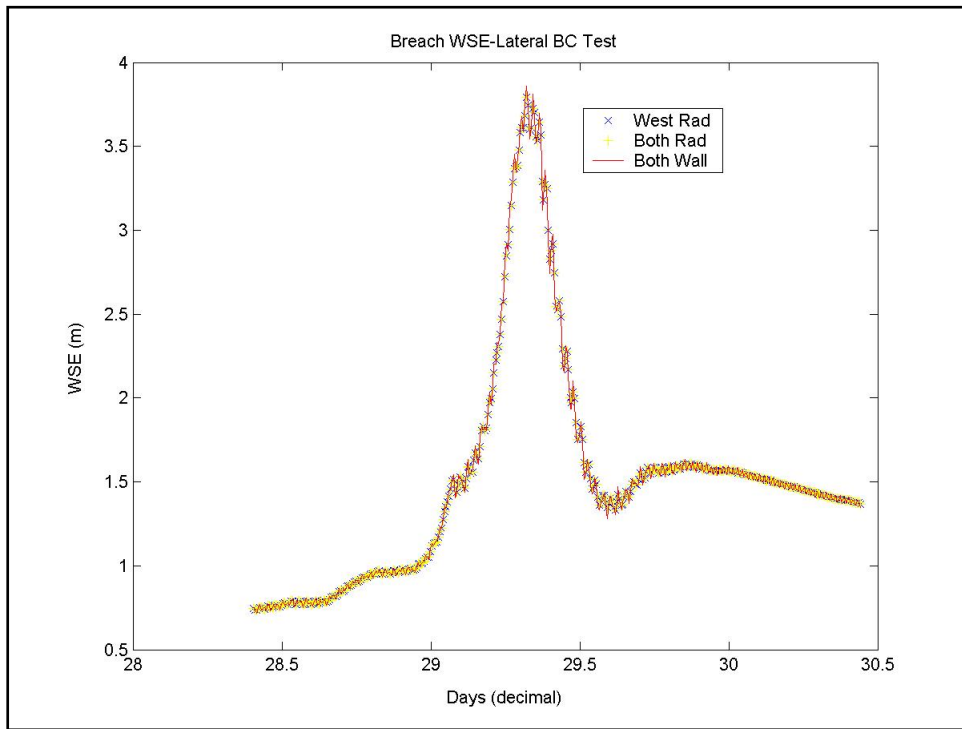


Figure V-56. Lateral boundary condition tests

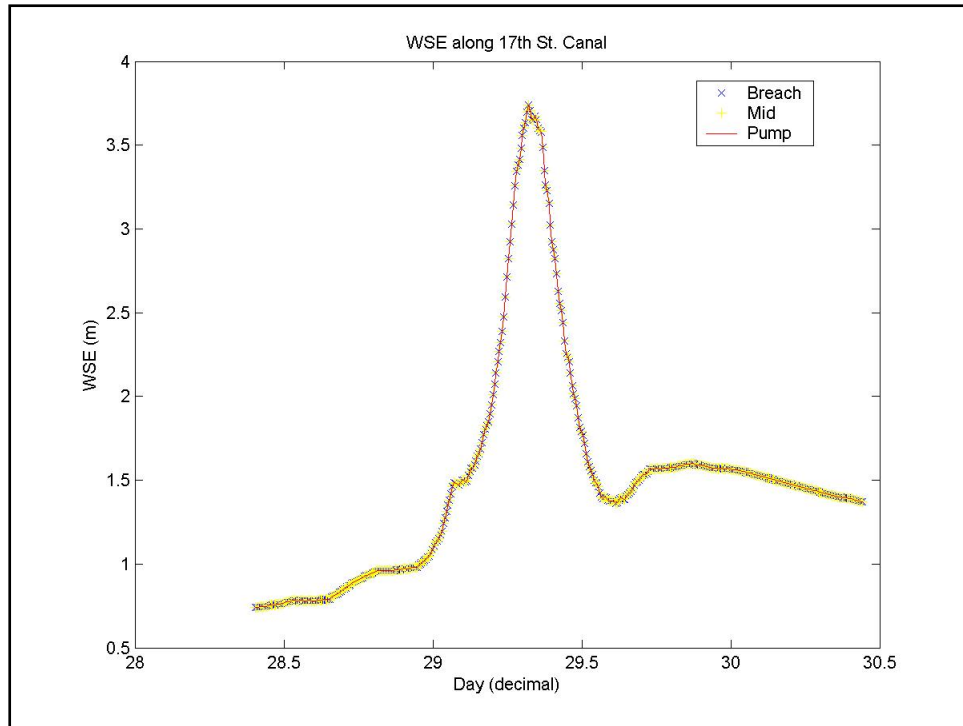


Figure V-57. Along channel water surface elevation variation. “Both Rad” lakeward boundary

Canal Side-Wall Boundary Condition. A series of tests were conducted to investigate the canal side-wall boundary condition using the London Avenue ADCIRC mesh. Two boundary conditions were tested: 1) a slip condition, representing an idealized flow at the canal walls and 2) a no-slip condition, representing the effects of viscosity on the flow at the canal walls. Figure V-58 gives snapshots of the velocity fields with the slip and no-slip boundary.

The impacts of this boundary condition are evident in the velocity magnitude patterns, where velocity magnitude drops to zero at the canal walls using the no-slip boundary condition. In contrast, the velocity magnitude across the canal is more uniform when a slip boundary condition is used. Peak velocity magnitude occurs at the canal entrance during rising surge for both the slip and no-slip scenarios and is 0.35 m/s and 0.25 m/s, respectively. While the percent difference is large, 30%, the velocity magnitudes in both scenarios are small.

While there are some differences in the velocity fields between the slip and no-slip cases, differences in water level within the canal are imperceptible. Furthermore, these differences in water level are well within the uncertainty of the water level hydrograph input and numerical model error.

Bottom Friction. To determine the relative impact of friction on the velocity fields and water levels within the canals, sensitivity tests were conducted using the London Avenue Canal ADCIRC mesh. Bottom friction was defined throughout the model domain using a quadratic friction law, with the dimensionless friction factor, C_f , held constant. Two values of the dimensionless friction factor

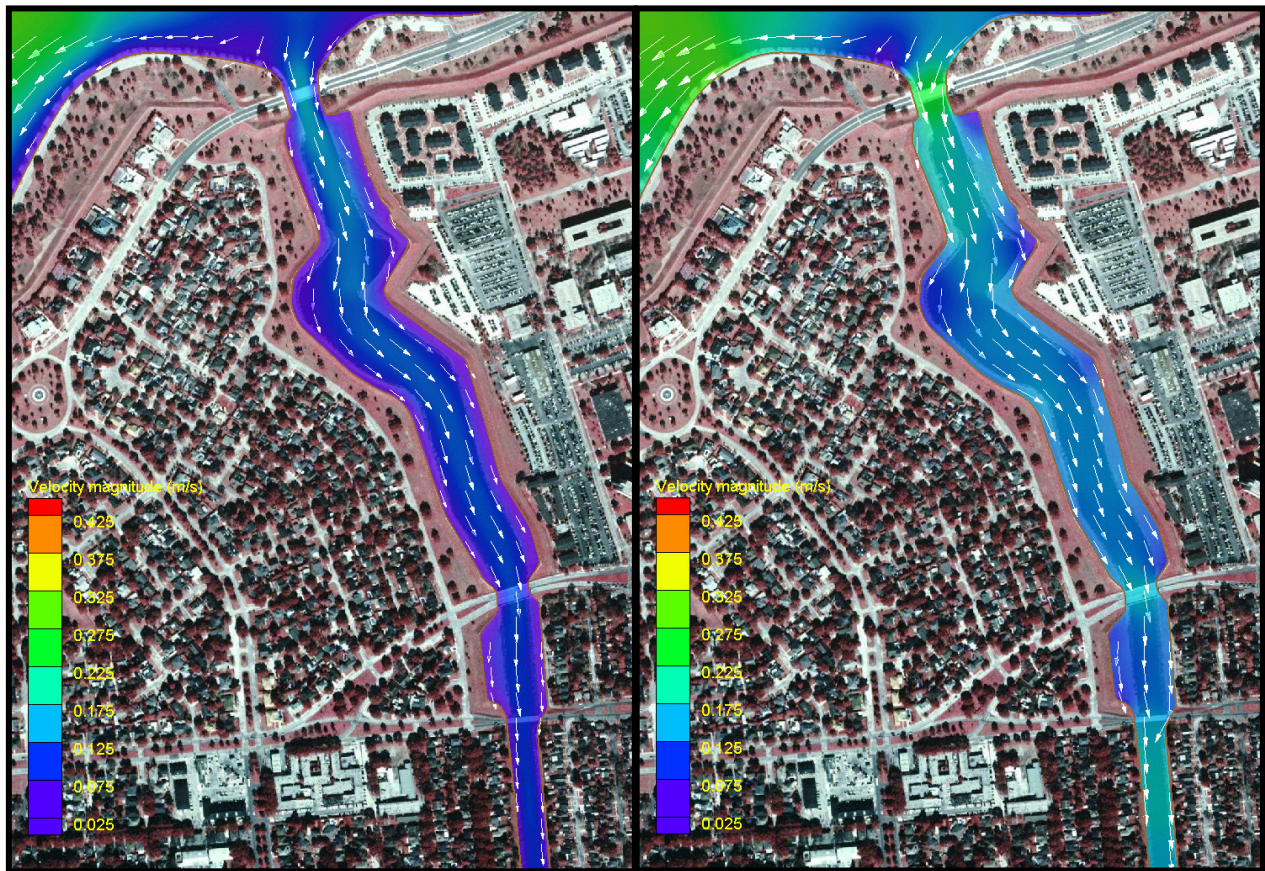


Figure V-58. Snapshot of ADCIRC velocity fields in London Ave Canal during rising surge for no-slip (left) and slip (right) boundary conditions

were assessed: 0.003, representing a smoother bottom, and 0.005, representing a rougher bottom. These values were selected to represent a reasonable range within the canals and follow the recommended values presented in Chow (1959). As with the side-wall boundary condition investigations, bottom friction impacts to water levels within the canal were imperceptible. In addition, the differences in velocity fields were small, with the largest differences occurring at the canal entrance during rising surge. Here, the largest difference was 0.01 m/s, or 3%.

Boussinesq Modeling

Basic Boussinesq Model Information: COULWAVE. COULWAVE (Cornell University Long and Intermediate Wave model) was developed by Patrick Lynett (Texas A&M) and Phil Liu (Cornell) at Cornell during the late 90's. The target applications of the model are nearshore wind wave prediction, landslide-generated waves, and tsunamis, with a particular focus on capturing the movement of the shoreline, i.e. runup, overtopping, and inundation.

COULWAVE has the capability of solving a number of wave propagation equations; however the applications for this project use the Boussinesq-type equations. To derive the Boussinesq-type model, one starts with the primitive equations of fluid motion, the Navier-Stokes equations, which govern the

conservation of momentum and mass. The fundamental assumption of the Boussinesq is that the wavelength to water depth ratio is large; thus the model is not applicable for deep water waves. This fundamental assumption yields additional physical limitations, such as the vertical variation of the flow must be small, and turbulence must be parameterized – physics such as wave overturning and overtopping of vertically-walled structures are, theoretically speaking, beyond the application bounds of the model. Applications for which COULWAVE has proven very accurate include wave evolution from intermediate depths to the shoreline, including turbulence dissipation from wave breaking and bottom friction.

Additional Details on Wave Simulation near and inside the 17th Street Canal. These two-horizontal-domain simulations use the ADCIRC grid in the vicinity of the canal. The ADCIRC grid is down-interpolated using an inverse distance weighted algorithm with care taken to eliminate coarse grid artifacts such as stepped bathymetry profiles. The total Boussinesq numerical grid is 1.8 mi², using a 4.9-ft grid step in both horizontal directions. The incident wave spectra are provided from STWAVE runs and water levels are provided from ADCIRC.

The first simulation recreates conditions near the canal at 0600 on August 29th; a time near the initiation of the breach. Waves approach the canal from the northeast with a significant wave height of 6.6 ft. The surge at this time was roughly 6.6 ft. Figure V-59 shows a snapshot in time of the wave field near the canal entrance. This simulation suggests that the marina just to the northeast of the canal entrance acts as an effective obstacle to wave energy approaching the canal. Wave heights in the canal are near 0.82 ft. Figure V-60 gives the canal-length profile of wave height, mean wave period, and mean bottom pressure oscillation (amplitude of the dynamic bottom pressure). Time series of free surface and bottom pressure are written to derive this data, and 15 minute segments are analyzed, taken 45 minutes after the start of the simulation. Generally, wave properties are constant through the canal, with slightly larger values at the northern segments south of the bridge. Note that this simulation likely underestimates the dissipation/reflection of wave energy by the marina and the residential area to the east of the canal, as the utilized elevation map characterizes this area as flat, and neglects the widespread infrastructure.

A second simulation was run using a wave spectra approaching the canal from a nearly normal direction, relative to the canal orientation. This situation corresponds to a time near 1200, with a wave height of 5.3 ft and surge of 6.6 ft. A snapshot of this simulation is shown in Figure V-61. Due to a more direct approach into the canal, wave heights in the canal are a much larger fraction of the incident wave, approaching 3.3 ft. This simulation also suggests the possibility of cross-channel modes, which can be inferred from the braided wave pattern in Figure V-61.

Additional Details on Wave Simulation along MRGO Levees. Wave impact on levees along MRGO are simulated at four specific transects, as shown in Figure V-62. The levee profiles are taken from the “Lake Pontchartrain, LA and Vicinity Design Memorandum No. 3”, dated November 1966. Incident wave

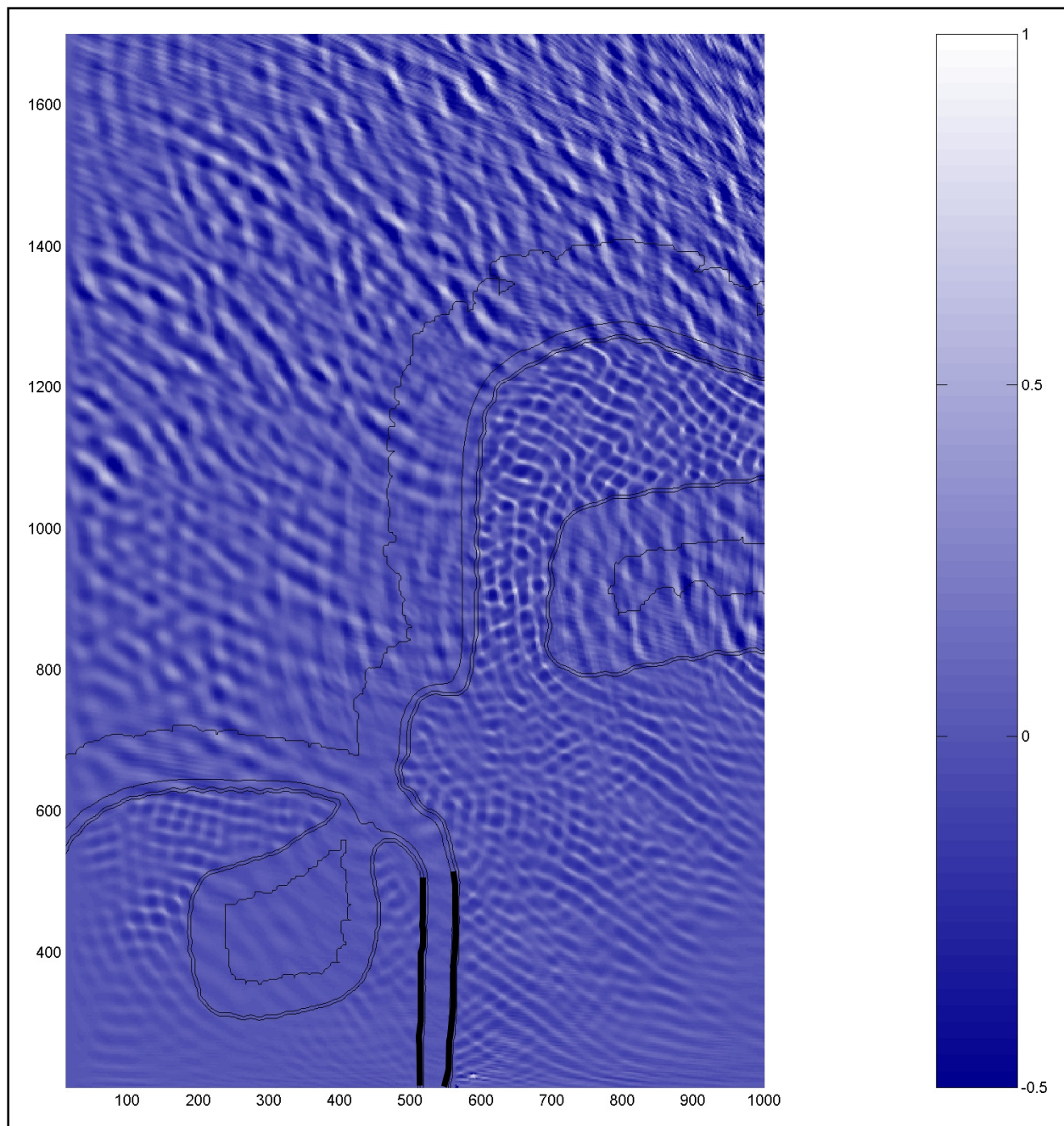


Figure V-59. Snapshot of Boussinesq simulation corresponding to a local time of 0600

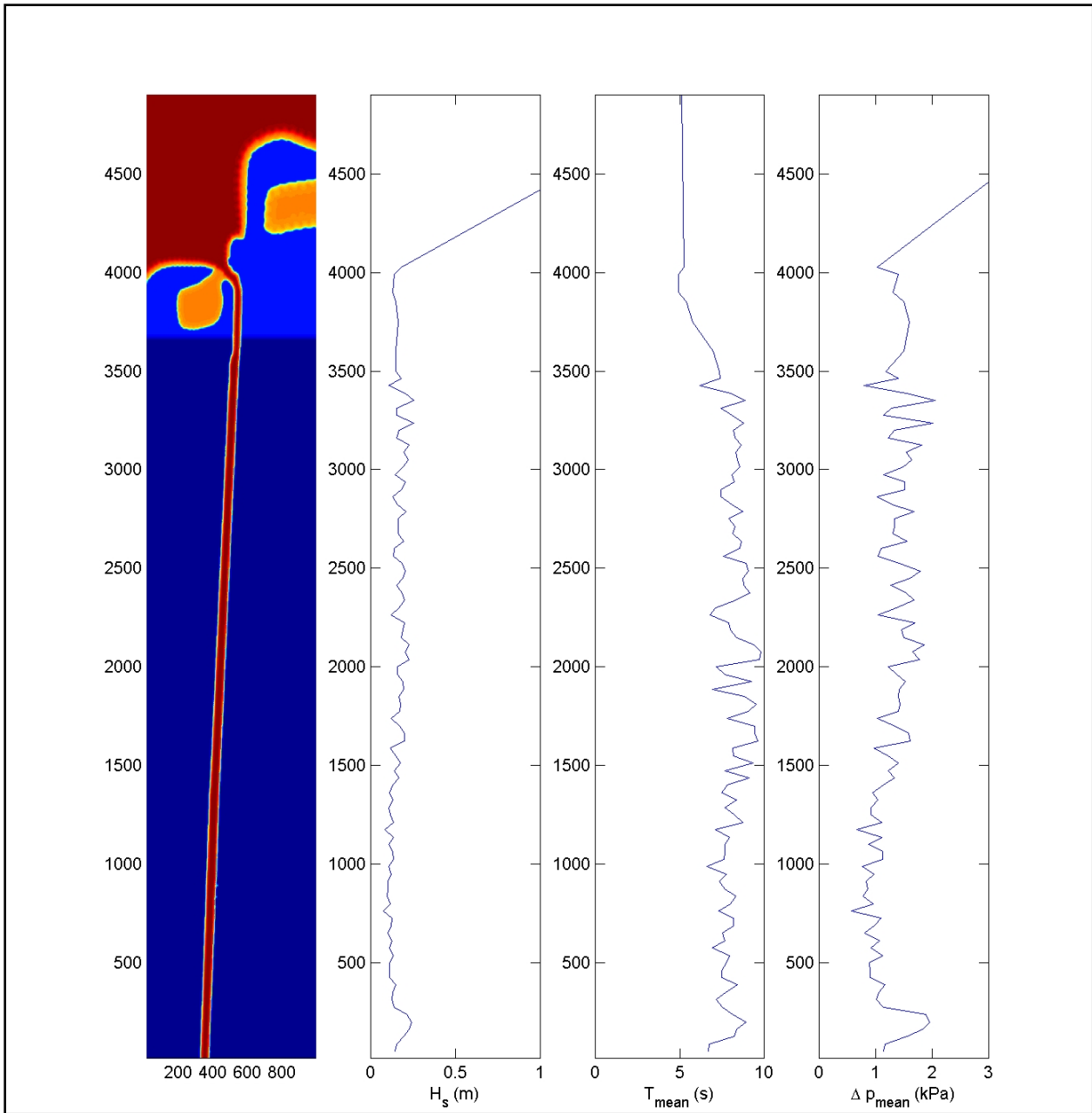


Figure V-60. Canal length profiles for the 0600 simulation

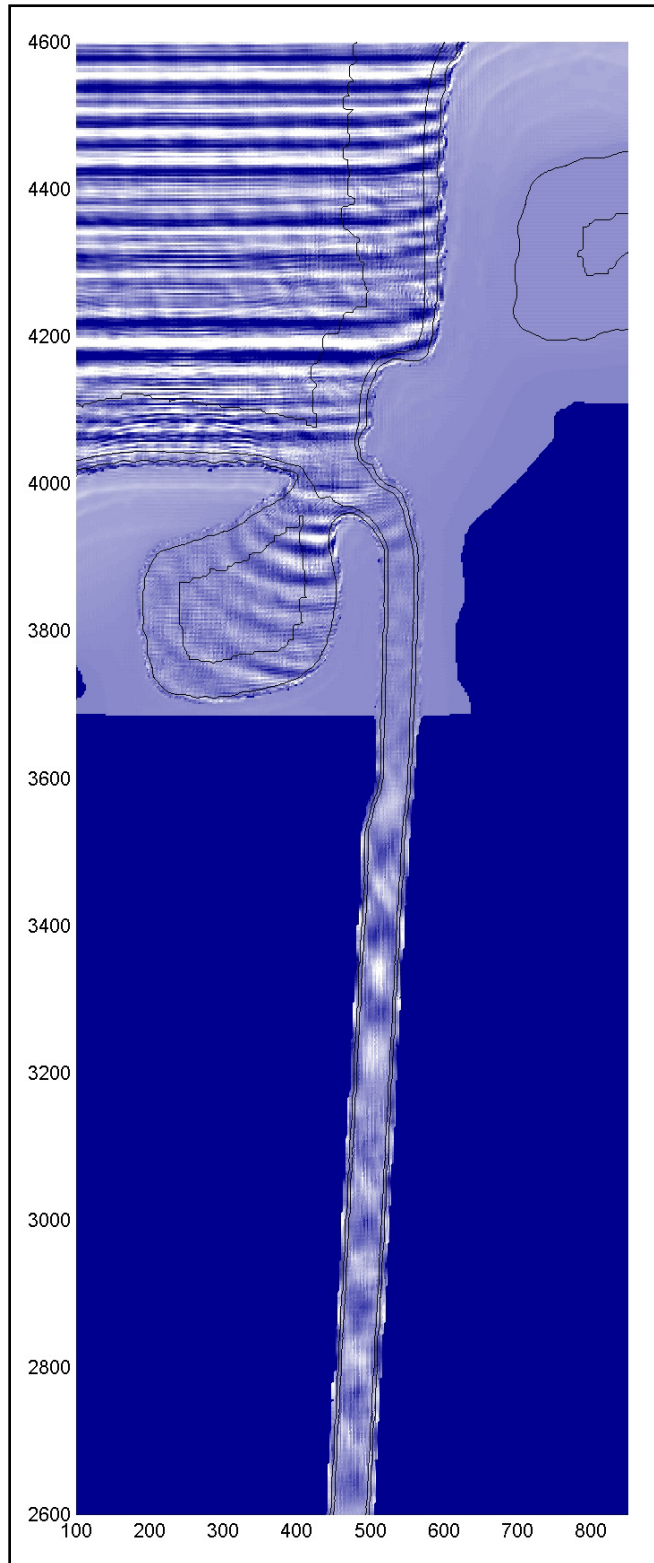


Figure V-61. Snapshot of free surface elevation for the normal incidence wave spectra

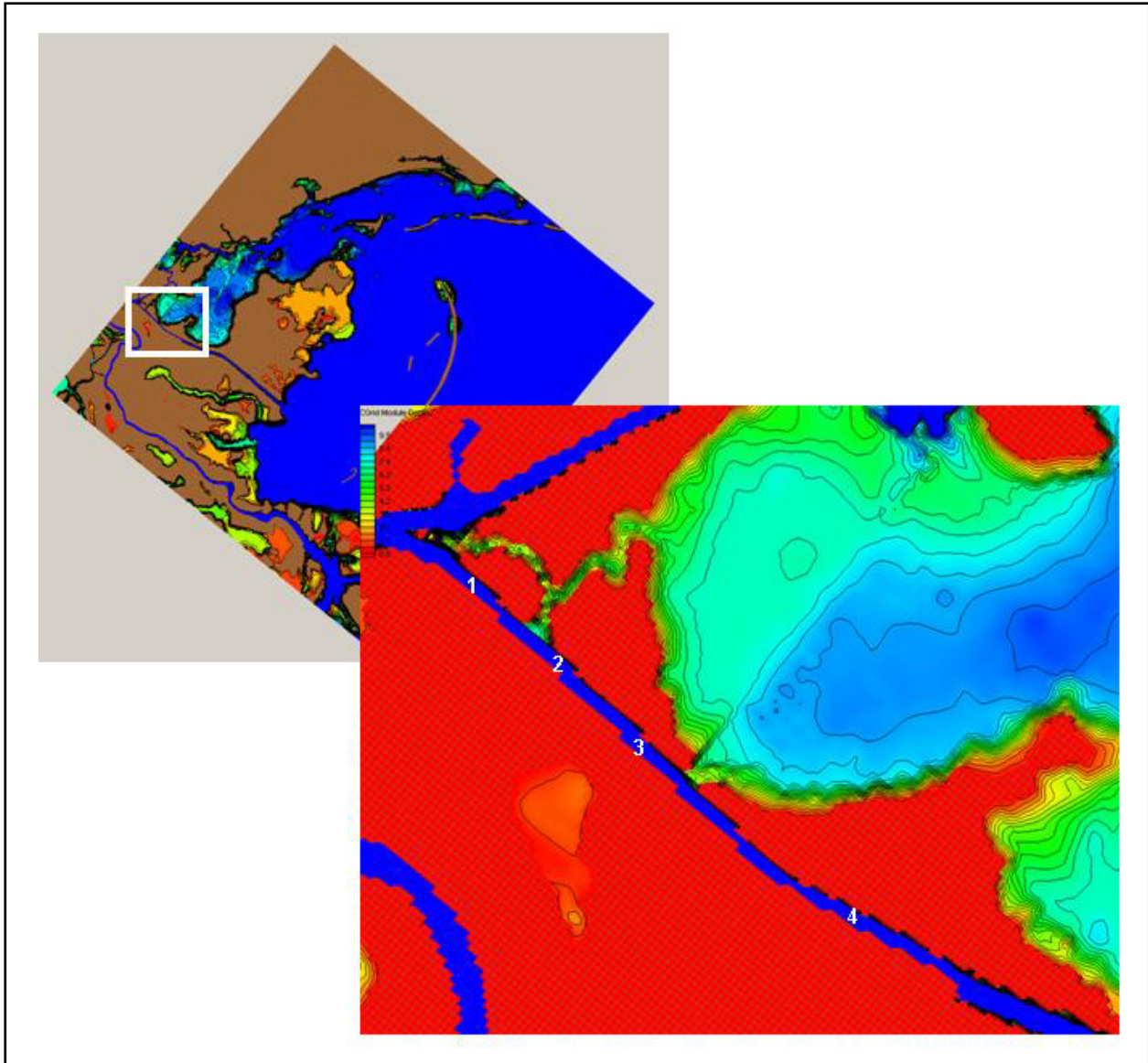


Figure V-62. Location of MRGO transects for simulation

conditions are provided by STWAVE and surge levels by ADCIRC. For each transect, wave spectra and surge levels are specified at 30 minute intervals, from 0600 to 1800 UTC (0100 – 1300 CDT). At each time interval, a simulation is run. An example snapshot from a simulation is given in Figure V-63. These simulations use a 1.64-ft grid, and are run for 30 minutes, with the last 15 minutes of output analyzed.

The time series output of each simulation is distilled into maximum and mean values of frontface runup, frontface velocities, overtopping flux, and backface velocities. Plots of these values for each station are given as Figures V-64 to V-67.

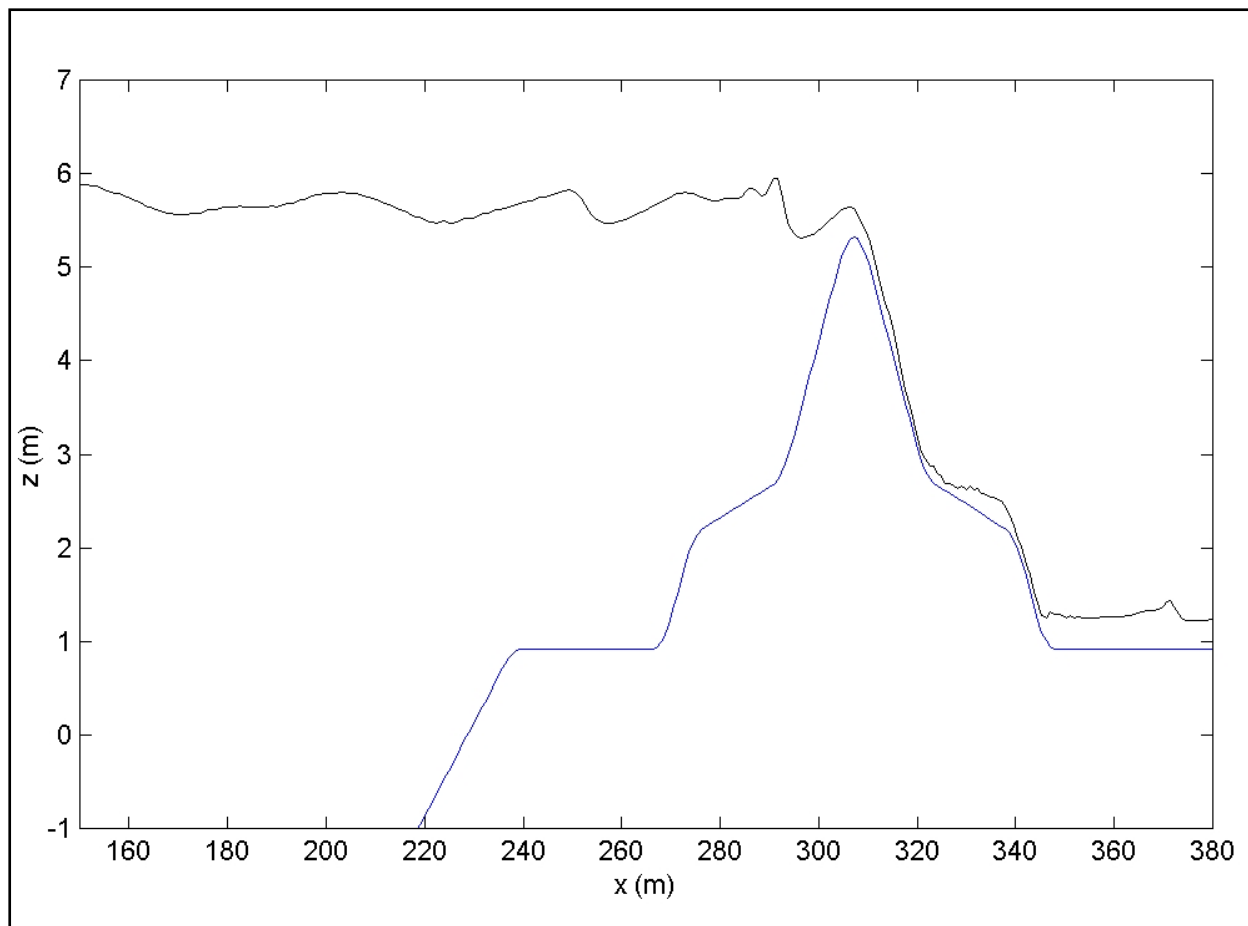


Figure V-63. Simulation snapshot from MRGO station 540 (location #2) at time 1200 UTC (0700 CDT)

Hydraulics of the I7th Canal Breach During Katrina Flooding

Introduction. This develops and provides a preliminary application of an engineering methodology for the analysis of the hydraulics in the 17th Street Canal. The analysis applies the time histories of the water levels at the two ends of the Canal and the geometric characteristics of the canal to estimate the flows through the breach at the 17th Street Canal as a function of time. Based on these results and eye witness accounts of the times of initial failure and later widening of the breach through the levee, approximate discharges through the breach and dimensions of the breach as a function of time are developed. The discharges through the breach will be used in conjunction with other information relating to flooding to improve understanding of the several sources contributing to and the timing of flooding.

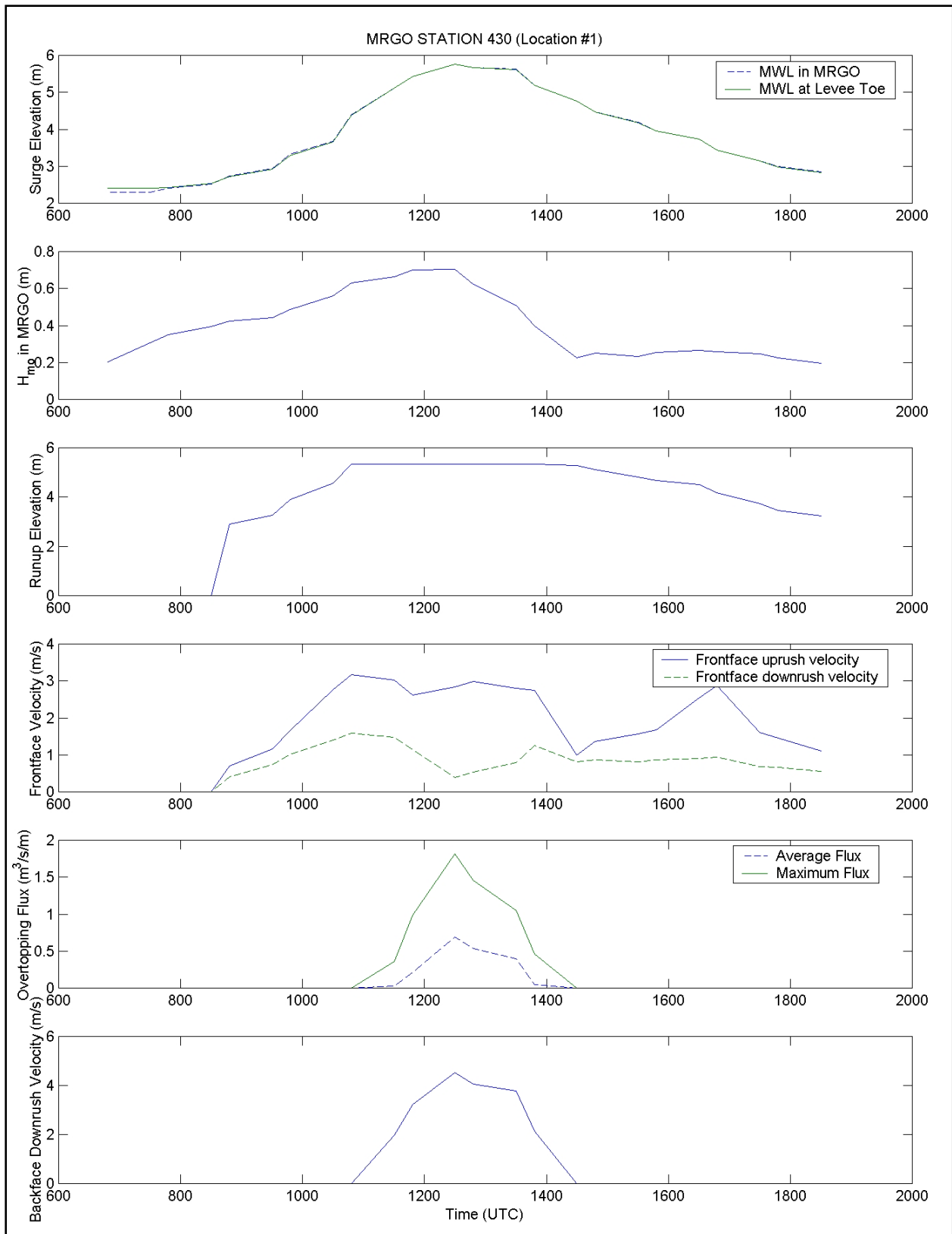


Figure V-64. Simulation summary for MRGO station 430

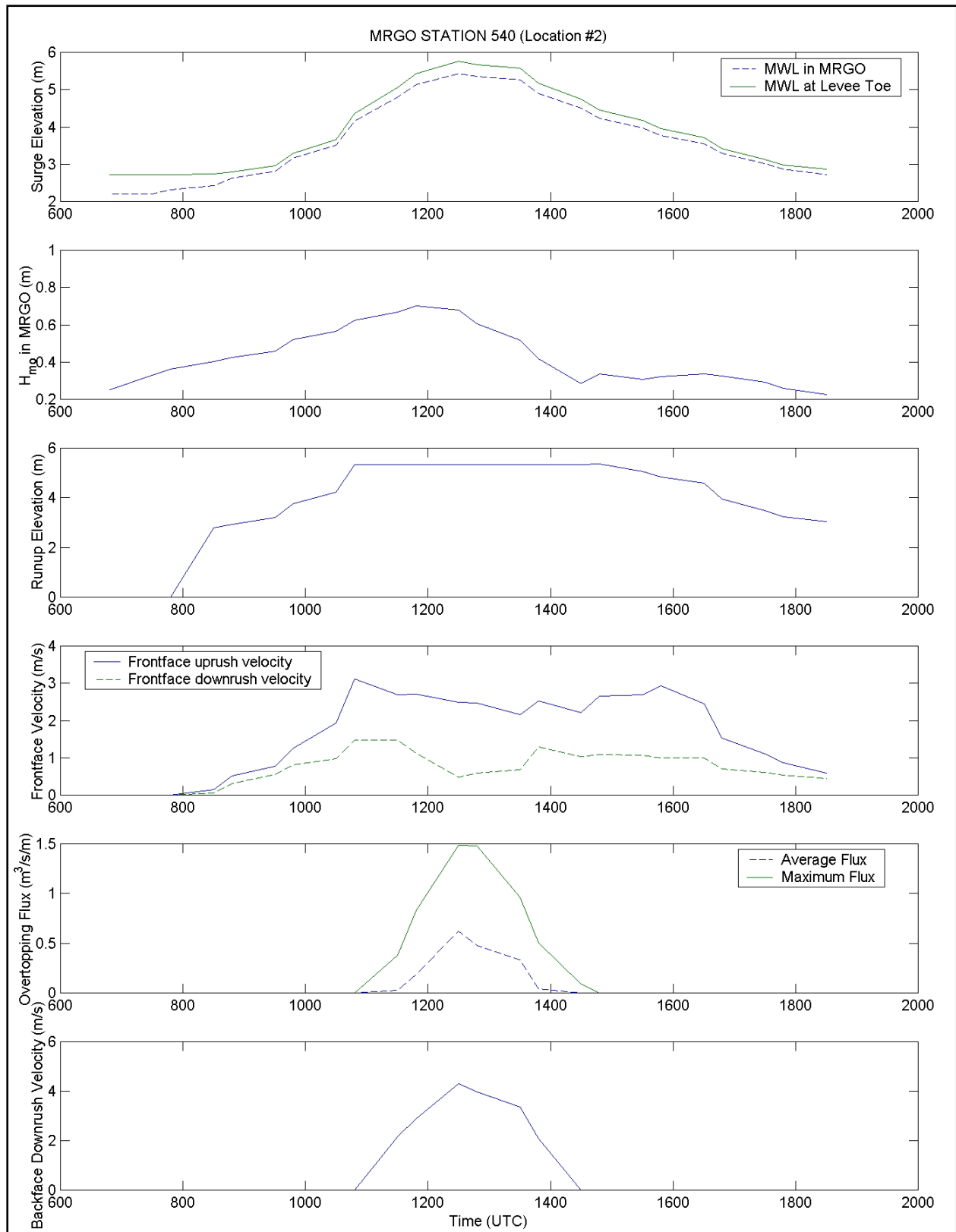


Figure V-65. Simulation summary for MRGO station 540

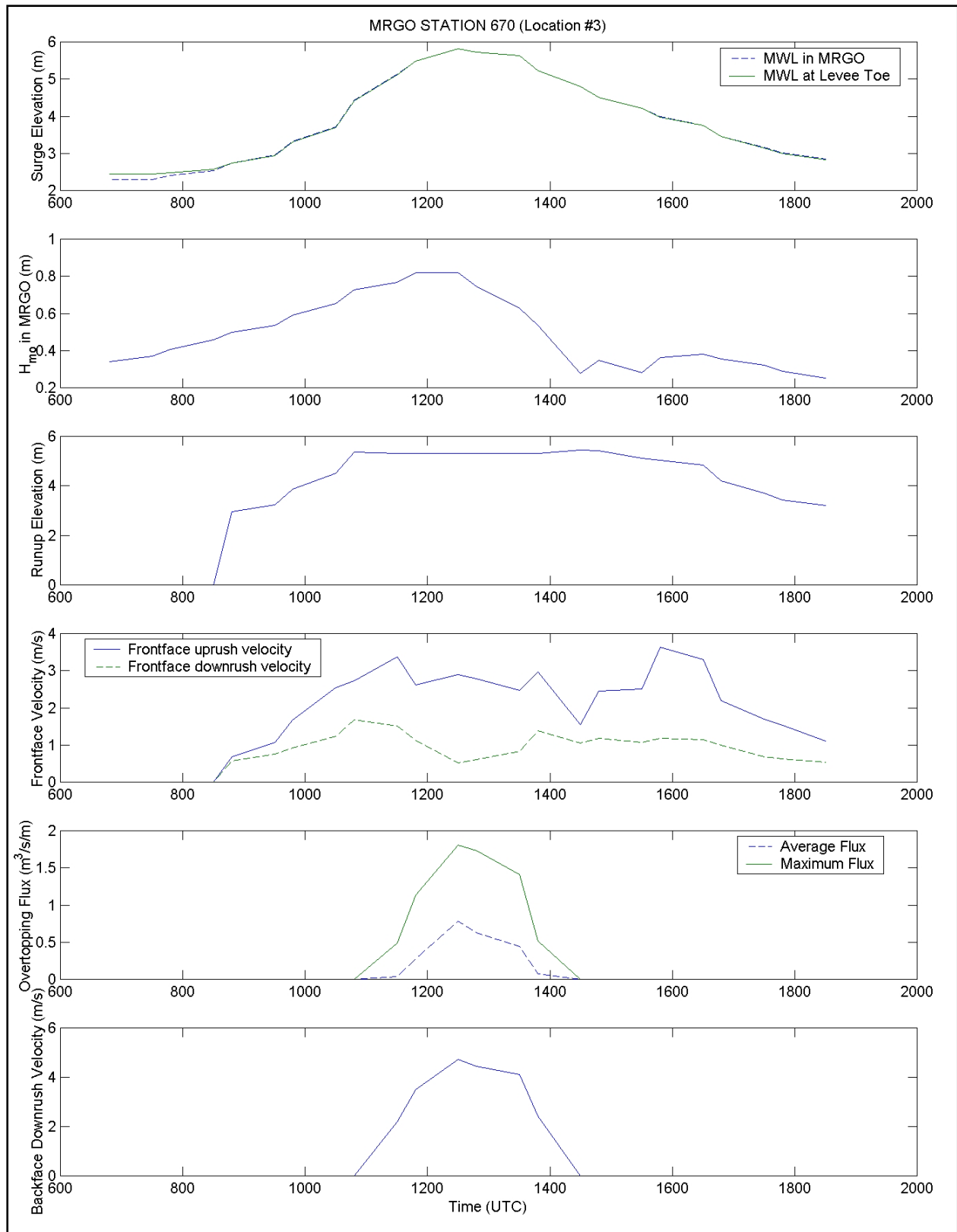


Figure V-66. Simulation summary for MRGO station 670

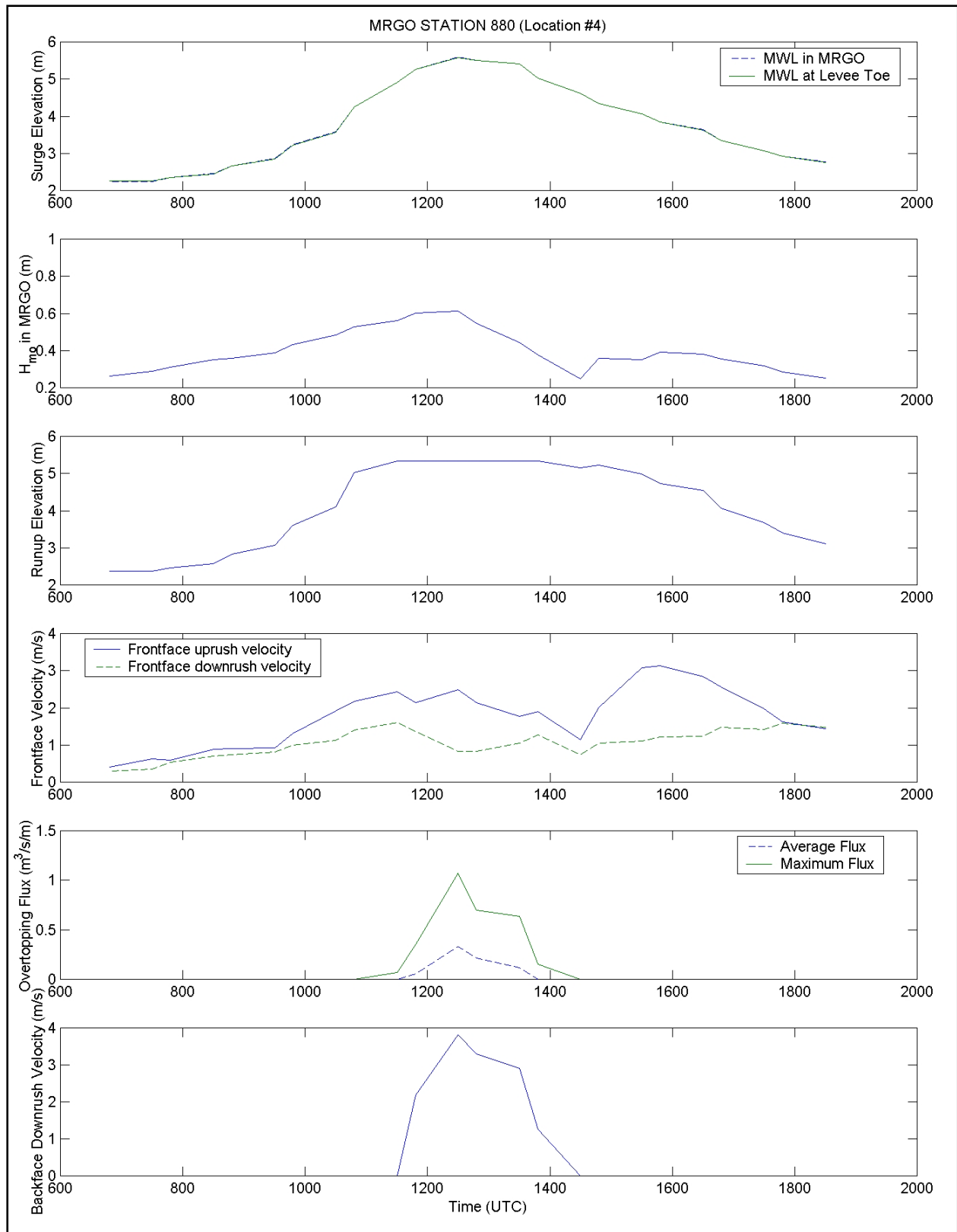


Figure V-67. Simulation summary for MRGO station 880

Available Information. The Data Collection and Management Group has developed the time history of water level in Lake Pontchartrain, η_o in the vicinity of the 17th Street Canal. Additionally, the pump operator at the south end of the 17th Street Canal conducted observations of water level, η_3 , on a graduated staff every one-half hour during Katrina. Both of these water level time histories are presented in Figure V-68.

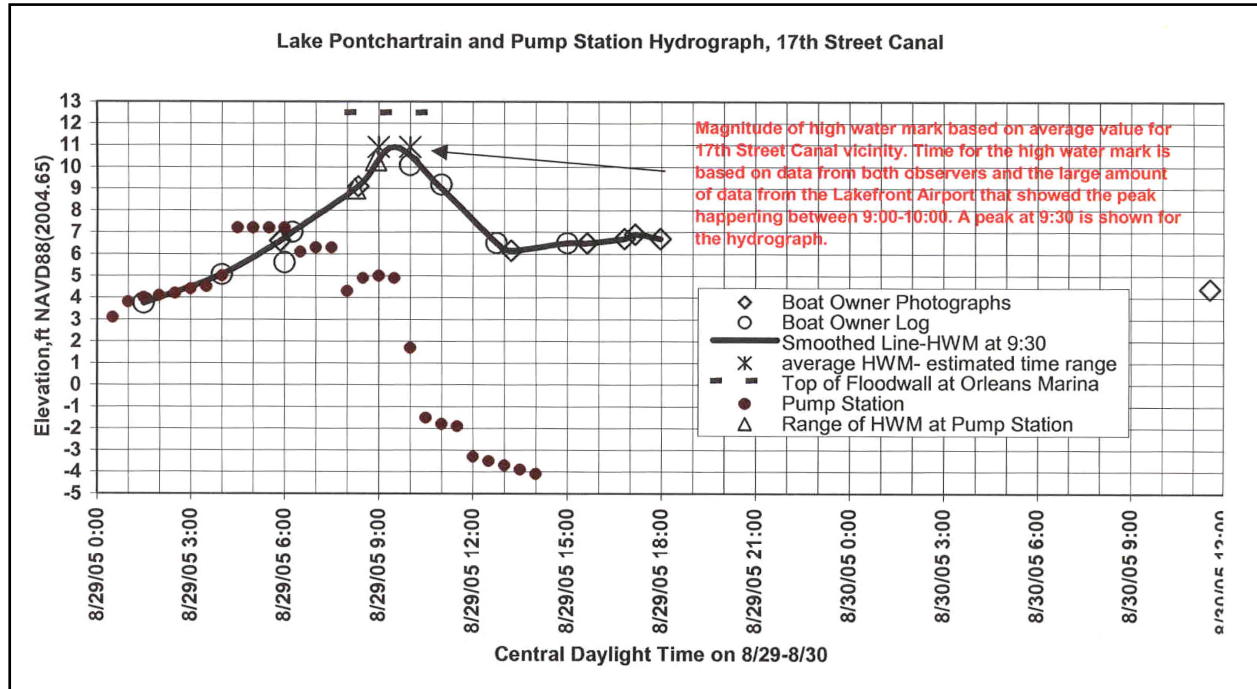


Figure V-68. Water level time histories in Lake Pontchartrain and at the south end of the 17th street canal

Although there is presently some uncertainty of the staff datum used by the pump operator and the validity of the associated elevations, they are the best information available of the water levels at the south end of the 17th Street Canal. Additional efforts will be made to evaluate these elevations.

Figures V-69 and V-70 present an idealized planview and cross-section of the 17th Street Canal, respectively.

Methodology. The equation relating the water level in Lake Pontchartrain, η_o , and the water level immediately inside the canal south of the bridge, η_1 , can be expressed as

$$\eta_o = \eta_1 + \frac{Q_1^2(1 + K_{en} + K_{BR})}{2gW^2(h + \eta_1)^2} \quad (V-1)$$

in which K_{en} is the entrance loss coefficient and K_{BR} is the bridge loss coefficient.

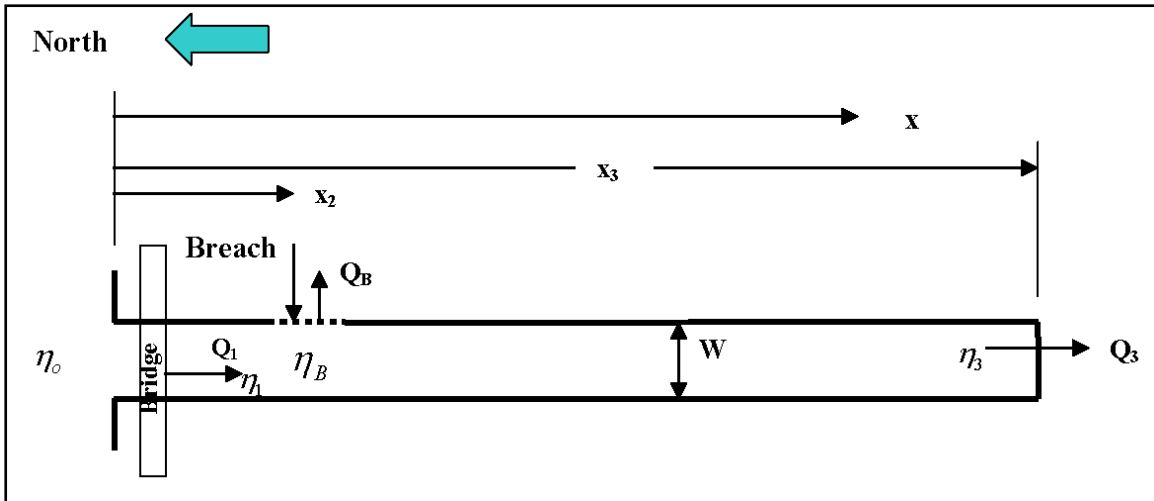


Figure V-69. Idealized planview of 17th street canal

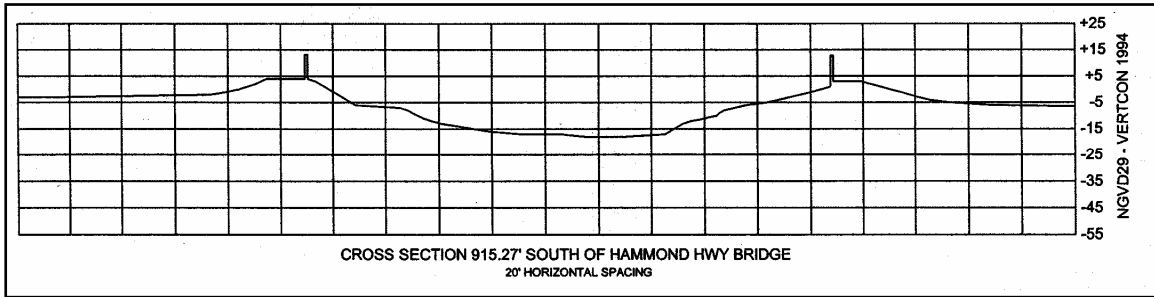


Figure V-70. Typical cross-section of the 17th street canal.

The equation relating conditions at Location 1 to those at the breach is

$$\eta_1 + \frac{Q_1^2}{2gW^2(h + \eta_1)^2} = \eta_B + \frac{fx_2Q_1^2}{8gW^2(h + \eta_{1,B})^3} \quad (V-2)$$

in which f is the Darcy-Weisbach friction coefficient and $(h + \eta_{1,B})$ represents the total effective canal depth between Location 1 and the breach.

Finally, the equation relating conditions at the breach to those at the south end of the canal is

$$\eta_B = \eta_3 + \frac{Q_3^2}{2gW^2} \left(\frac{1}{(h + \eta_3)^2} - \frac{f(x_3 - x_2)}{4(h + \eta_{2,3})^3} \right) \quad (V-3)$$

Equations 1, 2 and 3 provide relationships for the three unknowns, η_1 , η_B and Q_1 and can be solved directly for these three variables. With Q_1 known, the total flow through the breach can be determined as $Q_B = Q_1 - Q_3$. Of course, Q_3

is negative and will contribute to the flow through the breach during periods of pumping into the canal.

Breach Characteristics. With the discharge through the breach established, it is possible to estimate characteristics of the breach geometry and, to some extent, the reliability of the water level observations at the south end of the 17th Street Canal.

First, assuming that the breach is rectangular and that critical flow exists through the breach with unit discharge, $q_B = Q_B / W_B$ where W_B is the breach width, the depth on the breach sill, h_B is

$$h_B = \left[\frac{q_B^2}{g} \right]^{1/3}$$

and the elevation of the sill, z_S is

$$z_S = \eta_B - \frac{3}{2} h_B$$

Results. The above equations were applied to calculate the flows and breach characteristics for the following conditions and values of variables:

$f = 0.08$, $W = 200 \text{ ft.}$, $h = 10 \text{ ft.}$, $x_2 = 2,200 \text{ ft.}$, $x_3 = 12,200 \text{ feet}$, $W_B = 200 \text{ ft}$ up to time 0900 and = 450 ft after 0900¹. The pump discharge, $Q_3 = -5,000 \text{ cfs}$ up to time 0900 and = 0 cfs after 0900².

Figure V-71 presents Q_B , the flow through the breach and Figure V-72 presents the sill depth under the consideration that the flow is critical through the breach.

Consideration of Wind-Induced Barge Motions and Forces in the Inner Harbor Industrial Canal

Introduction. This addresses the issue of whether the barge that traversed from the Industrial Navigation Harbor Canal (INHC) through the flood wall to the Lower Ninth Ward could have been a cause of the levee failure in this area or whether the barge was simply transported through the levee subsequent to its failure. The Task 5 responsibility is to establish the associated forces relative to this issue.

¹ The timing of breach width increase is based on one eyewitness account that one section of floodwall was breached by 0630 and that a greater width of wall had been lost by 0930. The final breach width is approximately 450 feet.

² The time history of pump operations will be validated in the final version of this analysis.

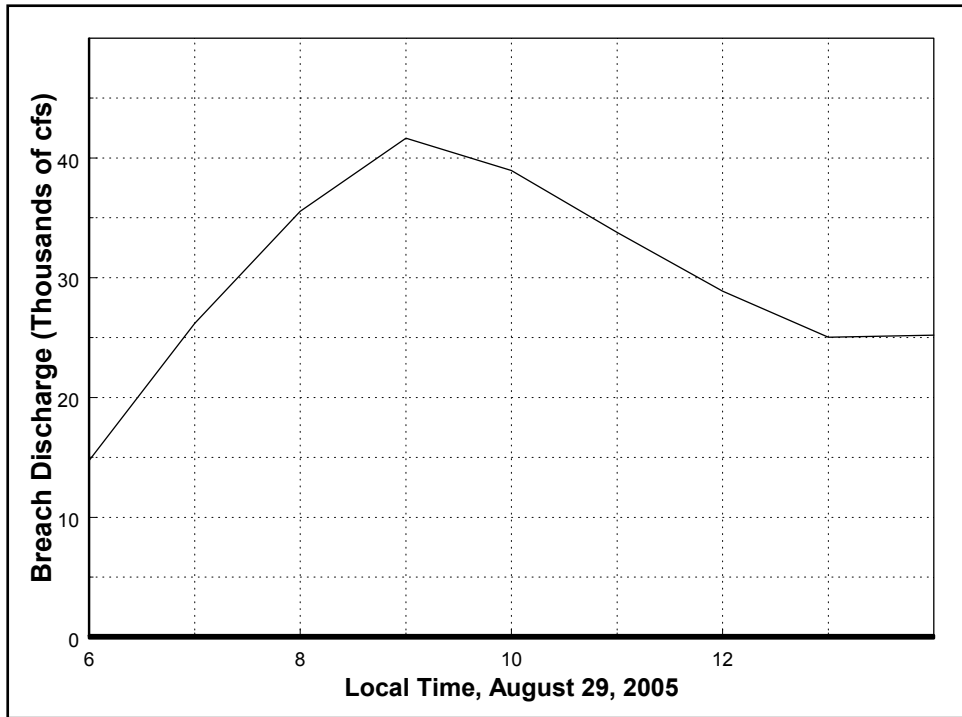


Figure V-71. Estimated breach discharge as a function of time

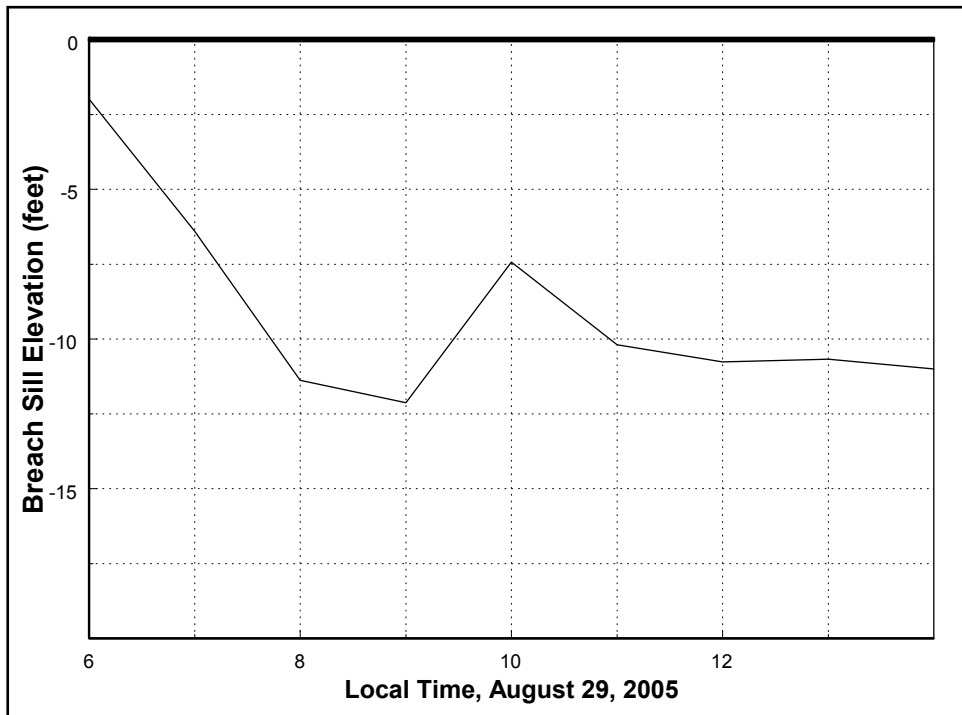


Figure V-72. Estimated time history of breach sill elevation

This brief report examines the wind forces exerted on the barge and the associated velocity, momentum and energy of the barge as it traverses a path across or diagonally along the canal to the location of levee failure. This analysis considers the situation prior to levee failure and no water current forces are considered. Following development of the velocity and trajectory equations, examples are presented to illustrate application of the methodology.

This report is organized as follows. “Barge Characteristics” describes, to the extent possible, the characteristics of the barge that was located outside the IHNC after the levee failed. The following section estimates the winds and wind forces on a barge immersed within the wind boundary layer. These wind forces on a static barge are compared with the static hydrodynamic forces which existed immediately prior to levee overtopping. The next section examines the dynamics of the barge for various drafts and provides a basis for quantifying the barge trajectory and momentum and energy upon impact with the east floodwall. Examples illustrating application of the methodology developed are presented in the next section. Recommendations and the summary and conclusions are presented in the final section.

The main focus of this report is to provide a method for quantifying the barge characteristics relative to its possible role in failure of the IHNC east flood wall. The detailed calculations employing this methodology will require improved estimates of the barge and other characteristics required by the methodology.

Figure V-73 shows a plan view of the barge in the INHC and the winds that were directed on the barge.

Barge Characteristics.

During the site visit on December 22, 2005, the dimensions of the barge identified as “ING 4727” were estimated as:

Hull Depth = 12 feet

Superstructure Height Including Covers for Contents = 11 feet

Barge Length = 200 feet

Barge Width = 35 feet

Figure V-74 presents these barge dimensions.

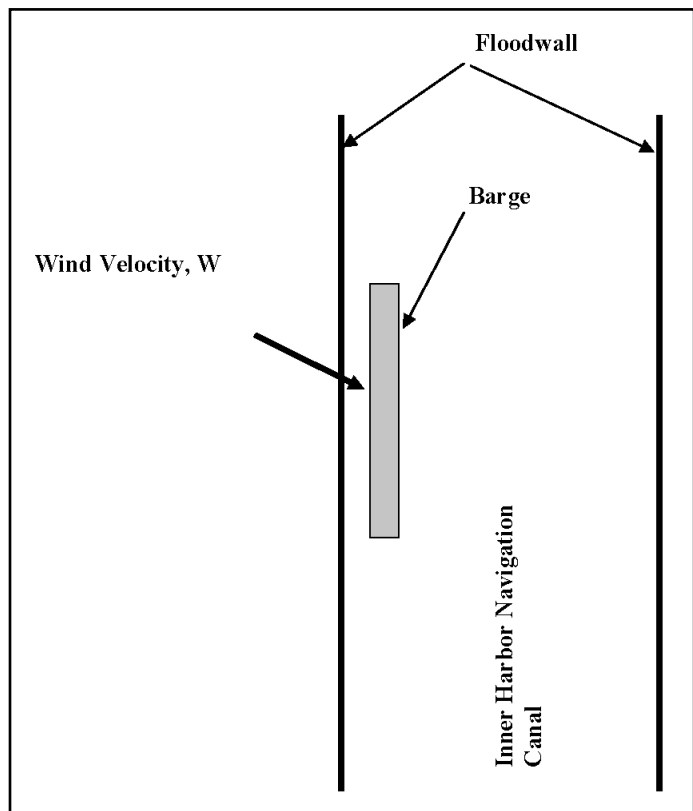


Figure V-73. Definition Sketch of Inner Harbor Navigation Canal and Wind Blowing on the Barge

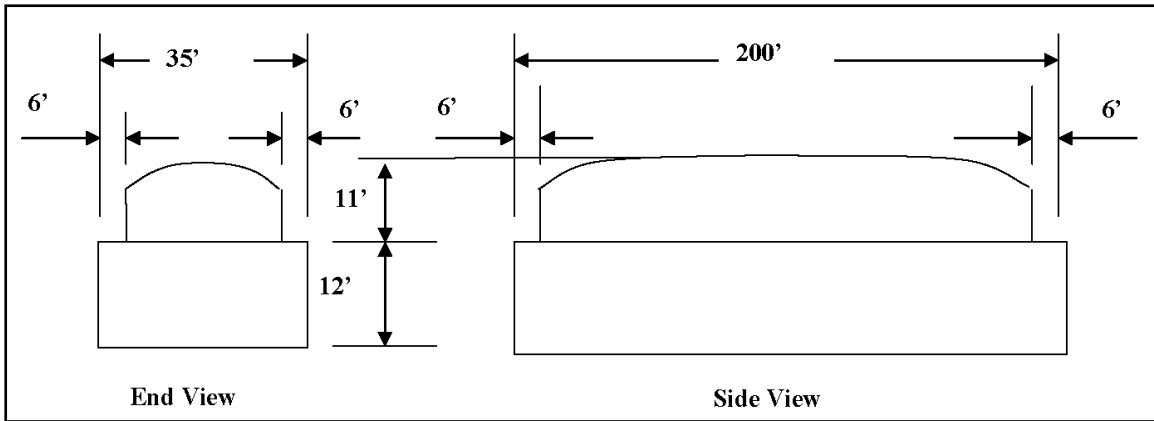


Figure V-74. Estimated Dimensions of Barge Observed on Site Visit to Lower Ninth Ward

Wind Loading and Comparison With Hydraulic Forces on East Flood Wall.

Wind Profile and Effective Wind Speed, W_{eff} . The relevant wind speed is that which is exerted on the barge. For a drag force relationship, this is the root-mean square of the wind speed over the vertical dimension of the above water portion of the barge. For purposes here, the following simple relationship for the vertical distribution of wind speed is considered

$$W(z) = W(30) \left(\frac{z}{30} \right)^{1/7} \quad (V-4)$$

in which z is the elevation above the water surface in feet and $W(30)$ is the reference wind speed at 30 feet above the water surface. The draft of the barge will be denoted as d . Thus the vertical dimension of the barge exposed to the wind is $(23 - d)$ feet. The effective wind speed, W_{eff} for drag force computations is therefore

$$W_{eff} = \sqrt{\frac{\int_0^{23-d} W^2(z) \ell(z) dz}{\int_0^{23-d} \ell(z) dz}} \quad (V-5)$$

in which $\ell(z)$ is the length of a barge element at elevation z and $23 - d$ is the height of the barge above the water level. Although the length of a barge element does vary slightly with elevation as shown in the previous section, this variation is reasonably small and for purposes here we will consider that $\ell(z)$ is uniform over the height, $23 - d$. This results in the effective velocity, W_{eff}

$$W_{eff} = 0.882 \left(\frac{23-d}{30} \right)^{1/7} W(30) \quad (V-6)$$

Wind Drag Forces on Barge. The drag force, $F_{D,a}$ exerted by the wind on the barge are given by

$$F_{D,a} = \frac{\rho_a C_{D,a} A_a W_{eff}^2}{2} \quad (V-7)$$

in which ρ_a is the mass density of air, $C_{D,a}$ is the so-called “drag coefficient” of the barge to winds and A_a is the “projected area” of the barge perpendicular to the wind velocity vector.

For purposes of examples presented in this report, we will consider the wind to be directed broadside to the barge, a wind mass density, $\rho_a = 0.002$ slugs/ft³ and a barge length = 200 feet. Thus, the relevant area in Equation V-7 is

$$A_a = 200(23 - d) \quad (V-8)$$

Static Hydraulic Forces and Moments on Flood Wall Immediately Before Overtopping

Figure V-75 depicts a typical section of the flood wall at an imminent overtopping condition.

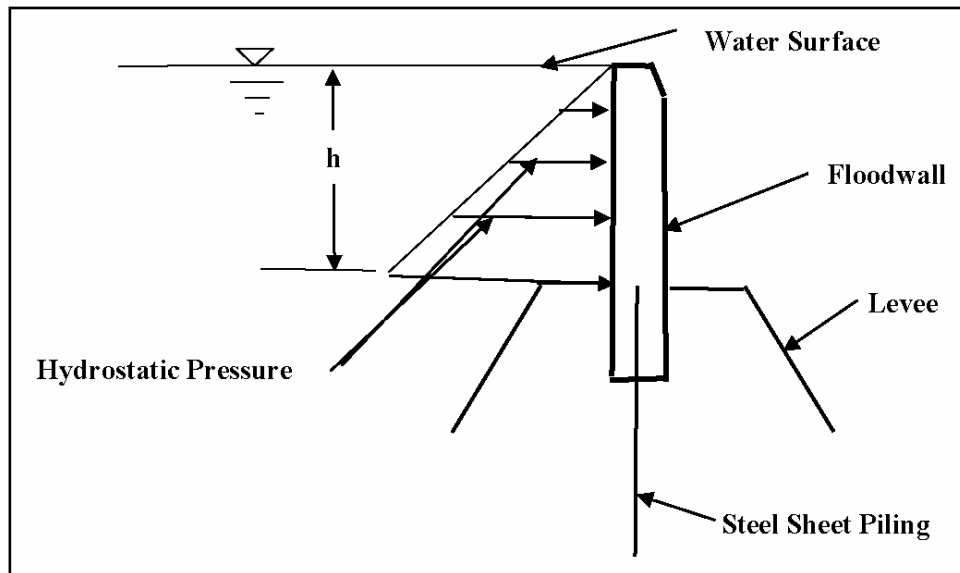


Figure V-75. Definition Sketch for East Floodwall at Imminent Overtopping Condition

The hydrostatic force, F_{HS} on the floodwall per unit floodwall length for the imminent overtopping condition shown in Figure V-75 is

$$F_{HS} = \rho_w g \frac{h^2}{2} \quad (V-9)$$

in which ρ_w is the mass density of water taken here as 1.94 slugs/ft³ and g is the acceleration of gravity.

The hydrostatic moment, M_{HS} about the base of the floodwall per unit length of flood wall is given by

$$M_{HS} = \rho_w g \frac{h^3}{6} \quad (V-10)$$

Comparison of Hydrostatic Forces and Moments With Static Wind forces and Moments

To calculate wind forces, we need to select a reference wind speed, W (30) as shown in Equation V-4. For most of the examples presented in this report, a reference wind speed of 100 miles per hour (146.7 ft/sec) and a wind drag coefficient, $C_{D,a} = 0.5$ have been selected for illustration purposes. To illustrate the maximum wind force, a lightly loaded barge condition is selected with a barge draft, $d = 4$ feet. Applying Equation V-6, the reference wind speed, $W_{eff} = 121.2$ ft/sec. The wind drag force per unit barge length f_{HS} , is then

$$f_{D,a} = \frac{\rho_a C_{D,a} (23 - d) W_{eff}^2}{2} = 139.5 \text{ pounds/foot} \quad (V-11)$$

This value is compared to the hydrostatic force per unit length of 1,999 pounds/foot based on a floodwall height = 8 feet. Thus, the static wind force is equal to approximately 7% of the hydrostatic force. However this result is based on a uniform transfer of the wind load on the barge to the floodwall. If this transfer is concentrated, the local wind related loads acting on the floodwall per unit length could be much greater than those calculated above.

The wind related moments about the bottom of the floodwall are considered to result from application of the wind related forces at the mid-elevation of the barge draft, i.e., 2 feet below the crest of the floodwall. In this case, the moment due to the wind is 837 foot pounds per foot compared to the hydrostatic moment of 5,331 foot pounds per foot or the wind moment is approximately 16% of the hydrostatic moment. However, the same comment applies to moments as was presented for forces regarding the consideration that the wind forces were applied uniformly along the wall.

The following section examines the dynamics of the floating barge.

Barge Dynamics Under the Action of Wind Forces

Equation of Motion and Solution. The equation of motion of the barge is:

$$m_T \frac{dV}{dt} = K_1 W_{eff}^2 - K_2 V^2 \quad (V-12)$$

in which m_T is the total effective mass of the floating barge and is the sum of the physical mass and the added mass, V is the barge velocity, t is time after the barge starts to float free, W_{eff} is the effective wind speed acting on the barge as described earlier. The factor, K_1 has been defined earlier as

$$K_1 = \frac{\rho_a C_{D,a} A_a}{2} \quad (V-13)$$

The factor K_2 is defined as

$$K_2 = \frac{\rho_w C_{D,w} A_w}{2} \quad (V-14)$$

in which ρ_w has been defined as the mass density of water, $C_{D,w}$ is the so-called “drag coefficient” of the barge to the water and A_w is the “projected area” of the barge perpendicular to the water velocity vector. In subsequent calculations, the following values of drag coefficients will be applied: $C_{D,a} = C_{D,w} = 0.5$. The dimensions of both K_1 and K_2 are “force/velocity squared.” The complete barge dimensions were presented in section above titled “Consideration of Wind-Induced Barge Motions and Forces in the Inner Harbor Industrial Canal” (see Figure V-74).

Estimation of K_1 and K_2 Factors and Steady State Velocities. From Equation V-10, it is seen that the steady state (or terminal) velocity of the barge, $V(\infty)$ is given by

$$V(\infty) = \sqrt{\frac{K_1}{K_2}} W_{eff} \quad (V-15)$$

The values of K_1 and K_2 will be estimated for the case of the barge fully loaded and loaded very lightly. The barge is considered broadside to the wind. The results of these estimates are presented in Table V-5. The values of the dimensionless terminal barge velocity, $V(\infty)/W_{eff}$ are also presented in

Table V-5. Note that the length of the barge acted upon by winds has been taken as 188 feet.

Table V-5				
Estimation of K_1 and K_2 for Two Cases				
Case	Description	K_1 (Pounds- sec²/ft²)	K_2 (Pounds- sec²/ft²)	$V(\infty) / W_{eff}$
1	Fully Loaded, Draft $d = 9$ feet	1.32	873	0.039
2	Lightly Loaded, Draft $d = 4$ feet	1.79	388	0.068

Non-Dimensionalization and Solutions of the Equation of Motion

It is useful to cast the equation of motion in non-dimensional form as:

$$\frac{m_T}{K_1 W_{eff}^2} \frac{dV}{dt} = 1 - \frac{K_2}{K_1} \frac{V^2}{W_{eff}^2} \quad (V-16)$$

from which the solution can be shown to be:

$$V(t) = V(\infty) \tanh \left(\sqrt{\frac{K_1 K_2}{m_T}} W_{eff} t \right) \quad (V-17)$$

The non-dimensionalizing time, t_* , is defined as

$$t_* = \frac{m_T}{\sqrt{K_1 K_2} W_{eff}} \quad (V-18)$$

and is the time at which the barge velocity is 76.2% of its terminal velocity. Choosing the non-dimensionalizing velocity as the terminal velocity, $V(\infty)$, and denoting non-dimensional quantities by primes (e.g., $t' = t / t_*$), the solution for the non-dimensional velocity, $V'(t')$ is

$$V'(t') = \tanh(t') \quad (V-19)$$

The non-dimensional barge displacement, $x'(t') = x(t) / x_*$, can be shown to be

$$x'(t') = \ln[\cosh(t')] \quad (V-20)$$

$$\text{where } x_* = \frac{m_T}{K_2} \quad (V-21)$$

The advantages of the non-dimensional solutions presented is that they depend on only one variable, t' .

Figure V-76 presents the non-dimensional solutions for the range $0 < t' < 5$ which will be shown to provide adequate information to analyze the case of the barge motions and forces in the INHC canal.

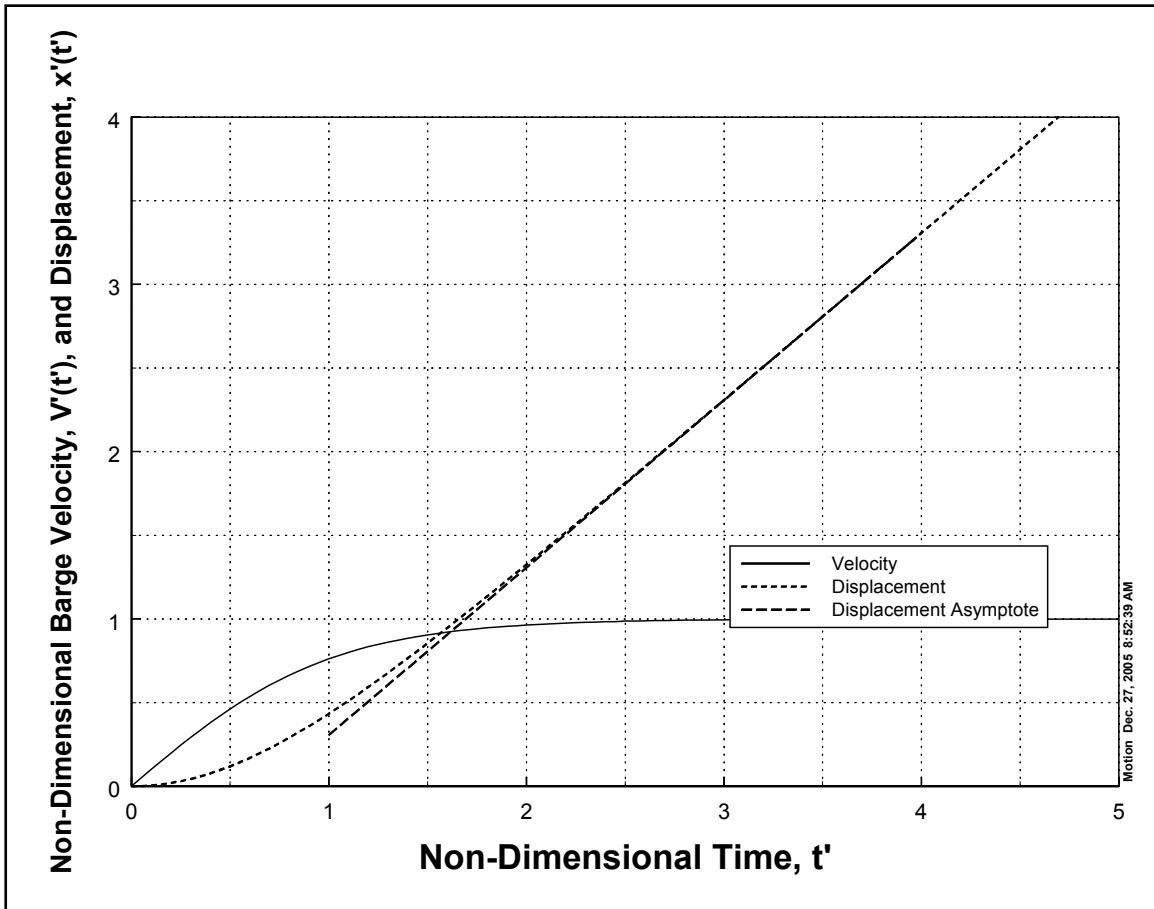


Figure V-76. Non-Dimensional Barge Velocity and Displacement

The non-dimensional relationships are plotted in a different manner in Figure V-77 which has advantages for our particular applications. Figure V-77 presents the non-dimensional barge velocity, $V'(t')$ as a function of the non-dimensional barge displacement, $x'(t')$. In applications, the quantity x is the path of the barge from its starting point to its ending point where it would impact the east flood wall of the INHC canal. This quantity is based on barge and other conditions and is the non-dimensional distance, x' . Entering Figure V-77 with

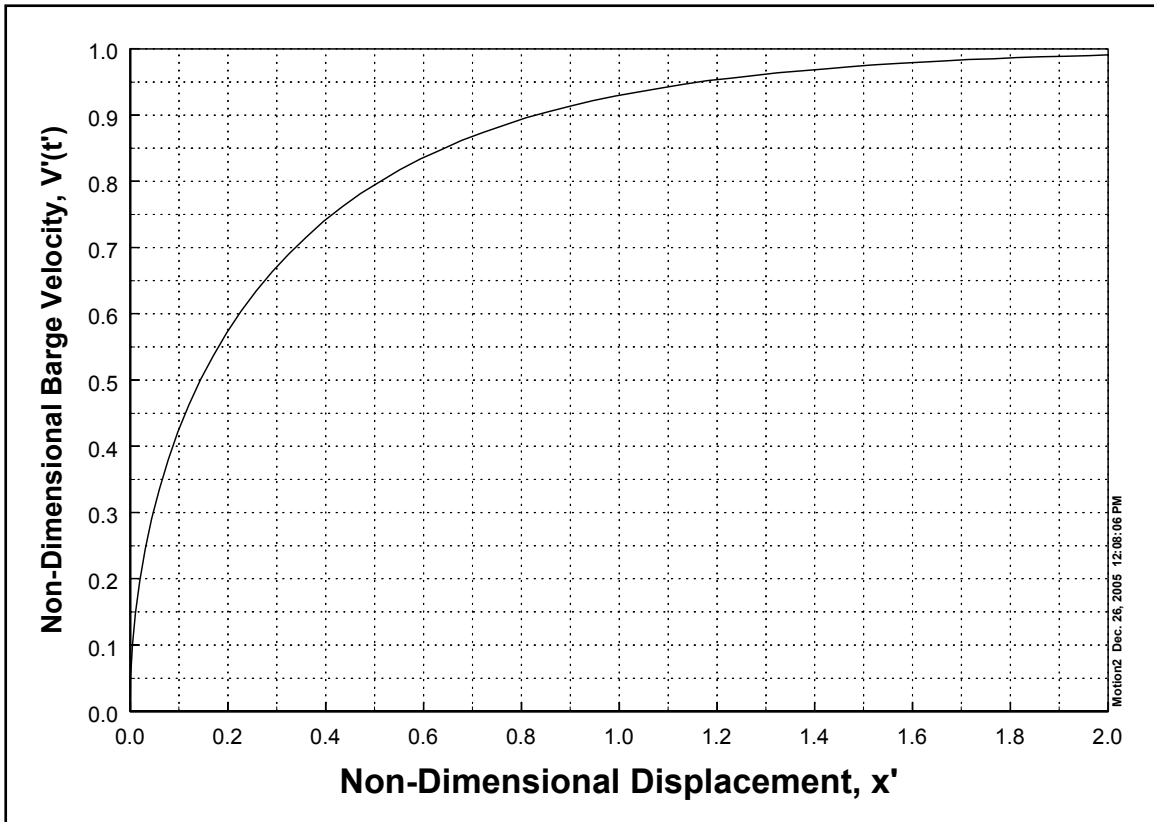


Figure V-77. Relationship Between Non-dimensional Barge Velocity, $V'(t')$ and one-dimensional Displacement, $x'(t')$

this x' quantity on the abscissa, the non-dimensional velocity, V' is determined. The dimensional velocity, V is then quantified. Finally the momentum and energy of the barge upon impact are determined as:

$$\text{Momentum} = m_T V \quad (\text{V-22})$$

$$\text{Energy} = \frac{m_T V^2}{2} \quad (\text{V-23})$$

The barge displacement, x , should increase linearly with time after the barge has reached its terminal velocity, $V(\infty)$ and this appears to be the case from Figure V-76 but is not so apparent from Equation V-20. However, from Equation V-18, for large t' ,

$$x'(t') = t' - \ell \ln(2) \quad (\text{V-24})$$

which is plotted as the asymptote in Figure V-76. Expressing Equation V-24 in dimensional form, this equation becomes

$$x(t) = V(\infty)t - \frac{m_T}{K_2} \ln(2) \quad (\text{V-25})$$

which demonstrates the expected linearity of the relationship for large time. The second term on the right hand side of the above equation accounts for the acceleration phase of the barge response, as can be appreciated by the role of the total mass, m_T , such that a larger mass tends to prolong the acceleration phase and thus reduce the displacement at any particular time.

The procedure for calculating barge motion characteristics will be illustrated in the following section of this report.

Examples Illustrating Application of the Methodology

Consistent with the results in Table V-5, two cases are considered: Case 1 in which the barge is fully loaded with a draft of 9 feet and Case 2 for which the barge draft is 4 feet. It is noted that the examples presented here are for illustrative purposes of the methodology. After the detailed characteristics of the barge are more fully established, the motion and force characteristics can be more fully quantified.

Case 1. Barge Fully Loaded. For Case 1, the total mass, m_T is the sum of the physical mass, m_p and the added mass, m_A . The physical mass is equal to the mass of the displaced water or 122,220 slugs. Assuming an added mass coefficient of 0.2, the total mass, $m_T = 144,664$ slugs.

For a barge exposure above water of 14 feet ($d = 9$ feet), based on Equation V-6, the reference wind velocity, W_{eff} is $0.791 \times W(30)$. Considering, as an example, $W(30) = 100$ mph = 146.7 ft/sec, $W_{eff} = 116.0$ ft/sec. The K_1 and K_2 values are 1.32 pound-sec²/ft² and 873 pound-sec²/ft², respectively as given in Table V-5. The non-dimensionalizing quantities are $t_* = 36.7$ sec, $V(\infty)$, the barge terminal velocity = 4.52 ft/sec, and $x_* = 165.7$ ft.

The distance across the IHNC from the western floodwall to the eastern floodwall is approximately 1,100 feet. Considering that this is the trajectory of the barge, the translation distance is 1,082.5 feet (the width of IHNC minus one-half the barge width). Thus the value of x' is 6.53. Referring to Figure V-77, it is clear that the barge would have achieved its terminal velocity, $V(\infty)$ of 4.52 ft/sec. Thus the momentum and energy upon impacting the wall are:

Impact Momentum = 653,900 pound sec.

Impact Energy = 1.48 million foot pounds.

This example is provided as an illustration of the application/interpretation of the impact momentum. Consider this momentum to be transferred in, say 10 seconds allowing for barge deformation. If the form of the transfer is triangular, that is the force starts at zero, rises to twice the average value, then decreases to zero force in 10 seconds, then the maximum force acting on the flood wall would be 130,780 pounds. This is compared to the hydrostatic force of 399,000 pounds over the barge length of 200 feet. Thus, for this impact time of 10 seconds, the maximum impact force is 33% of the hydrostatic force. It is cautioned that: (1) The actual impact time would require a careful analysis of the barge and floodwall deformation characteristics and consideration of various barge orientations upon impact. Shorter impact times will result in greater maximum impact forces, and (2) The impact forces may be localized thus resulting in greater impact forces per unit length of the floodwall.

Case 2. Barge Lightly Loaded. The draft for this case is 4 feet as shown in Table V-5. As for Case 1, the total mass, m_T is the sum of the physical mass, m_p and the added mass, m_A . The physical mass is equal to the mass of the displaced water or 54,320 slugs. Again assuming an added mass coefficient of 0.2, the total mass, $m_T = 65,184$ slugs.

For a barge exposure above water of 19 feet ($d = 4$ feet), based on Equation V-6, the reference wind velocity, W_{eff} is $0.826 \times W(30)$. Considering $W(30) = 100$ mph = 146.7 ft/sec, $W_{eff} = 121.2$ ft/sec. Considering $C_{D,a} = C_{D,w} = 0.5$, the K_1 and K_2 values are 1.79 pound-sec²/ft² and 388 pound-sec²/ft², respectively as given in Table V-5. The non-dimensionalizing quantities are $t_* = 20.4$ sec, $V(\infty)$, the barge terminal velocity = 8.24 ft/sec, and $x_* = 168.0$ ft.

Considering the same barge trajectory as for Case 1, the value of x' is 6.44. As for Case 1, referring to Figure V-77 it is clear that the barge would have achieved its terminal velocity, $V(\infty)$ of 8.24 ft/sec. Thus the momentum and energy upon impacting the wall are:

$$\text{Impact Momentum} = 537,120 \text{ pound sec.}$$

$$\text{Impact Energy} = 2.21 \text{ million foot pounds.}$$

General Case of Arbitrary Draft

It has been demonstrated that for a reference wind speed of 100 miles per hour, the barge will reach its terminal velocity regardless of the draft and with a minimum distance of the IHNC width translation distance (minus one-half the barge width). Thus, it is possible to develop the following simple equations for impact momentum and energy for the barge of interest.

Impact Momentum. For the barge of interest and considering that the barge had reached its terminal velocity at impact, the equation for the terminal momentum can be written as

$$\text{Terminal Momentum} = 275.2\sqrt{d}(23-d)^{9/14}W(30) \text{ (in pound sec)}$$

Note that consistent units must be used in these equations. Thus $W(30)$ is in ft/sec.

Impact Energy. For the same considerations as above for terminal momentum, the terminal energy can be shown to be

$$\text{Terminal Energy} = 2.32(23-d)^{9/7}(W(30))^2 \text{ (in foot pounds)}$$

Plots of the impact momentum and impact energy are presented in Figure V-78.

Figure V-78 presents non-dimensional plots of terminal momentum and energy versus barge draft. For purposes here, the non-dimensional terminal momentum and velocity have been defined as the ratio of these quantities to the values for a 9 foot barge draft and for a wind speed, $W(30) = 144.67$ ft/sec (100 miles per hour).

Thus the terminal momentum for any draft and wind speed is determined by multiplying the value for 9 feet (653,900 pound sec) by the appropriate value in Figure V-78 and the ratio of the wind speed of interest, $W(30)$ to 146.7 (all in feet/sec).

Similarly, the terminal energy is determined by multiplying the terminal energy for a draft of 9 feet (1.48 million foot pounds) by the appropriate value in Figure V-78 and the ratio of the square of the wind speed of interest, i.e., $W^2(30)$ to $(146.7)^2$ where all wind speeds are in ft/sec.

Interim Results Summary

The equations governing the effective wind speed acting on a barge present in the wind boundary layer have been examined and an effective wind speed defined for drag force calculations. Static wind forces and moments acting on a lightly loaded barge and then transferred to the east IHNC floodwall due to a wind speed of 100 miles per hour have been examined and found to represent a reasonably small fraction of the hydrostatic forces and moments exerted directly on the floodwall. These forces and moments have been expressed as averages per unit length on the floodwall although the barge related forces were likely transferred in a concentrated manner rather than in a uniform manner.

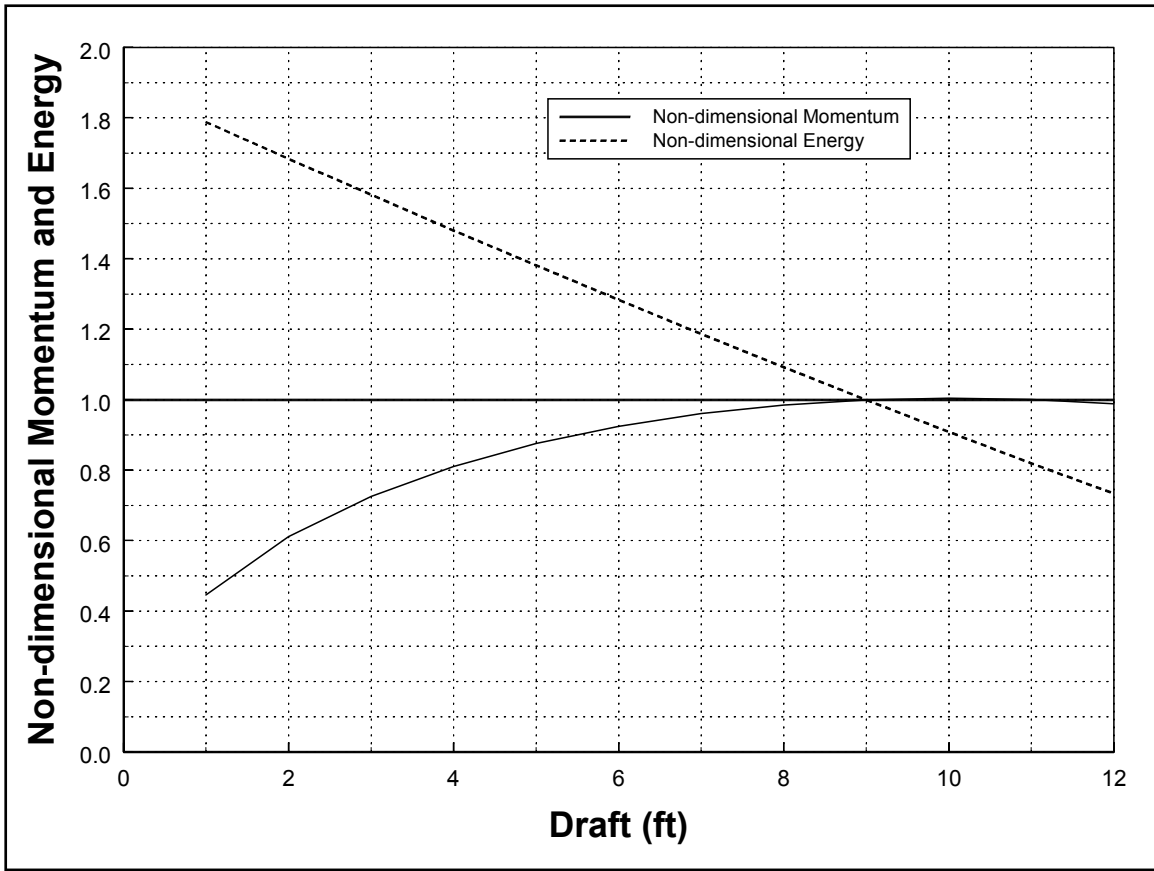


Figure V-78. Non-dimensional Barge Terminal Momentum and Energy vs Barge Draft

The equation of motion of a freely floating barge has been developed and cast in non-dimensional form for easy application. The equations include development of the terminal velocity of the barge. The equation is solved for the non-dimensional velocity and displacement.

It is found that the terminal velocity of the barge is achieved rather quickly for the wind speed examined (100 miles per hour) and that for barge conditions in the INHC the momentum and energy impact on the east flood wall depend primarily on the draft of the barge during the event. Simplified equations have been presented for terminal momentum and energy for use by others in evaluating whether the barge was a contributor to the failure of the INHC flood wall in the Lower Ninth Ward area.

Physical Model

Since the last report, the 14,000 sq ft, 1:50 scale model of the 17th St Canal has been constructed, with completion of concrete placement and molding as of 25 Feb 06. The model will be painted; gauges located, and wave generator calibration begun the following week. Data collection will begin 9 March 06. Figure V-79 shows the layout of the region modeled in the 150-ft-wide by 190-ft-long test basin.

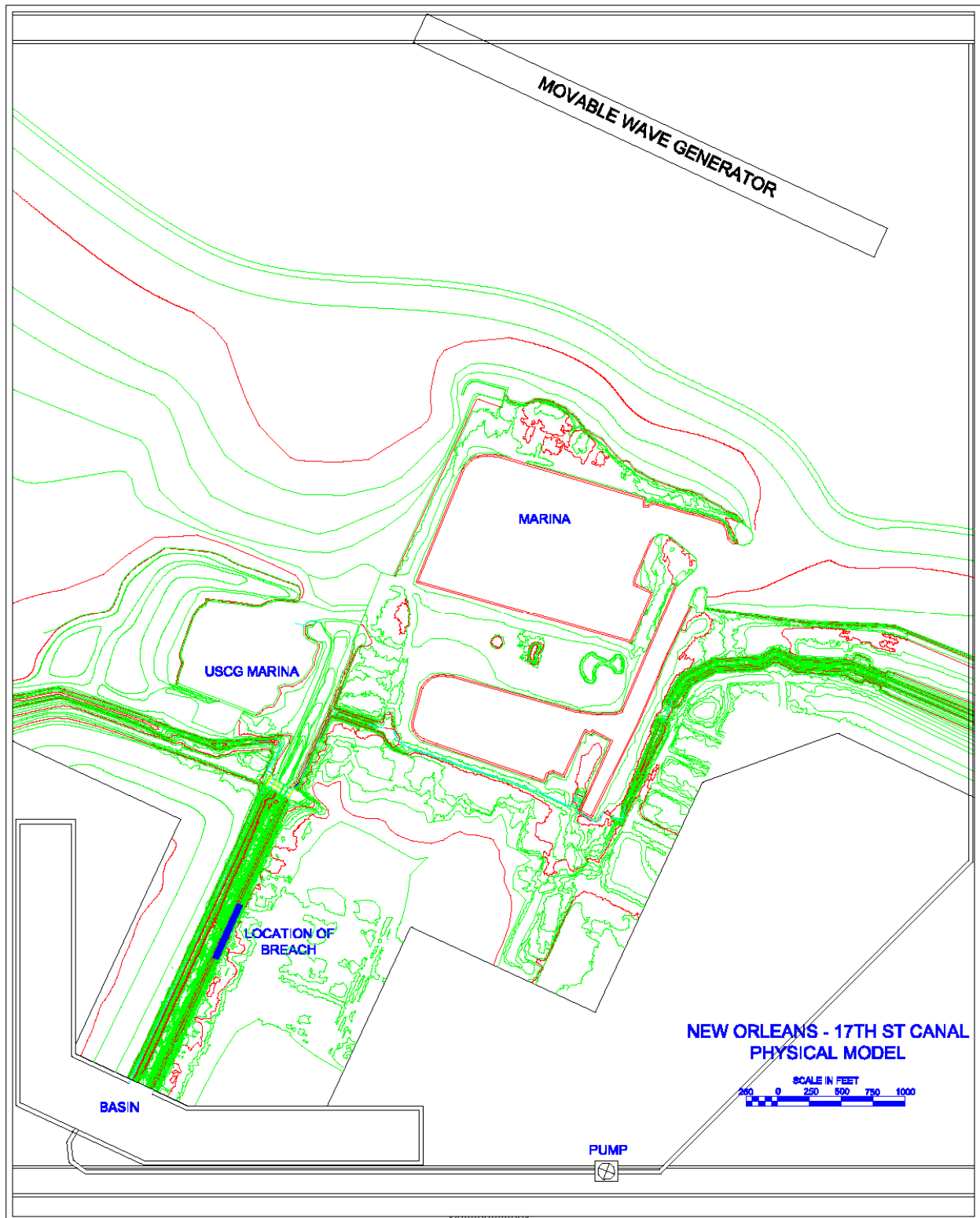


Figure V-79. Layout of 17th St Canal physical model

The physical model includes one-half mile of the 17th St Outfall Canal from the Hammond Highway Bridge to the breach area and 1,200 feet beyond the breach in accurate detail. The remainder of the surface area of the canal is included as a basin region to provide storage area for wave setup and to provide an input region for flow to simulate the pumping system flow.

Input for reproduction of waves and water level was received from Surge and Wave Model Group and Estimation of Forces on Levee Group. Figure V-80 shows the surge height, wave height, period and direction as the storm progressed through time near the 17th Street Canal. Wave information was calculated for four locations evenly spaced across the one mile of lakefront that the physical model reproduces. As can be noted in Figure V-80, the wave data for the four locations plot nearly on top of one another, indicating uniformity in wave height and direction for the 17th St region of lakefront.

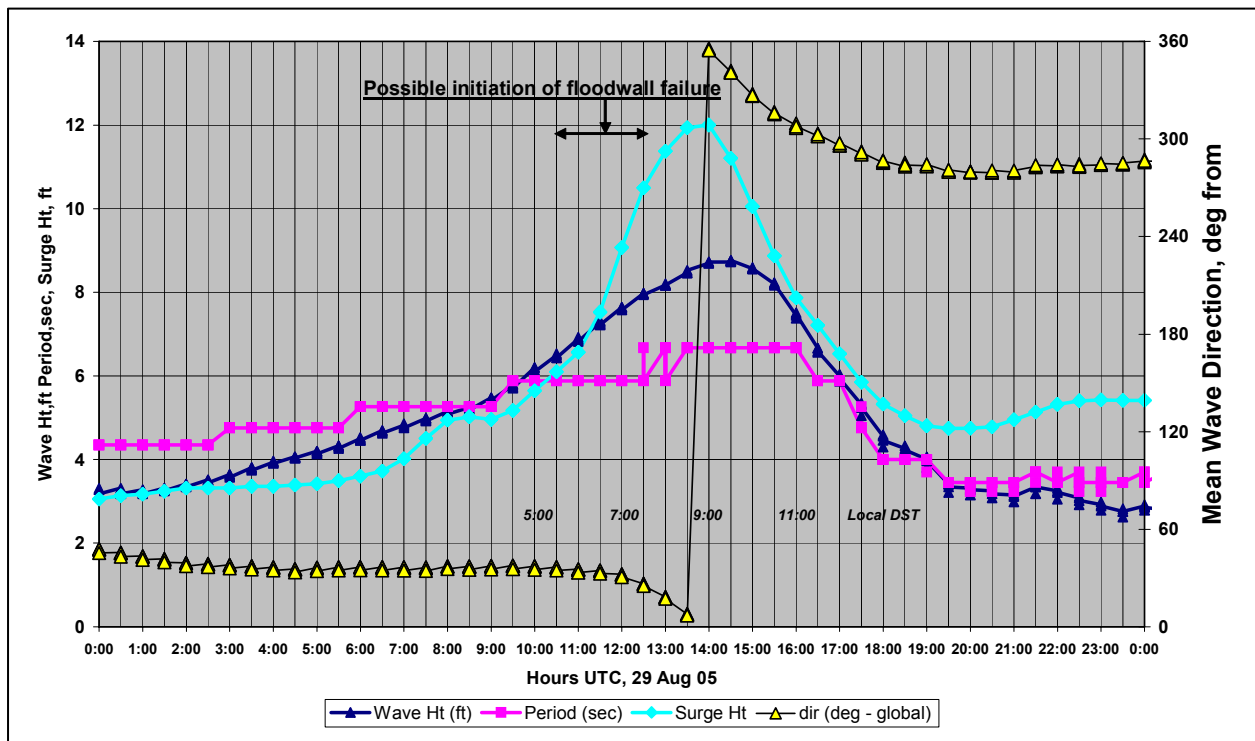


Figure V-80. Surge height and wave information at 17th Street Canal, 14-ft contour, in Lake Pontchartrain

Status of Efforts Remaining

Although it has been demonstrated that the barge terminal momentum and energy could have been considerable and thus possible contributors to the levee failure at the Lower Ninth Ward, this is not evidence that the barge did contribute to the failure. Thus it is recommended that other types of forensic evidence be sought including indications of whether evidence of substantial impact with the flood walls is present on the barge and as much as possible about the mooring arrangement and conditions of the mooring lines after levee failure. Other types of forensic evidence may also be available.

ADCIRC. Subsequent test simulations are planned to incorporate inflow at the pump station, flow into the canals generated by wave setup, flow out of the canals due to breaching, and the effects of bridges. The testing of bridge piers and pump station flows is underway. The conceptual development of representing breaches is underway.

Wave Modeling. Detailed time histories of wave impact on levees will be performed near the failures on the Intracoastal Waterway and the Industrial Canal. The method of simulation here will be comparable to that already performed along MRGO locations; 1HD transects will be examined. As these locations contain vertical T-walls, when the Boussinesq simulations predict strong overtopping, the simulations will be checked with a Boussinesq-RANS (Reynolds-Averaged Navier-Stokes, 2D-vertical) hybrid model, where the T-wall will be located in the RANS domain. This approach permits physically reasonable representation of the overtopping and associated forces during interaction with a vertically-walled structure.

Similar to the analysis presented for the 17th Street Canal, wave simulations will be undertaken for the entire lengths of the London Avenue Canal, Orleans Avenue Canal, and the Industrial Canal, including wave generation effects estimated via STWAVE. These simulations will be run for selected times, and the wave heights and related dynamic pressures/forces will be examined.

Status of Remaining effort for Analytical Analysis of Levee System. Analytical modeling of flow over levees, through breaches, flow in canals, runoff and overtopping of levees, rubble armor stability and damage, and forces on levees and floodwalls has been conducted for some of the major features of the levee system. These modeling techniques have been discussed in preliminary reports. Detailed analysis of flow in the 17th street canal has been conducted. However, because bathymetric and topographic data have only just been received, this task has progressed at a slow rate. Bathymetric and topographic data now exist to allow detailed analysis of flow near and within the 17th Street Canal, London Canal and lakefront areas. Data are still being processed but should be ready soon for analyzing flow in the IHNC, MRGO, and lower Mississippi River areas (Plaquemines Parish). Assuming that these data are supplied in the next two weeks, the bulk of this analysis will be completed for the next 90% report

Plans for Additional Breach Flow Analysis. The final analysis of the hydraulics in the 17th Street Canal and the breach flow and geometric characteristics will be refined through: (1) Evaluation and, if necessary, modification of the time history of the water levels at the south end of the 17th Street Canal, (2) Consideration of the effective canal width as a function of water level in the canal, (3) Inclusion of the hydraulics of the bridge as appropriate (The lower member of the bridge is at an elevation of approximately +6 feet, although this elevation requires verification), and (4) Evaluating whether the inertia terms require consideration in the analysis (A preliminary assessment indicates that they are relatively small).

Planned Efforts to Investigate Breaching in London Avenue and IHNC Canals. The London Avenue and IHNC Canal breaches are considerably more complicated than that in the 17th Street Canal. Both of these canals experienced multiple breaches and considerably less data exist to support the breach analysis/interpretation in these canals. Thus the “piecing together” of the limited information to form coherent scenarios of the timing and sequence of the various breaches will be quite difficult and will necessarily encompass greater uncertainty. It is possible that more useful information will emerge, although in view of the past thorough efforts of Task 1, it is doubtful that this will add significantly to the presently available information.

The data available for the two additional breached canals include the water level time histories in Lake Pontchartrain, eye witness accounts and limited photographic information. Most of this information was collected by Task 1. This information includes some accounts of when flooding was first observed at particular locations and the rates of water level rise at locations.

The time dependence of breaching adds complications to the analysis/interpretation. If the breaching mechanism of canals depended only on the instantaneous loading, it could be argued that multiple breaches could only occur if the more distant breaches from Lake Pontchartrain occurred first because breaches at other locations would reduce the water levels in those portions of the canal more distant from Lake Pontchartrain, thereby reducing breaching potential. Because the mechanisms of breaching are time dependent, the above logic does not strictly apply; however, breaching would lower water levels at more distant locations from Lake Pontchartrain. Thus, combined with geotechnical and flooding analysis, considerations of this type may be useful in establishing breaching characteristics.

In summary, the investigation of hydraulics and breaching timing in the London Avenue and IHNC canals will be complicated by the limited data and may result in several equally plausible scenarios. However, the effort will combine all available data and will be coordinated closely with the geotechnical and flooding investigations, thus providing a basis for identifying the most probable scenarios that are consistent with all sources of reliable information.

Physical Model. Wave height and velocity data will be collected in the canal region and at various locations approaching the canal. Twenty locations can be measured simultaneously for wave height using capacitance-type wave gauges. Velocity will be measured with acoustic Doppler velocimeters. Referring to Figure V-80 above, data will be collected at hours 10, 11, 12 (rising surge level), at hour 14 (peak surge level) and possibly at hours 15 and 16 (falling surge level). Focus will be on times of rising and peak surge levels, as failure of the floodwall likely occurred during this time frame. For each time, repeat tests will be run, the water level will be varied around the numerical surge prediction, and wave height varied around the numerical wave model prediction to produce a suite of wave height values.

Figure V-81 shows an example of the wave spectra providing wave input for the physical model's wave generator. In the first phase of data collection a uni-directional wave generator will be operated, with a directional wave generator coming available later, if required. Also a debris field will be created to determine wave height sensitivity to waves transmitting past the Hammond St. Bridge where photos did indicate a debris field against the bridge after the storm (see Figure V-82).

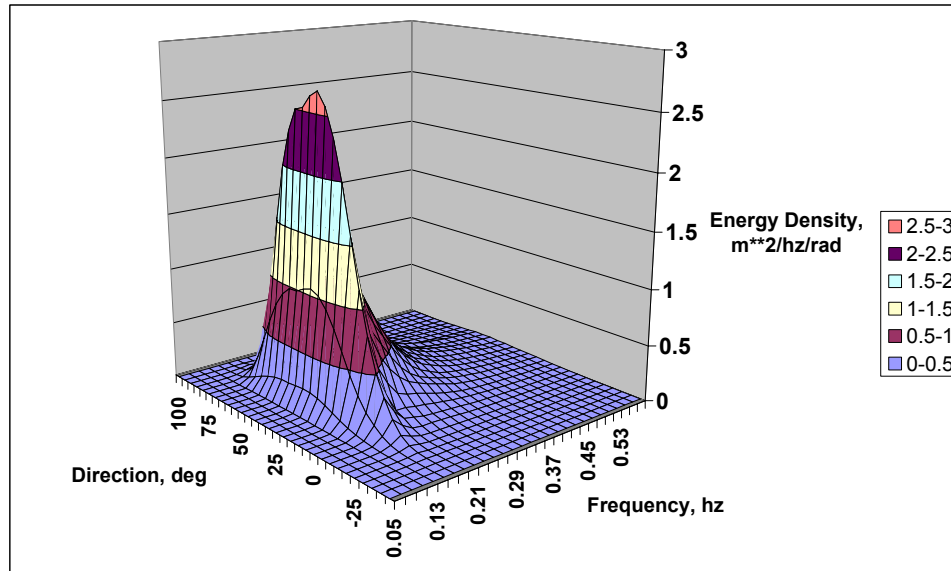


Figure V-81. Wave spectra example at hr 1000 UTC, 29 August 2006 (6.2-ft, 5.9 sec, 37-deg wave)

Figure V-83 shows the Hammond St Bridge profile and its position relative to the highest surge level. This indicates that the bridge had a blocking effect as the surge level rose above the 6-ft level. The testing will provide the effects of the bridge on wave transmission toward the breach region.

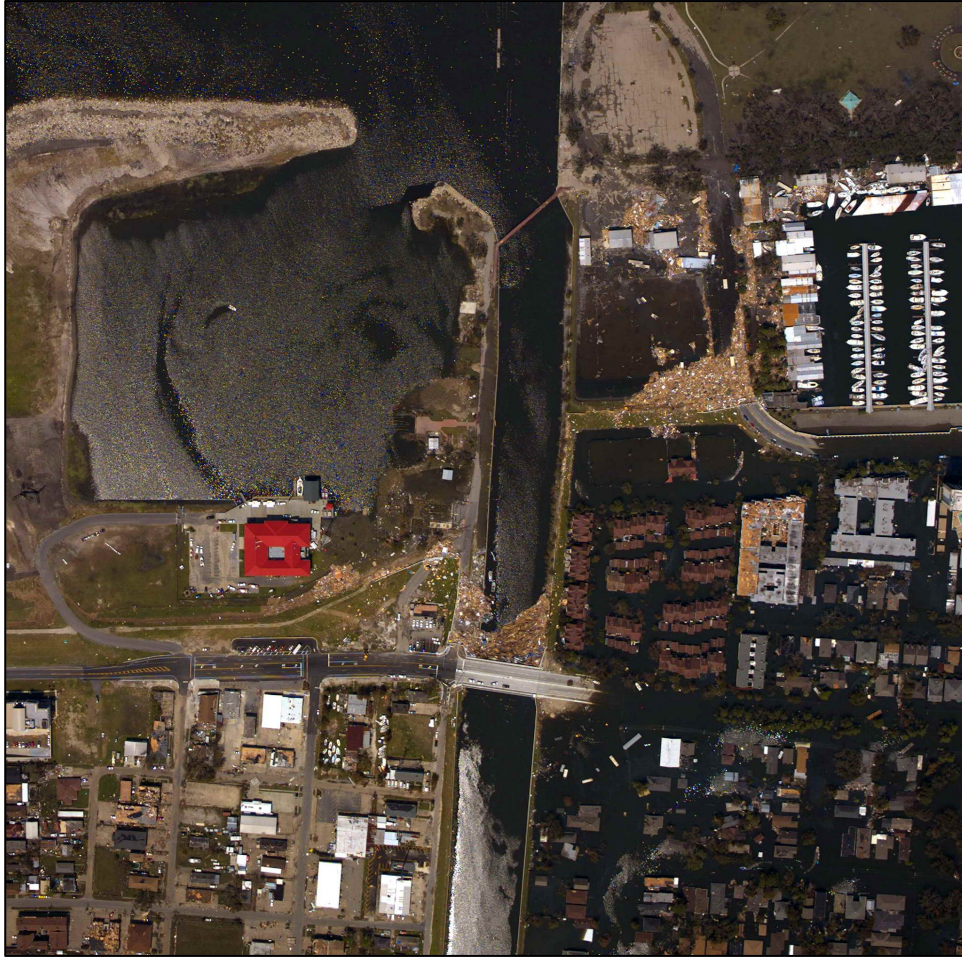


Figure V-82. Debris field against Hammond St. Bridge

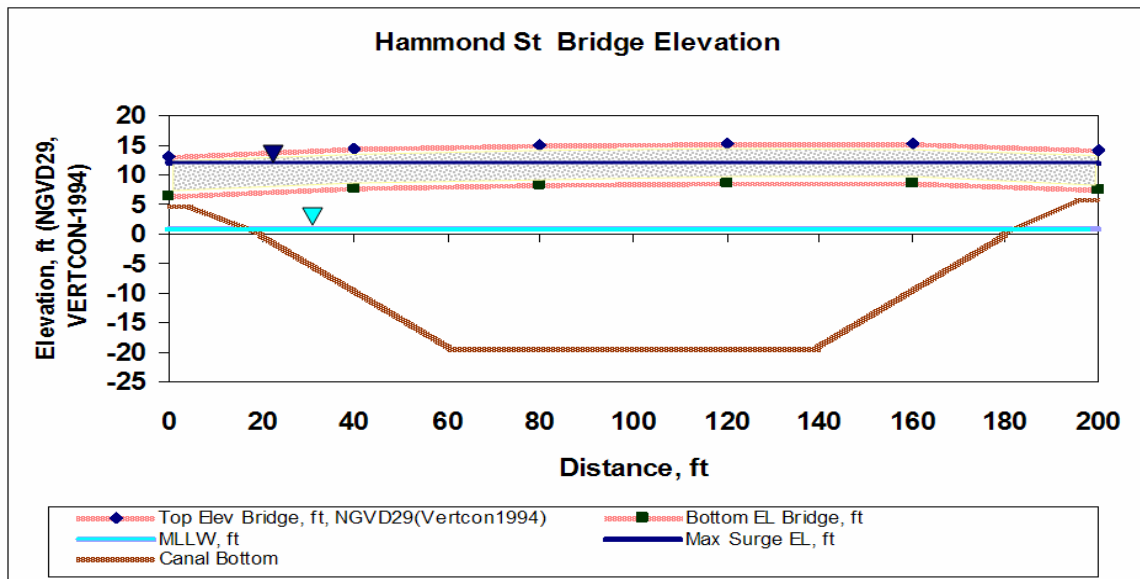


Figure V-83. Location of maximum surge level relative to Hammond St. Bridge